PEPTIDE MONOLAYERS: AN ELECTROCHEMICAL STUDY

A Thesis Submitted to the College of

Graduate Studies and Research

In Partial Fulfillment of the Requirements

For the Degree of Doctor of Philosophy

In the Department of Chemistry

University of Saskatchewan

Saskatoon

By

GRZEGORZ ARTUR ORLOWSKI

PERMISSION TO USE

In presenting this thesis in partial fulfilment of the requirements for a Postgraduate degree from the University of Saskatchewan, I agree that the Libraries of this University may make it freely available for inspection. I further agree that permission for copying of this thesis in any manner, in whole or in part, for scholarly purposes may be granted by the professor or professors who supervised my thesis work or, in their absence, by the Head of the Department or the Dean of the College in which my thesis work was done. It is understood that any copying or publication or use of this thesis or parts thereof for financial gain shall not be allowed without my written permission. It is also understood that due recognition shall be given to me and to the University of Saskatchewan in any scholarly use which may be made of any material in my thesis.

Requests for permission to copy or to make other use of material in this thesis in whole or part should be addressed to:

The Head

Department of Chemistry

University of Saskatchewan

Saskatoon, Saskatchewan

S7N 5C9

ABSTRACT

Understanding electron-transfer (ET) processes in proteins is of fundamental importance. In a series of photophysical studies of well-behaved peptide model systems, it has become evident that the ET through peptide spacers is greatly influenced by the separation between the acceptor (A) and the donor (D), the nature of the peptide backbone, the amino acid sequence, and the resulting flexibility of the peptide conjugates. In particular, it was suggested in the literature that the presence of H-bonding will increase the rate of ET, and there is experimental evidence, mostly in proteins, to suggest that H-bonding indeed increases the rate of ET.

My aim was to develop a potential-assisted deposition method for ferrocene peptide disulfides onto gold surfaces and investigate the electrochemical properties of these films. We made use of two classes of Fc-peptides: acylic ferrocenoyl (Fc)-peptide disulfides and cyclo-1,1'-Fc-peptide disulfides, allowing the preparation of tightly packed films of cyclic and acylic Fc-peptides on gold surfaces within 30 minutes. This is a significant benefit compared to the conventional "soaking" method of self-assembly requiring several days for the assembly of well-packed films. Such films exhibited considerably improved stability. This electrodeposition method should find wide-spread applications for the formation of tightly-packed films from disulfides. Our studies allowed a direct comparison of the electron transfer kinetics of cyclic and acyclic Fc-peptide disulfide systems. Our results showed faster ET kinetics for films prepared from cyclic Fc-peptide conjugates compared to the acyclic systems, presumably as a result of

the enhanced rigidity of the Fc-peptide conjugates on the surface and/or an increase of the number of "conductive peptide wires" to the surface. Following the idea of peptide dynamics as a major contributor to the observed electron transfer rate in peptides and peptide conjugates, variable temperature electrochemical studies of Fc-peptide films were performed. An estimation of the reorganization energy associated with ferrocene/ferrocenium (Fc/Fc^+) redox process allowed us to probe the role of peptide dynamics. Three counter-ions were tested, exhibiting different strengths of association with the Fc^+ group ($BF_4^- < ClO_4^- < PF_6^-$) and the reorganization energies were evaluated in each case. The highest reorganization energy was obtained for the weakly interacting anion BF_4^-. Weakly interacting anions also showed significant broadness in the redox peaks and emergence of the second oxidation peak which is attributed to phase separation of the ferrocene group. Ferrocene agglomeration was not observed for any of the cyclic Fc-peptide conjugates but occurred for some of the acyclic systems. In particular, for acyclic Val and Leu containing Fc-peptide conjugates agglomeration were observed and was presumably caused by lateral interactions between the hydrophobic side-groups of the peptides. Further experiments involving the interaction of Fc-peptide films with alkali metal ions gave additional evidence that electron transfer is influenced significantly by peptide dynamics.

ACKNOWLEDGMENTS

I have worked with a number of great people whose contribution in various ways needs to be acknowledged. It is a pleasure to express my gratitude to all of them in this humble recognition.

In the first place, I would like to express my gratitude to my supervisor Bernie Kraatz for his guidance, supervision, and advice throughout my research adventure. Freedom to play, explore and experiment that he granted, allowed me to developed strong passion for the research and enormously enriched my experience as a student and scientist. I will benefit, in years to come, from this acquaintance.

I would like to thank the members of my advisory committee:

Professor A. Baranski for electrochemical instrumentation and electrochemical advice, Professor David Sanders and Professor Alex Moewes for their advice during the program.

I am also grateful to past and present members of Kraatz group: Somenath, Amir, Anas, Song, Demian, Khan, Yitao, Khaled, Mark, Marek Jr, Thara, Kagan, Regan, Armando and Francis. It was a pleasure to work with you guys !!!

A special gratitude will go to Professor Todd Sutherland for extremely valuable discussions about chemistry, but not only.

I am also grateful to Alex Boika for interesting discussions about HOT electrodes.

I would also like to acknowledge the people that I was collaborating with:

Gareth Nealon – Gaz, soon we all going to love Australian Possums and beer, believe me. Maybe you can build a "Sar-cage" to keep one in.

Jorg Schachner, Clinton Lund & Professor Jens Muller – electrochemistry of [1.1] ferrocenophanes was very entertaining. (I deliberately ate all "umlauts").

I also would like to acknowledge Department of Chemistry and University of Saskatchewan for place to work and funding.

DEDICATION

I would like to dedicate this work for my dear wife
Izabella
For her ongoing Support and Love

TABLE OF CONTENTS

page

LIST OF TABLES

Table page

LIST OF FIGURES

Figure page

LIST OF ABBREVIATIONS

A	Acceptor
ACV	Alternating current voltammetry
AFM	Atomic force microscopy
Aib	α-Aminoisobutyric acid
Ala	Alanine
B	Bridge/linking element
CA	Chronoamperometry
CV	Cyclic voltammogram/cyclic voltammetry
CSA	Cystamine
d	Distance in Å
D	Donor
DPV	Differential pulse voltammetry
e	elementary charge $1.6*10^{-19}$ C
E	Potential
E^0	Standard potential
$E^{0'}$	Formal potential
E_a	Energy of activation
E_p	Peak potential
ΔE_p	Difference in the peak potential
ΔE_{DB}	Energy gap between donor and bridge
E_{fwhm}	Full width of the peak at half maximum
ED	Electrodeposition
ET	Electron transfer
ESI	Electronic supplementary data
EtOH	Ethanol
EQCM	Electrochemical quartz crystal microbalance
F	Faraday constant 96485 C/mol
Fc	Ferrocene
Fc^+	Ferrocenium
ΔG	Gibbs free energy
$\Delta G^{\#}$	Free energy of activation
G	Guanine
GC	Glassy carbon electrode
Gly	Glycine
H_{AD}	Electronic coupling between Donor and Acceptor
H^0	Electronic coupling matrix
ILIT	Indirect laser induced temperature jump
k_{ET}	Electron transfer rate
k_f	Forward electron transfer rate
k_b	Backward electron transfer rate
k^0	Standard electron transfer rate
k_B	Boltzmann constant $1.38*10^{-23}$ J/K

Leu ..... Leucine
i ..... Current
Ile ..... Isoleucine
j ..... Current density A/cm^2
OPE ..... Oligophenyleneethynylene
OPV ..... Oligophenylenevinylene
Pro ..... Proline
ν ..... Scan rate usually in V/s
V ..... Volt
Val ..... Valine
SA ..... Self-assembly
SAM ..... Self-assembled monolayer
SCE ..... Saturated calomel electrode
STM ..... Scanning tunneling microscopy
T ..... Temperature
THF ..... Tetrahydrofuran
TRIS ..... tris(hydroxymethyl)aminomethane
Trp ..... Tryptophan
Tyr ..... Tyrosine
QCM ..... Quartz crystal microbalance
UHV ..... Ultra high vacuum
XPS ..... X-Ray photoelectron spectroscopy
α_{LA} ..... Atomic orbital coefficient between bridge and acceptor
α_{DL} ..... Atomic orbital coefficient between donor and bridge
β ..... Attenuation factor
Γ ..... Surface concentration mol/cm^2
λ ..... Reorganization parameter
ħ ..... Dirac constant1.054*10^{-34} Js

CHAPTER 1
INTRODUCTION

Ferrocene (Fc) terminated self-assembled monolayers are one of the most studied redox-active assemblies on metal surfaces[1-10]. These films have been extensively used as suitable ensembles of well-defined composition, structure and thickness. Fc-terminated films have been often used as model systems to probe electrical double layer properties and electron transfer. A self-assembled monolayer can be described as a donor-bridge-acceptor system (D-B-A), which can be correlated to electrode-spacer-redox couple (Au-B-Fc/Fc^+). In this study, I decided to investigate the role of peptides as a bridging element. Peptide-mediated electron transfer is of extreme importance in many biological processes like photosynthesis, cellular respiration and metabolism. The electron transfer in such systems can occur across various peptide chains, which separate the donor from the acceptor. Folding and functions of some proteins have been associated with electron transfer events. The secondary structure of peptides[11-13] and hydrogen bonding[14-17] are also known to affect efficiency of the ET process.

1.1 Immobilization Methods

In the literature, we can find a large number of references describing the deposition of sulphur-containing compounds on metal surfaces. Recently, thorough reviews were

presented by Whitesides[18] and Gooding.[19] Finklea[20] and Ulman[105] reviewed earlier achievements in this field.

The concept of chemisorption of alkenes on the metal surface was first demonstrated for dialkyl disulfides by Nuzzo[21], even though current scientific reports are mainly describing thiol compounds. The resulting chemisorbed thiolate anions have a high value of activation energy of desorption estimated at approximately150 kJ/mol.[22] In the case of a gold surface immersed in a solution of an alkyl thiol, it is generally assumed that a hydrogen atom is abstracted from a thiol molecule and the resulting radical species undergoes precipitation on the surface, forming a covalent Au–S bond. Chemical equation of the deposition of the alkene thiol on the gold surface can be presented as[104]:

$$R-S-H+Au_n(0) \rightarrow R-S^- - Au^+ \bullet Au_n(0)+1/2H_2 \quad (1.1)$$

For disulfides deposition can be described as an oxidative addition of S-S bond to the gold surface:

$$R-S-S-R+Au_n(0) \rightarrow 2R-S^- - Au^+ \bullet Au_n(0) \quad (1.2)$$

Major methods that can be used for the deposition of thiols (RSH) and disulfides (RSSR) can be summarized as follows:

Less popular method of deposition is the adsorption of thiols and disulfides from the gas phase in UHV. However, this method suffers mainly from its limited application as

many compounds have low volatility and additional chemical modification is often necessary.[23, 24]

Adsorption from solution, where a metal substrate is immersed in diluted (1-10 mM) ethanolic solution of thiol or disulfide, is more versatile.[24] The incubation is usually carried out for a period ranging from minutes for simple alkenethiols, up to a few days in the case of more complicated disulfide compounds. A dense coverage of the adsorbate is obtained just after tens of seconds but second step called organization is much slower (Figure 1.1).

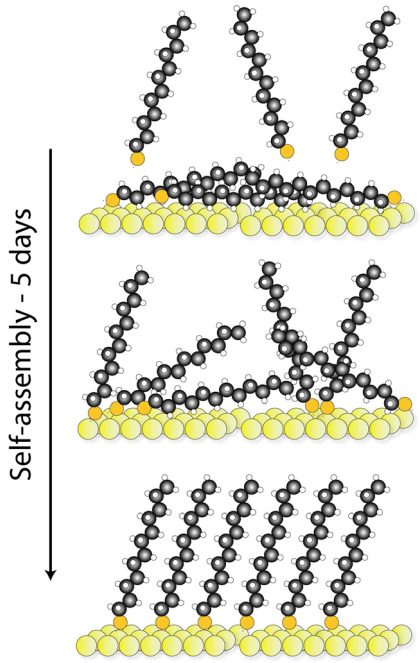

Figure 1.1 Schematic representation of self-assembly steps of alkenethiols on the gold surface.[60] During the first stage, a few second after immersion, alkenethiols are horizontally oriented on the surface. During the second, the lengthiest step, alkenethiols are self-organizing and attaining vertical orientation on the surface.

A number of factors can affect the structure of the SAM on the surface prepared this way like concentration, solvent, temperature, purity of the adsorbate and cleanliness of

the substrate, just to mention the most important ones. The formation of the film at elevated temperatures (above room temperature) can improve quality of the monolayer.[25, 26] Concentration and deposition time are inversely related, the lower the concentration, the longer immersion time is necessary. There is extensive evidence that monolayers formed from disulfide and thiols actually result in films that have very similar structures. Nevertheless disulfides conjugates are less often used mainly due to their lower solubility.[18, 27]

In the literature, we can also find minor number of examples where electrochemical deposition of thiols was used to improve the quality of the deposited film and reduce the time of deposition. Such method was reported by Porter and coworkers[25] for the first time, but a qualitative description of the formed monolayers was not provided. Stratman[28] showed that a small positive potential can increase the speed of thiol adsorption to the gold surface. Ron and Rubinstein[29] reported rapid deposition of alkanelthiols with assistance of a highly positive potential +1.5 V vs. SCE. High positive potential of 1.2 V vs. $Ag/AgNO_3$ was also applied by Ferguson[30] for the deposition of alkanelthiols from THF. In a very recent contribution, Lennox and Ma[31] reported very rapid deposition (ca. 15 minutes) of well organized alkanethiol monolayers when modest (+200-600 mV vs Ag/AgCl) positive potential was applied. Similar results were reported by Vericat.[32,33]

Interestingly there is very little known about electrochemically enhanced deposition of disulfide compounds on the metal surface even though scientific investigation on thiol chemisorption started from disulfide compounds.[21] In the literature electrodeposition of

chemically modified disulfides conjugates is practically absent. In my research I decided to work with disulfide compounds mainly due to availability of cystamine (H_2N-$(CH_2)_2$-S-S-$(CH_2)_2$-NH_2) and simplicity of the synthetic procedures that can be used for making new bio-conjugate compounds.

1.2 Electron Transfer Theory

A comprehensive understanding of electron transfer (ET) processes is vital for future development in many fields of technology and science, ranging from molecular electronics to gaining detailed understanding of some biological enzymes. Over the past few decades, the development of the systems that helped to probe ET has been considerably expanded. In particular electrochemical studies on of redox-active films have contributed much to understanding of the parameters governing interfacial ET. Many different bridging elements have been proposed for use in investigations on the nature of electron transfer process but only few so far had biological relevance. Electron transfer rate can be feasibly obtained by application of various physicochemical methods ranging from electrochemical methods chronoamperometry (CA), cyclic voltammetry (CV),[9, 34-39] alternating current voltammetry (ACV),[35, 40, 41] electrochemical impedance spectroscopy (EIS)[42, 43] through indirect laser induced temperature jump (ILIT)[44] to many photo-physical approaches.[45, 46]

Chidsay[47, 48] was the first one to propose application of Ferrocene-modified monolayers to assess ET rates through alkane chain.

The reduction and oxidation of an electroactive group at a gold electrode can be written:

$$ox + e^- \underset{k_b}{\overset{k_f}{\rightleftharpoons}} red \qquad (1.3)$$

where *ox* is the oxidized form of ferrocene (ferrocenium/ Fc^+) and *red* is the reduced form (ferrocene/Fc). The reaction free energy ΔG^0 can be described as:

$$-\Delta G^0 = e\left(E - E^0\right) \qquad (1.4)$$

where e is electron charge, E is the potential of the electrode and E^0 is the standard potential. When $E = E^0$, the forward rate constant k_f is equal to the backward rate constant k_b. The net reaction rate constant is expected to increase with decrease of the reaction free energy. By changing of the potential, kinetics and free energy of the reaction can be easily controlled.

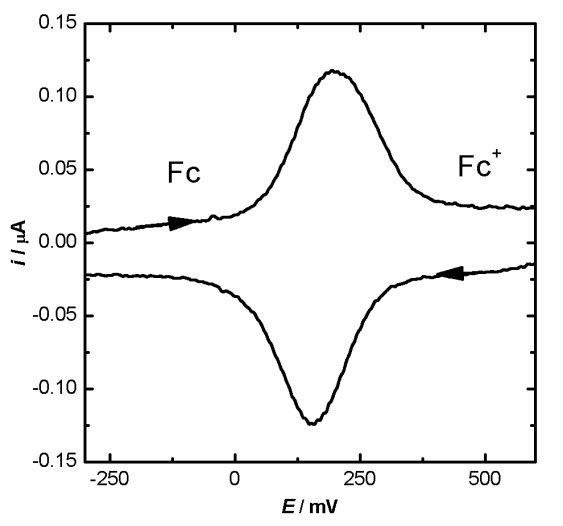

Figure 1.2 Typical electrochemical response in a form of simple cyclic voltammogram of a surface immobilized ferrocene conjugate.

In Figure 1.2, the electrode potential is initially scanned in positive direction through E^0 and the oxidation of the ferrocene to ferrocenium is observed. Then potential is scanned in the negative direction where reduction of the ferrocenium to ferrocene can occur. In the ideal case for very slow scan rate peak separation should be equal to zero.

According to the Laviron[49] formalism, the peak separation is directly related to the electron transfer rate. However, this approach has many drawbacks (huge sensitivity toward solution resistance) and usually is suitable for larger peak separations (above 200 mV).

More direct evaluations of the electron transfer kinetics can be achieved by applying Butler-Volmer formalism.[50]

$$k_f + k_b = k^0 \exp\left[\frac{\alpha e\left(E - E^0\right)}{k_B T}\right] + k^0 \exp\left[\frac{-(1-\alpha)e\left(E - E^0\right)}{k_B T}\right] \qquad (1.5)$$

where k^0 is the standard rate constant, α is the electron transfer coefficient, k_B is the Boltzmann constant and T is temperature in Kelvin. α is an activation barrier symmetry parameter.

Marcus and Hush[51-53] description provides crucial foundation, by which the rate constant for intermolecular electron transfer k_{ET} in the solution can be related to thermodynamic factors. The main dependencies are described in equations 1.6 to 1.8.

$$k_{ET} = \frac{2\pi}{\hbar} \frac{\left|H_{DA}\right|^2}{\sqrt{4\pi k_B T \lambda}} \exp\left(-\frac{\Delta G^{\#}}{k_B T}\right) \quad (1.6)$$

$$\Delta G^{\#} = \frac{\left(\Delta G^0 + \lambda\right)^2}{4\lambda} \quad (1.7)$$

$$H_{DA} = H_0 \exp\left(-\beta d\right) \quad (1.8)$$

where λ is the reorganization energy, H_{DA} is the electronic coupling matrix, ΔG^0 is the change in Gibbs free energy accompanying electron transfer, d is the separation between donor and acceptor, β is the attenuation factor describing the conductivity of the molecular linker, and $\Delta G^{\#}$ is the free energy of activation.

A key feature of this theory is the change in the free energy of activation and its parabolic dependence on the reorganization and free Gibbs energy. The reorganization energy parameter λ contains contributions from both inner (nuclear) and outer (solvation) energy term. It can be also easily derived from Equation 1.6 that electronic coupling matrix H_{DA} should depend on the distance between donor and acceptor and should decrease exponentially with increasing distance.

Super-exchange represents an expansion of the Marcus theory,[54-56] in which the electron transfers from the donor to the acceptor through the path of "virtual" orbitals localized on the linking element even if bridge itself does not engage as a real intermediary element in ET process.

$$H_{DA} = \frac{\alpha_{DL}\alpha_{LA}}{\Delta E_{DB}} \qquad (1.9)$$

where α_{DL} and α_{LA} are atomic orbital coefficients describing coupling between donor and the first linking element and the last linking element with acceptor. The most important aspect of this theory is that coupling element H_{DA} can be related to the band gap (ΔE_{BD}) between orbitals on the donor and the bridging element. A large band gap can be interpreted as weak electronic coupling and thus a slower ET rate. ΔE_{BD} is determined by the electronic properties of the linking element.

1.3 Electron Transfer in Biomolecules

Although there is significant experimental evidence for the validity of Marcus' description of electron transfer, recent studies of the long-range ET through DNA[57, 58] and long helical peptides[37, 59, 60] have shown significant deviations from typical tunnelling and slow ET was observed which cannot be rationalized by Marcus theory. To explain the unusually slow ET rate through peptide, DNA linkers and DNA, the

discrepancies of the observed distance dependence of the ET rate, a new type of mechanism called "hopping" was proposed.[57, 61, 62] The "hopping" mechanism is widely recognized as a working route in DNA charge transfer through "$G^{+\cdot}$ hole" hopping. An electron can hop to and from a guanine base that is operating as an intermediate donor/acceptor on the bridge (Figure 1.3).[62, 63]

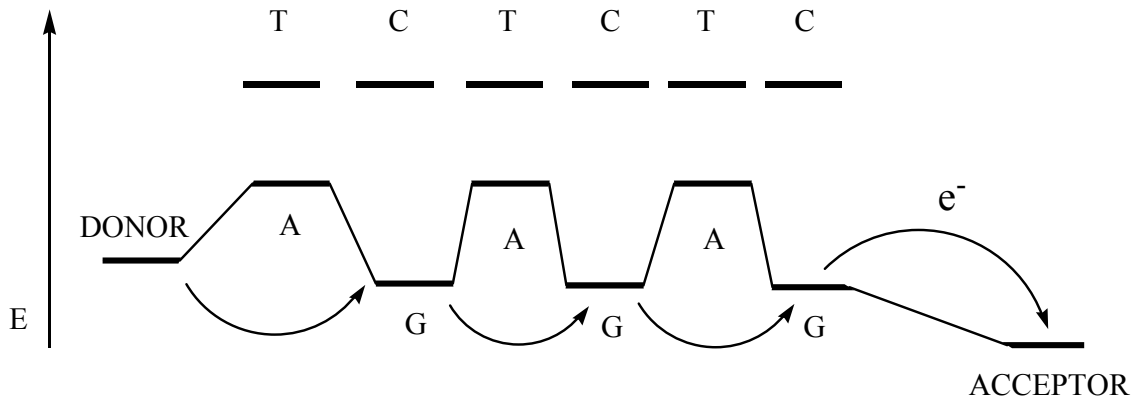

Figure 1.3 DNA charge transfer through "$G^{+\cdot}$ hole" hopping

A thorough description of the problems associated with electron transfer in biomolecules can be found in recent reviews from Benniston,[64] Adams,[65] Giese,[66] and Kraatz[67]. Earlier achievements in this field with a detailed description of the photochemical studies of ET in peptide conjuguates was described by Isied.[46]

A photophysical solution study performed by Isied and coworkers[45], one of the pioneers of peptide charge transfer, on a series of oligopeptide conjugate systems, showed that charge transfer through the peptide backbone is significantly affected not only by the

distance between the donor and the acceptor, but also the nature of the amino acid sequence.[1, 45]

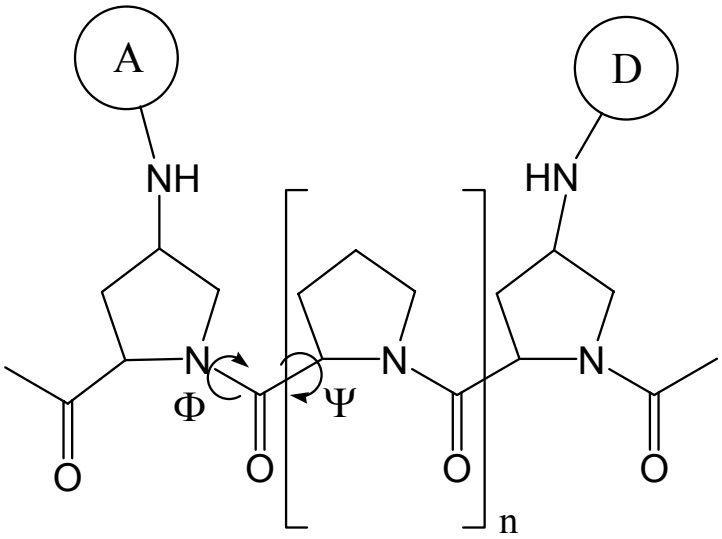

Figure 1.4 Model systems of the oligoprolines used by Isied[1, 45, 68, 69] Giese[70] and Meyer[71] their ET research. Angles Ψ and Φ are used to define secondary structure of the peptide chain.

More recent results appear to indicate that there is a transition in the ET mechanism from a super-exchange mechanism to electron hopping with increasing peptide chain length.[1, 69] However this mechanistic interpretation is not widely accepted.

Meyer[71, 72] for instance argued that electron transfer rates obtained by Isied could have been strongly influenced by changes in the orientation and conformation of the molecules in the bridge. Further evidence that molecular dynamics could significantly alter ET rates was provided by Ogawa.[73] By employing oligoglutamic acid chain in his

study he was able to connect the reorientation of the whole complex in the transition state with the ET rate and activation energy.

Jones[74] studied longer α-helical peptides. In his report, he encountered a wide distribution of observable ET rates. To explain this unusual result Jones invoked considerable conformational changes in the structure of "rigid" helical peptides as a major parameter responsible for significant variations in ET rate.

Newton, Isied[11] and co-workers also reported a theoretical study providing an explanation for differences that were observed in electron transfer kinetics between peptides of various secondary structures. With the help of oligoproline system, Isied presented a model in which the ET kinetics are strongly affected by the differences in the magnitude and directional dipole, occurring along peptide backbone. It is postulated that the dipole moment can significantly contribute to the total electronic coupling between the donor and acceptor group $|H_{AD}|$. Isied's results showed that there are major differences between α- and polyproline-II helices and extended β-strand-like secondary structure. The electronic coupling will be higher for helical structures compared to the strand-like structure, resulting in a final observation as faster ET in helices.

Similar theoretical results were lately reported by Senthikumar[12]. He used polyglycine unit with a different secondary motifs to calculate electron coupling matrix H_{AB}. The differences in the dihedral angles had immense impact on the charge transfer.

The solution electrochemistry experiments performed on α-aminoisobutyric (Aib)-homo-oligomers linked to a phthalimide or p-cyanobenzamide donors showed a unusual picture of the ET process.[60] Non-natural peptides containing Aib aminoacid are known to form very stable 3_{10}-helices that have very strong intramolecular hydrogen bonding[75].

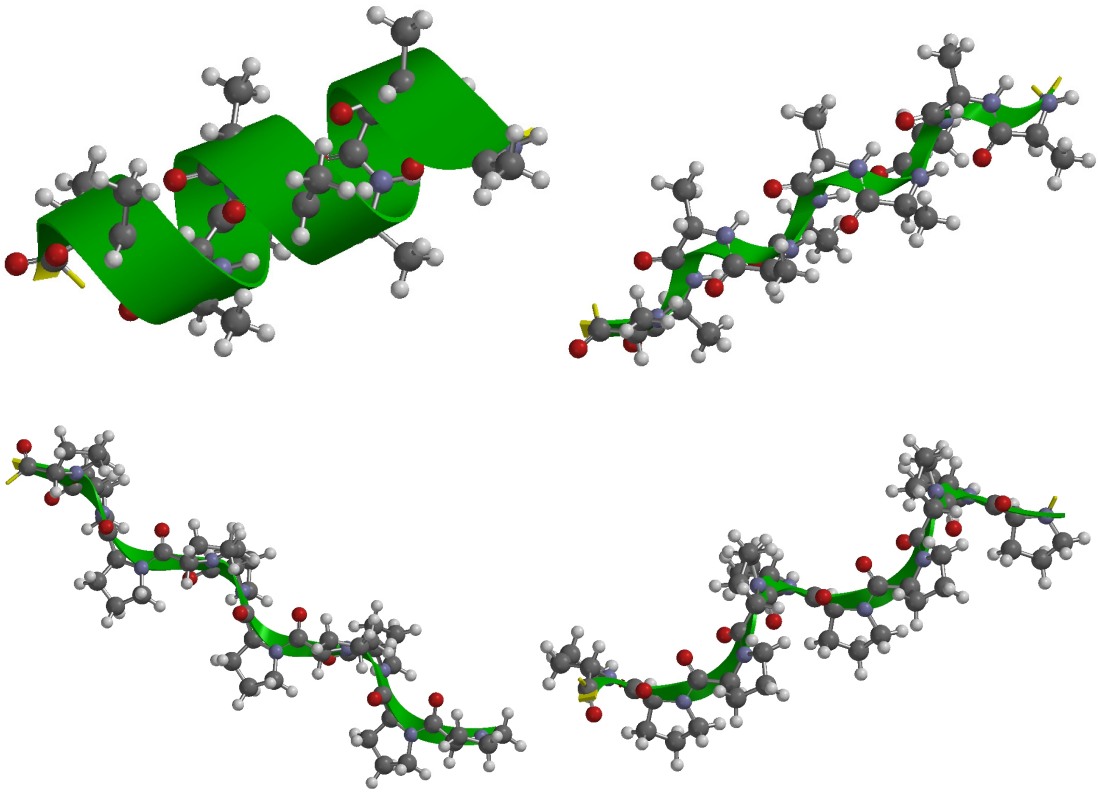

Figure 1.5. Various secondary motifs used in the ET studies: α- helical structure, 3_{10} – helical structure, polyproline I and polyproline II. Each of the structures has different Ψ and Φ angles resulting in diverse H-bonding patterns.

The number of H-bonds increases with the length of the peptide. Maran[60] found that the ET rate exhibits only very weak distance dependence. In some cases, where phthalimide was used as the donor, the ET rate appears to increase with distance. In order to increase the driving force and increase energy gap between donor and acceptor thus favor a hopping mechanism Maran employed p-cyanobenzamide. Interestingly, the distance-ET rate correlation for both systems was much smaller than expected. Maran rationalized the obtained results by invoking a super-exchange mechanism in which the peptide bridge was involved. The evidence, from variable temperature experiments, suggests that a hopping mechanism is not operative in these systems at all. It has to be emphasized that even though both groups have studied helical peptides, Isied's systems are not able to form in inter- or intramolecular bonds while Maran's Aib-systems possess strong intra-molecular hydrogen bonds. The effect of hydrogen bonding and its impact on electron transfer needs to be investigated in more details.

Giese[70] showed that electron transfer through a peptide backbone can be efficient only when peptides with aromatic rings like tyrosine or phenylealanine were employed. It is reported that electron directly hops between neighboring phenol rings with a solvent as a mediator.

Petrov and May[76] have provided a solid theoretical foundation for the description of hopping and super-exchange mechanism. The "hopping" mechanism is also proposed to explain long range electron transfer through the peptide chain. However, this is still disputed.[70, 77]

A systematic investigation of the peptide spacer as a bridging element in electron transfer studies is lacking. In most cases, the research was rather focused on elucidating the distance dependence of ET though peptide chains. Knowledge about the role of a single amino acid may be helpful in rationalizing the electrochemical response and surface behavior of more complex systems.

1.4 Ferrocene-containing Monolayers and Peptide Films

A number of thorough reviews on this subject have been written by Benniston *et al.* [64] and Adams *et al*.[65] Early achievements in this field have been described by Finklea.[20]

A convenient way to study interfacial ET and processes associated with it is to measure kinetics of ET reactions of redox moieties irreversibly attached to the electrode surface as a part of stable, well-organized structure in a form of a self-assembled monolayer (SAM). The purpose is to investigate and characterize the role of the chemical composition and the physical properties of the bridging element in mediating interfacial electron transfer. There are many reasons why monolayers are so attractive from research point of view. Firstly, the redox moiety is located at a well-defined distance from the surface. Secondly, the distance and the composition of the bridge or even the electrode material can be varied. Diffusive and convective contributions to the ET process can be neglected[48]. Consequently such systems are ideal for the study of the fundamental physical factors that control interfacial ET processes. The electronic coupling $|H_{AB}|$ between a redox group and the electrode strongly depends on the chemical nature of the bridge.

ET through alkyl spacers has been extensively studied and such systems were used to create basic theories describing heterogeneous ET processes.[9] In addition, extensive work was done on bridges consisting of conjugated π-electron systems oligophenylacetylenes or oligophenylvinylenes.[44] These studies provided insight into the distance dependence of the interfacial ET through electron pathways created by π-electron systems. Smalley and Dudek[6, 78] employed phenylene rings in the bridge to show that molecular orientation and the rigidity can affect the electronic coupling and as a result be an important parameter controlling ET.

Slow change in the molecular conformation of the neighbouring phenyl groups was mainly responsible for obtained values of the ET process (Figure 1.6)

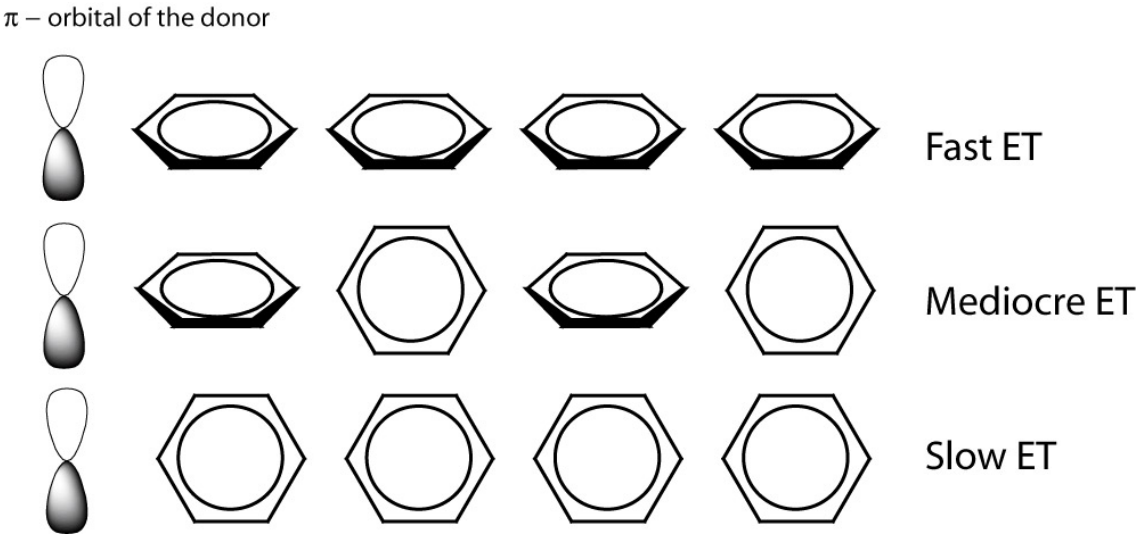

Figure 1.6 The orientation of phenylene elements of the bridge has tremendous effect on the ET rate[78].

The conductivity of oligophenyleneethynylene bridge depends on the slow rotation of the phenylene rings. Incomplete conjugation between connected phenylene rings will significantly affect interfacial ET. It was also suggested by Kauffman *et al.* that solvent dynamics might strongly affect ET rate and is responsible for conformational changes of the molecules in the bridge.[79, 80]

Benniston *et al*.[64] focused on the molecular conformation as one of the major parameters affecting ET. A continuous medium of overlapping orbitals is necessary to provide conjugated pathway for effective electron transfer. Fan *et al*.[81] reported similar observation that electron transfer occurred by conjugated pathway of localized orbitals in phenylene-ethylynen compounds.

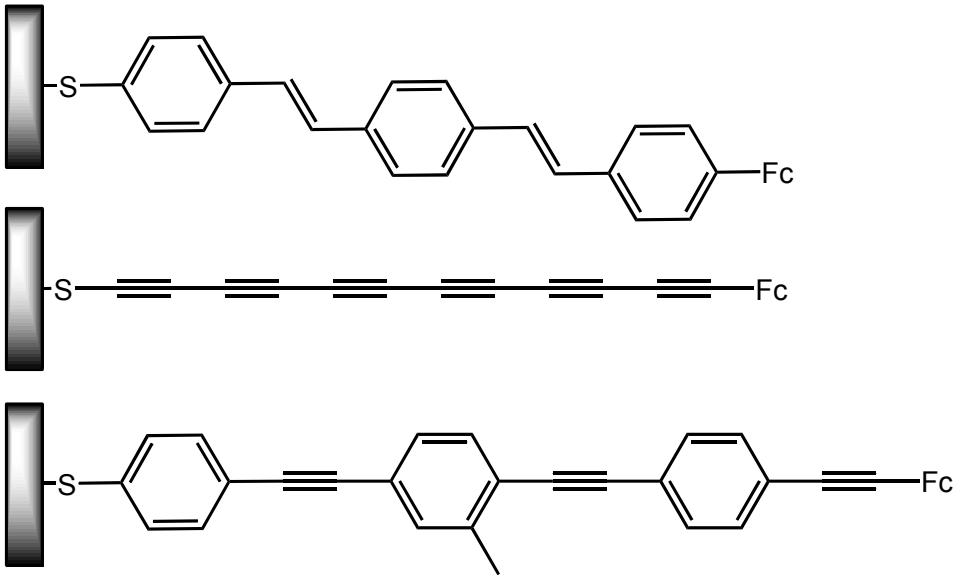

Figure 1.7 π-Electron conjugated systems used in the study by Sikes[82], Smalley[47] and Fan[81]

One of the most important issues is how the electronic coupling and pathway can be modulated by the presence of the covalent bonds and by hydrogen bonding. So far several studies on SAM's have shown that H-bonded systems can have significant contribution to the electronic coupling between Donor and Acceptor.[14-16]

In the literature we can also find very few examples in which redox induced changes in the thickness of the films were reported. Uosaki[83] studied ferrocene-alkenethiols (Fc-CO-$(CH_2)_{11}$-SH) immobilized on the gold surface. By combining electrochemical quartz crystal microbalance (EQCM) and infrared spectroscopy, he was able to observe changes in the orientation of the ferrocene and fluctuations of thickness during redox process caused by facile interaction of Fc^+ with approaching couter-ions. Similar observations were reported by Viana *et al.*[84, 85] for shorter chains (Fc-CO-$(CH_2)_n$-SH, where n = 3 - 10) Fc-alkenethiols. Unfortunately, none of these observations were related to the electron transfer rates and reorganization energies.

Adams *et al.*[65] in his review, focused on describing modern theories describing electron transfer rate. Electron transfer rate is always closely associated with the movement of counter-ions. Overall driving force of the charge transfer in many cases can be limited by kinetics and interactions with counter-ions[86]. Generation of an ion in a place that is isolated from the access of counter-ion (like in a case of the ferrocenium groups buried in alkenethiol) is energetically costly and that cost should be either considered in a form of additional reorganization energy, or treated as completely separate process. ET rate

in the case of buried Fc group is much slower than for the one that is exposed to the access of anions from the solution (Figure 1.8).

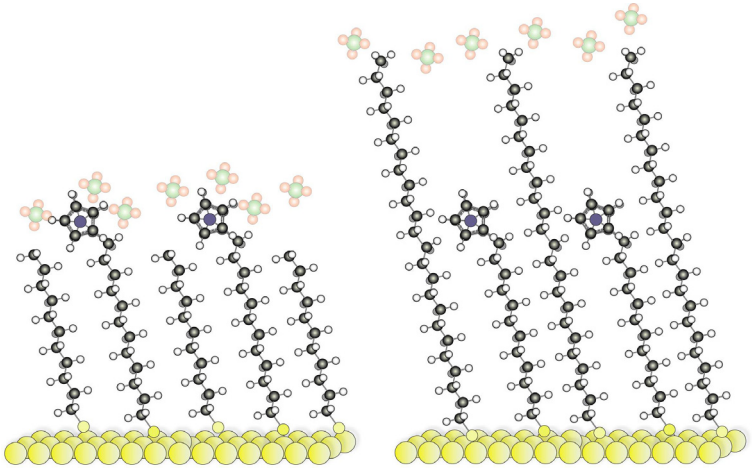

Figure 1.8 (Right) Electron transfer rate for buried ferrocene is two orders of magnitude slower then for the exposed one (left).[79]

The questions, which will allow us to further understand ET in peptides are: can we effectively shield the ferrocene group by placing aminoacids containing larger more hydrophobic groups in close vicinity to the Fc group? What will be the effect of such shielding in a term of electron transfer rate and counter-ion reorganization energy? Can this effect be efficiently evaluated by the measurements of the reorganization energy of the film? Those questions will be tackled further in the main body of the thesis (Chapter 5).

1.5 Ferrocene-peptide Films

Investigations have shown that the ET in peptides can occur across long distances separating the donor from the acceptor.[87] The secondary structure of peptides, as well as

the intramolecular hydrogen bonding network are known to affect the ET process.[69, 87-89] Electrochemical investigations of peptides immobilized on gold surface have become a practical way to study the electron transfer processes and to obtain important parameters like molecular footprint on the surface,[90] resistance,[91, 92] capacitance, activation and reorganization energies.[35] It was demonstrated by Chidsey[48] and others[35] that the solvation energy of the ferrocene significantly contributes to the activation energy and thus is affecting ET rate. The orientation of molecules on the surface and its vast impact on the electron rate was described by Mirkin[93] and Kaifer.[94]

Bilewicz and co-workers studied the effect of increasing glycine and alanine amino acids in Fc-peptide films anchored to the gold electrode. Their STM (scanning-tunneling microscopy) results indicated that polyglycine films were structurally well ordered and extremely well packed (specific area ~30 $Å^2$).[95] Similar surface concentrations were observed for helical polyalanine films.[88] In this contribution, the effect of the dipole on the symmetry of the Tafel plot was addressed. Her results showed a decrease in k_{ET} upon increasing the number of Glycine residues in the peptide. These changes were attributed to potential changes in the secondary structure of oligoglycine chain. However, a change in mechanism from a bridge-assisted superexchange to electron hopping could not be ruled out.

Kimura and coworkers addressed the problem of an electron transfer mechanism by working on very long helical peptides. By incorporating non-natural amino acids containing naphthyl[96] or ferrocene[96-98] residue in the side chain they were trying to find the theory that will explain the nature of long-range electron transfer. An electron transfer mechanism by “hopping” of the electron through the peptide immobilized on

the surface was proposed.[98] Kimura for his α-helical systems suggested that hopping involves amide to amide ET transfer due to partially double bond nature of the amide linker[14] However, this mechanism is highly debatable as the peptides the he used in his studies are lacking amino acids (e.g. Tyr, Trp containing π-electron rich peptides that can work as an electron donor/acceptor groups similarly to guanidine) and do not display any redox activity in a biologically accessible regime. In a recent STM study, Kimura and coworkers[98] observed that long helical peptides are able to change the length depending on the applied potential. The conformation of long helical peptides has changed from 3_{10} to α-helical structure. These observations may suggest that molecular dynamics of the molecules on the surface should be considered in all attempts to estimate ET rate. Vast changes in the thickness of Fc-modified double stranded DNA immobilized on the surface were reported by Demaille.[99, 100] Bending motion of the rigid DNA helix caused by the redox reaction of the ferrocene was responsible for an unusual electrochemical response that was observed.

The electrochemical properties of helical Fc-oligoprolines were investigated in our research group.[36] Oligoprolines are unable to form intra- or inter-strand H-bonding patterns and create inflexible structure. This aspect was used to provide some insight into the complicated mechanism of the ET process, which may imply that molecular dynamics is less pronounced in rigid systems. In this system a linear relationship between distance and electron transfer rate was found. In another publication[38] collagen-like peptides (Pro-Pro-Gly unit) were used to explain the effect of inter-strand and intermolecular H-bonding influence on ET process. Interestingly, the effect of the repulsion between Fc head-groups and resultant changes in film structure were

observed. It can be speculated that at least in the case of the Fc-peptide films that movements of the entire molecule, such as breathing motions of the H-bonding network or rocking motions of the individual Fc-peptide strands, could be responsible for the observed electrochemical effect. It was shown by Jones[74, 101] that the molecular dynamics can contribute significantly to the ET rate. In the Fc-peptide conjugates we can also assume that dynamics is playing an important role in determining the ET rate.

In results presented by Kimura, Bilewicz and from our own work, a significant issue arises. How can one distinguish a purely electrochemical response from an electrochemical signal distorted by the molecular motion of the molecules on the surface? The time scale of the electron movement from the ferrocene to the gold surface through the peptide spacer in most electrochemical experiments is often slower than the time scale of molecular motions, especially when external electric field are applied, forcing charged molecule to align itself within the field gradient. Clearly, the dynamic properties of the molecules have to be taken into account in order to describe the electron transfer process correctly. In addition, one part of the puzzle is a proper description of the reorganization energy of the system and its link to the dynamic properties of the system. It also critical to understand molecular behavior of the films under applied potential, effect of H-bonding, interactions with supporting electrolyte, conformational changes and changes in the orientation of the redox group happening during electron transfer event. Coupled ion/Fc^+ electron transfer mechanism is at question as well. How neighboring molecules can affect ET rate? Can counter-ion have direct effect on the ET mechanism or possibly on the molecular dynamics of the molecules? What is the effect of the rigidity, breathing motion associated with redox

response of the ferrocene/ferrocennium couple and what will be the effect of limited degree of freedom (Figure 1.9)? Can we successfully address those issues with an electrochemical approach?

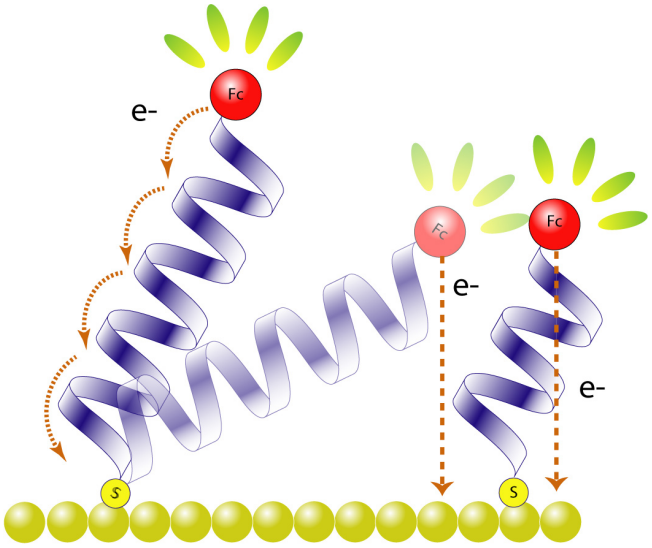

Figure 1.9 Major mechanism of ET occurring in surface bound Fc-peptide conjugates: hopping[37], peptide mobility and tunneling[48].

Another interesting observation was made by Barnett[102] and coworkers who reported that thermal motions of hydrated sodium cations were strongly influencing charge transport along DNA double helix. Similar changes in the ET transport through DNA were reported by Bard in a single molecule STM experiments.[103] Immediately relevant questions can be asked: what will be the effect of different cations on electrochemical response of Fc-peptide conjugates? Can we apply observed changes, if any, to construct aminoacid based cation detector? Can ET rate be effectively tuned by the presence of different metal cations through? The scientific problems presented above will be tackled in Chapter 6.

1.6 Research Objectives

The objective of this work is two-fold:

- To find a suitable method for rapid deposition of compounds containing redox active disulfide conjugates
- To gain a thorough understanding of the electron transfer process in peptide films by investigating the chemical and physical parameters affecting it

Ferrocene-modified peptides were used in this study and the film behavior on the electrified metal surface has been investigated. These studies have been carried out mainly by application of electrochemical techniques, such as cyclic voltammetry (CV), alternating current voltammetry (ACV) and chronoamperometry (CA).

Cyclic voltammetry was my primary technique. From the CV response, I am able to extract direct information about the electron transfer rate. Integration of the current from CV peaks (Figure 1.2) gave the charge Q, which allowed for calculation of the surface concentration Γ of Fc-bioconjugates. The current I(E) and surface concentration Γ(E) at various overpotentials were then related to each other and resulted in easily obtainable electron transfer rate for forward and backward process (oxidation-reduction of Ferrocene group). All calculations were done in an Excel® spreadsheet. Relevant equations are described in detail in Chapter 4.

In Chapters 2 and 3, the development of a new method for the preparation of molecular films on gold by electrodeposition of disulfides from solution is described in detail. The mechanism of electrochemical deposition of disulfide conjugates onto gold is not discussed and requires future investigation.

The electrodeposition method was fine-tuned throughout the chapters of the thesis. First attempts were explained in earlier chapters, where final method is described in details in latter chapter 6.

Supplementary information given in Chapter 2 contains comparison of the Fc-peptide films obtained by electrodeposition and typical incubation method. The material provided in Chapter 2 compares ET rates obtained with chronoamperometry (CA) as method that directly relates decay in the current with electron transfer rate by ET rates obtained by CV.

Equation used to obtain ET rate from chronoamperometric experiments is:

$$I(t) = k\,Q\,\exp(-kt) \qquad (1.7)$$

where Q is a charge I is a current t is time and k is ET rate.

The stability of electrochemically immobilized Fc-peptide films (by multiple CV experiments) is depicted in supplementary information of Chapter 2.

Neutral ferrocene-peptide conjugates and cationic cobalt sarcophagine peptide conjugates were investigated, that allowed the demonstration of the scope of the method. In the course of the study, several interesting discoveries were made, such as

the field-dependent structural changes that occurred in films prepared from cationic sarcophagine peptide conjugates and the differences that exist in the electron transfer rates in ferrocene peptide conjuguates. This led to an in depth discussion, in chapter 4, of a simple method for the evaluation of electron transfer rates by cyclic voltammetric experiments. In the course of the experiments, it was discovered that the forward and backward rates are not symmetrical but appear to be influenced by the nature of the amino acid. In particular, the bulkiness of the amino acid side chain and the penetration of the supporting electrolyte into the peptide film appear to play a role in the electron transfer. Clearly, the effect of the supporting electrolyte required additional study, the details of which are described in Chapter 5. Here, the effect of various anions on the ET rate of ferrocene peptide films is investigated and major questions about molecular dynamics (rigidity), ferrocene shielding by a larger hydrophobic groups, ferrocenium ion-pairing, and their effects on the ET rates and the reorganization energy are tackled. In the penultimate chapter, the effect of cations is investigated in order to provide a complete picture of the environmental effects on the ET rates. In the course of the study, it was discovered that some cations appear to cause significant surface restructuring, an effect that has previously not been observed in peptide films. Finally, Chapter 7 provides a summary of the research achievements within the context of the reported research.

1.7 References

1. Malak, R. A.; Gao, Z.; Wishart, J. F.; Isied, S. S., *J. Am. Chem. Soc.* **2004,** 126, 13888-13889.

2. York, R. L.; Nguyen, P. T.; Slowinski, K., *J. Am. Chem. Soc.* **2003,** 125, 5948-5953.

3. Li, C.-Z.; Long, Y.-T.; Kraatz, H.-B.; Lee, J. S., *J. Phys. Chem. B* **2003,** 107, 2291-2296.

4. Fan, F.-R. F.; Yang, J.; Cai, L.; Price, D. W., Jr.; Dirk, S. M.; Kosynkin, D. V.; Yao, Y.; Rawlett, A. M.; Tour, J. M.; Bard, A. J., *J. Am. Chem. Soc.* **2002,** 124, 5550-5560.

5. Nitzan, A., *Annu. Rev. Phys. Chem.* **2001,** 52, 681-750.

6. Dudek, S. P.; Sikes, H. D.; Chidsey, C. E. D., *J. Am. Chem. Soc.* **2001,** 123, 8033-8038.

7. Morita, T.; Kimura, S.; Kobayashi, S.; Imanishi, Y., *Chem. Lett.* **2000**, 676-677.

8. Creager, S. E.; Wooster, T. T., *Anal. Chem.* **1998,** 70, 4257-4263.

9. Smalley, J. F.; Feldberg, S. W.; Chidsey, C. E. D.; Linford, M. R.; Newton, M. D.; Liu, Y.-P., *J. Phys. Chem.* **1995,** 99, 13141-13149.

10. Chidsey, C. E. D.; Bertozzi, C. R.; Putvinski, T. M.; Mujsce, A. M., *J. Am. Chem. Soc.* **1990,** 112, 4301-4306.

11. Shin, Y.-G. K.; Newton, M. D.; Isied, S. S., *J. Am. Chem. Soc.* **2003,** 125, 3722-3732.

12. Santhanamoorthi, N.; Kolandaivel, P.; Senthilkumar, K., *J. Phys. Chem. A* **2006,** 110, 11551-11556.

13. Santhanamoorthi, N.; Kolandaivel, P.; Senthilkumar, K., *Chem. Phys. Lett.* **2007,** 440, 302-307.

14. Lewis, P. A.; Smith, R. K.; Kelly, K. F.; Bumm, L. A.; Reed, S. M.; Clegg, R. S.; Gunderson, J. D.; Hutchison, J. E.; Weiss, P. S., *J. Phys. Chem. B* **2001,** 105, 10630-10636.

15. Clegg, R. S.; Hutchison, J. E., *Langmuir* **1996,** 12, 5239-5243.

16. Terrill, R. H.; Postlethwaite, T. A.; Chen, C.-h.; Poon, C.-D.; Terzis, A.; Chen, A.; Hutchison, J. E.; Clark, M. R.; Wignall, G.; et al., *J. Am. Chem. Soc.* **1995,** 117, 12537-12548.

17. Clegg, R. S.; Reed, S. M.; Hutchison, J. E., *J. Am. Chem. Soc.* **1998,** 120, 2486-2487.

18. Love, J. C.; Estroff, L. A.; Kriebel, J. K.; Nuzzo, R. G.; Whitesides, G. M., *Chem. Rev. (Washington, DC, U. S.)* **2005,** 105, 1103-1169.

19. Gooding, J. J.; Mearns, F.; Yang, W.; Liu, J., *Electroanalysis* **2003,** 15, 81-96.

20. Meyers, R. A.; Finklea, H. O., *Self-assembled monolayers on electrodes*. John Wiley & Sons Ltd.: 2000.

21. Nuzzo, R. G.; Zegarski, B. R.; Dubois, L. H., *J. Am. Chem. Soc.* **1987,** 109, 733-740.

22. Nuzzo, R. G.; Dubois, L. H.; Allara, D. L., *J. Am. Chem. Soc.* **1990,** 112, 558-569.

23. Badia, A.; Lennox, R. B.; Reven, L., *Acc. Chem. Res.* **2000,** 33, 475-481.

24. Dubois, L. H.; Nuzzo, R. G., *Annu. Rev. Phys. Chem.* **1992,** 43, 437-463.

25. Weisshaar, D. E.; Lamp, B. D.; Porter, M. D., *J. Am. Chem. Soc.* **1992,** 114, 5860-5862.

26. Cavalleri, O.; Kind, H.; Bittner, A. M.; Kern, K., *Langmuir* **1998,** 14, 7292-7297.

27. Finklea, H. O., *Self-assembled monolayers on electrodes*. Meyers, R. A. ed.; John Wiley & Sons Ltd.: 2000.

28. Rohwerder, M.; de Weldige, K.; Vago, E.; Viefhaus, H.; Stratmann, M., *Thin Solid Films* **1995,** 264, 240-245.

29. Ron, H.; Rubinstein, I., *J. Am. Chem. Soc.* **1998,** 120, 13444-13452.

30. Hsueh, C.-C.; Lee, M.-T.; Freund, M. S.; Ferguson, G. S., *Angew. Chem., Int. Ed.* **2000,** 39, 1228-1230.

31. Ma, F.; Lennox, R. B., *Langmuir* **2000,** 16, 6188-6190.

32. Vericat, C.; Vela, M. E.; Gago, J.; Salvarezza, R. C., *Electrochim. Acta* **2004,** 49, 3643-3649.

33. Vericat, C.; Vela, M. E.; Benitez, G. A.; Gago, J. A. M.; Torrelles, X.; Salvarezza, R. C., *J. Phys.: Condens. Matter* **2006,** 18, R867-R900.

34. Forster, R. J.; O'Kelly, J. P., *J. Phys. Chem.* **1996,** 100, 3695-3704.

35. Weber, K. S.; Creager, S. E., *J. Electroanal. Chem.* **1998,** 458, 17-22.

36. Galka, M. M.; Kraatz, H.-B., *ChemPhysChem* **2002,** 3, 356-359.

37. Morita, T.; Kimura, S., *J. Am. Chem. Soc.* **2003,** 125, 8732-8733.

38. Bediako-Amoa, I.; Sutherland, T. C.; Li, C.-Z.; Silerova, R.; Kraatz, H.-B., *J. Phys. Chem. B* **2004,** 108, 704-714.

39. Yang, Y. J.; Khoo, S. B., *Electrochem. Commun.* **2004,** 6, 87-90.

40. Brevnov, D. A.; Finklea, H. O.; Van Ryswyk, H., *J. Electroanal. Chem.* **2001,** 500, 100-107.

41. Lambert, C.; Kriegisch, V.; Terfort, A.; Zeysing, B., *J. Electroanal. Chem.* **2006,** 590, 32-36.

42. Li, J.; Schuler, K.; Creager, S. E., *J. Electrochem. Soc.* **2000,** 147, 4584-4588.

43. Chang, B.-Y.; Hong, S.-Y.; Yoo, J.-S.; Park, S.-M., *J. Phys. Chem. B* **2006,** 110, 19386-19392.

44. Sikes, H. D.; Smalley, J. F.; Dudek, S. P.; Cook, A. R.; Newton, M. D.; Chidsey, C. E.; Feldberg, S. W., *Science (New York)* **2001,** 291, 1519-1523.

45. Isied, S. S.; Ogawa, M. Y.; Wishart, J. F., *Chem. Rev. (Washington, DC, U. S.)* **1992,** 92, 381-394.

46. Isied, S. S., *Prog. Inorg. Chem.* **1984,** 32, 443-517.

47. Smalley, J. F.; Finklea, H. O.; Chidsey, C. E. D.; Linford, M. R.; Creager, S. E.; Ferraris, J. P.; Chalfant, K.; Zawodzinsk, T.; Feldberg, S. W.; Newton, M. D., *J. Am. Chem. Soc.* **2003,** 125, 2004-2013.

48. Chidsey, C. E. D., *Science (Washington, DC, U. S.)* **1991,** 251, 919-922.

49. Laviron, E., *J. Electroanal. and Interf. Chem.* **1979,** 101, 19-28.

50. Bard, A. J.; Faulkner, L. R., *Electrochemical Methods: Fundamentals and Applications*. 2nd ed.; 2001.

51. Marcus, R. A., *J. Chem. Phys.* **1956,** 24, 966-978.

52. Marcus, R. A., *J. Chem. Phys.* **1957,** 26, 872-877.

53. Hush, N. S., *Electrochim. Acta* **1968,** 13, 1005-1023.

54. McConnell, H. M., *J. Chem. Phys.* **1961,** 35, 508-515.

55. Naleway, C. A.; Curtiss, L. A.; Miller, J. R., *J. Phys. Chem.* **1991,** 95, 8434-8437.

56. Redmore, N. P.; Rubtsov, I. V.; Therien, M. J., *J. Am. Chem. Soc.* **2003,** 125, 8769-8778.

57. Meggers, E.; Michel-Beyerle, M. E.; Giese, B., *J. Am. Chem. Soc.* **1998,** 120, 12950-12955.

58. Murphy, C. J.; Arkin, M. R.; Jenkins, Y.; Ghatlia, N. D.; Bossmann, S. H.; Turro, N. J.; Barton, J. K., *Science (Washington, DC, U. S.)* **1993,** 262, 1025-1029.

59. Felts, A. K.; Pollard, W. T.; Friesner, R. A., *J. Phys. Chem.* **1995,** 99, 2929-2940.

60. Antonello, S.; Formaggio, F.; Moretto, A.; Toniolo, C.; Maran, F., *J. Am. Chem. Soc.* **2003,** 125, 2874-2875.

61. Giese, B.; Spichty, M.; Wessely, S., *Pure Appl. Chem.* **2001,** 73, 449-453.

62. Davis, W. B.; Naydenova, I.; Haselsberger, R.; Ogrodnik, A.; Giese, B.; Michel-Beyerle, M. E., *Angew. Chem., Int. Ed.* **2000,** 39, 3649-3652.

63. Kelley, S. O.; Jackson, N. M.; Hill, M. G.; Barton, J. K., *Angew. Chem., Int. Ed.* **1999,** 38, 941-945.

64. Benniston, A. C.; Harriman, A., *Chem. Soc. Rev.* **2006,** 35, 169-179.

65. Adams, D. M.; Brus, L.; Chidsey, C. E. D.; Creager, S.; Creutz, C.; Kagan, C. R.; Kamat, P. V.; Lieberman, M.; Lindsay, S.; Marcus, R. A.; Metzger, R. M.; Michel-Beyerle, M. E.; Miller, J. R.; Newton, M. D.; Rolison, D. R.; Sankey, O.; Schanze, K. S.; Yardley, J.; Zhu, X., *J. Phys. Chem. B* **2003,** 107, 6668-6697.

66. Giese, B., *Bioorg. Med. Chem.* **2006,** 14, 6139-6143.

67. Long, Y.-T.; Abu-Irhayem, E.; Kraatz, H.-B., *Chem.--Eur. J.* **2005,** 11, 5186-5194.

68. Issa, J. B.; Salameh, A. S.; Castner, E. W., Jr.; Wishart, J. F.; Isied, S. S., *J. Phys. Chem. B* **2007**, ACS ASAP.

69. Ogawa, M. Y.; Moreira, I.; Wishart, J. F.; Isied, S. S., *Chem. Phys.* **1993,** 176, 589-600.

70. Giese, B.; Napp, M.; Jacques, O.; Boudebous, H.; Taylor, A. M.; Wirz, J., *Angew. Chem., Int. Ed.* **2005,** 44, 4073-4075.

71. Striplin, D. R.; Reece, S. Y.; McCafferty, D. G.; Wall, C. G.; Friesen, D. A.; Erickson, B. W.; Meyer, T. J., *J. Am. Chem. Soc.* **2004,** 126, 5282-5291.

72. Serron, S. A.; Aldridge, W. S., III; Fleming, C. N.; Danell, R. M.; Baik, M.-H.; Sykora, M.; Dattelbaum, D. M.; Meyer, T. J., *J. Am. Chem. Soc.* **2004,** 126, 14506-14514.

73. Liu, L.; Hong, J.; Ogawa, M. Y., *J. Am. Chem. Soc.* **2004,** 126, 50-51.

74. Jones, G., II; Zhou, X.; Vullev, V. I., *Photochem. Photobiol. Sci.* **2003,** 2, 1080-1087.

75. Toniolo, C.; Bonora, G. M.; Barone, V.; Bavoso, A.; Benedetti, E.; Di Blasio, B.; Grimaldi, P.; Lelj, F.; Pavone, V.; Pedone, C., *Macromolecules* **1985,** 18, 895-902.

76. Petrov, E. G.; Shevchenko, Y. V.; Teslenko, V. I.; May, V., *J. Chem. Phys.* **2001,** 115, 7107-7122.

77. Polo, F.; Antonello, S.; Formaggio, F.; Toniolo, C.; Maran, F., *J. Am. Chem. Soc.* **2005,** 127, 492-493.

78. Smalley, J. F.; Sachs, S. B.; Chidsey, C. E. D.; Dudek, S. P.; Sikes, H. D.; Creager, S. E.; Yu, C. J.; Feldberg, S. W.; Newton, M. D., *J. Am. Chem. Soc.* **2004,** 126, 14620-14630.

79. Saleh, N. i.; Kauffman, J. F., *J. Phys. Chem. A* **2004,** 108, 7139-7146.

80. Kauffman, J. F.; Khajehpour, M.; Saleh, N. i., *J. Phys. Chem. A* **2004,** 108, 3675-3687.

81. Fan, F.-R. F.; Lai, R. Y.; Cornil, J.; Karzazi, Y.; Bredas, J.-L.; Cai, L.; Cheng, L.; Yao, Y.; Price, D. W., Jr.; Dirk, S. M.; Tour, J. M.; Bard, A. J., *J. Am. Chem. Soc.* **2004,** 126, 2568-2573.

82. Sikes, H. D.; Smalley, J. F.; Dudek, S. P.; Cook, A. R.; Newton, M. D.; Chidsey, C. E. D.; Feldberg, S. W., *Science (Washington, DC, U. S.)* **2001,** 291, 1519-1523.

83. Shen, Y.; Haba, T.; Sato, Y.; Shimazu, K.; Uosaki, K., *Phys. Chem. Chem. Phys.* **1999,** 1, 3653-3659.

84. Viana, A. S.; Jones, A. H.; Abrantes, L. M.; Kalaji, M., *J. Electroanal. Chem.* **2001,** 500, 290-298.

85. Viana, A. S.; Abrantes, L. M.; Jin, G.; Floate, S.; Nichols, R. J.; Kalaji, M., *Phys. Chem. Chem. Phys.* **2001,** 3, 3411-3419.

86. Sumner, J. J.; Creager, S. E., *J. Phys. Chem. B* **2001,** 105, 8739-8745.

87. Skourtis, S. S.; Beratan, D. N., *Adv. Chem. Phys.* **1999,** 106, 377-452.

88. Sek, S.; Misicka, A.; Swiatek, K.; Maicka, E., *J. Phys. Chem. B* **2006,** 110, 19671-19677.

89. Kraatz, H.-B.; Bediako-Amoa, I.; Gyepi-Garbrah, S. H.; Sutherland, T. C., *J. Phys. Chem. B* **2004,** 108, 20164-20172.

90. Rowe, G. K.; Creager, S. E., *Langmuir* **1994,** 10, 1186-1192.

91. Creager, S. E.; Rowe, G. K., *J. Electroanal. Chem.* **1997,** 420, 291-299.

92. Weber, K.; Hockett, L.; Creager, S., *J. Phys. Chem. B* **1997,** 101, 8286-8291.

93. Herr, B. R.; Mirkin, C. A., *J. Am. Chem. Soc.* **1994,** 116, 1157-1158.

94. Wang, Y.; Cardona, C. M.; Kaifer, A. E., *J. Am. Chem. Soc.* **1999,** 121, 9756-9757.

95. Sek, S.; Moszynski, R.; Sepiol, A.; Misicka, A.; Bilewicz, R., *J. Electroanal. Chem.* **2003,** 550-551, 359-364.

96. Watanabe, J.; Morita, T.; Kimura, S., *J. Phys. Chem. B* **2005,** 109, 14416-14425.

97. Kitagawa, K.; Morita, T.; Kawasaki, M.; Kimura, S., *J. Polym. Sci., Part A: Polym. Chem.* **2003,** 41, 3493-3500.

98. Kitagawa, K.; Morita, T.; Kimura, S., *J. Phys. Chem.*, ACS ASAP.

99. Wang, K.; Goyer, C.; Anne, A.; Demaille, C., *J. Phys. Chem. B* **2007,** 111, 6051-6058.

100. Anne, A.; Demaille, C., *J. Am. Chem. Soc.* **2006,** 128, 542-557.

101. Jones, G., II; Vullev, V.; Braswell, E. H.; Zhu, D., *J. Am. Chem. Soc.* **2000,** 122, 388-389.

102. Barnett, R. N.; Cleveland, C. L.; Joy, A.; Landman, U.; Schuster, G. B., *Science (New York)* **2001,** 294, 567-571.

103. Liu, B.; Bard, A. J.; Li, C.-Z.; Kraatz, H.-B., *J. Phys. Chem. B* **2005,** 109, 5193-5198.

104. Ulman, A. *Chem. Rev.* **1996,** 96, 1533-1554.

CHAPTER 2
ELECTRODEPOSITION OF FERROCENOYL PEPTIDE DISULFIDES

This chapter is based on the manuscript by G. A. Orlowski, S. Chowdhury, Y.-T. Long, T. C. Sutherland, H.-B. Kraatz. "Electrodeposition of ferrocenoyl peptide disulfides". *Chem. Commun.*, **2005**, 1330-1332.

I am the main contributor in this manuscript. I have performed all electrochemical experiments and calculations. S. Chowdhury provided compounds, the synthesis of which is described elsewhere. Y.-T. Long was responsible for the interpretation of the XPS data. T.C. Sutherland helped in preparation of the first draft of the manuscript. The final version of the manuscript was obtained in an iterative writing process with my supervisor.

2.1 Connecting Text

This chapter outlines the critical first step in my investigations and describes a new method for the electrochemical deposition of ferrocene-peptide disulfides onto gold surfaces. Detailed information about electron transfer rates through a series of Fc-peptide conjugates is presented, together with a discussion of the role of the linker on the ET process. And a thorough comparison between films prepared by

electrodeposition versus the typical incubation method is provided, showing that my method is a useful route for the immobilization of disulfides onto gold surfaces resulting in tightly packed films. This chapter lays the foundation for my work described in the subsequent chapters making use of the film preparation methods described here.

2.2 Introduction and Discussion

Self-assembled monolayers (SAMs) have been extensively studied over the last 20 years.[1-5] It was shown that the formation of alkylthiol SAMs can be aided by electro-deposition of the film on the gold surface,[6] cutting the time from days to minutes for the preparation of a monolayer. Additionally, the packing of a monolayer prepared in this fashion is denser and appears to lack some of the disorder associated with an incomplete monolayer formation. An electro-deposition step for the corresponding disulfides, which are often used to prepare SAMs has not been reported and usually takes several days.[7, 8]

Our aim was twofold: a) to develop an electro-deposition method for disulfides onto gold surfaces, b) to investigate the electrochemical properties of these monolayers. We made use of two classes of Fc-peptides: acylic ferrocenoyl (Fc)-peptide disulfides[9] and cyclic 1,1'-Fc-peptide disulfides,[10] which upon deposition onto a gold surface should give rise to two different structures on the surface, as indicated in Figure 2.1 Acyclic systems will have the Fc group linked to the surface by a single amino acid linker, whereas the cyclic system can link the Fc group to the surface using both amino acid spacers. This would suggest differences in the rigidity of the attached molecule, which in turn may influence the electron transfer (ET) kinetics of the film.

We investigated the electro-deposition of the acyclic [Fc-CSA]$_2$ (**1-a**), [Fc-Gly-CSA]$_2$(**2-a**), [Fc-Ala-CSA]$_2$ (**3-a**), [Fc-Val-CSA]$_2$ (**4-a**) and [Fc-Leu-CSA]$_2$ (**5-a**)[9] and of the corresponding cyclic 1,1'-Fc[CSA]$_2$ (**1-c**), 1,1'-Fc[Gly-CSA]$_2$ (**2-c**), 1,1'-Fc[Ala-

CSA]$_2$ (**3-c**). 1,1'-Fc[Val-CSA]$_2$ (**4-c**) and 1,1'-Fc[Leu-CSA]$_2$ (**5-c**)[10] and the properties of the corresponding films.

The electro-deposition was accomplished by placing a freshly oxidized (electrochemical cycling from 0.2 V to 1.6 V *vs*. Ag/AgCl in 0.5 M H_2SO_4) microelectrode (diameter: 25 μm) into a 10 mM ethanolic Fc-peptide disulfide solution and applying -1.3 V for 30 min. Note the absence of supporting electrolyte. Longer applied potential times were tested, but afforded no change in monolayer coverage and more anodic potentials did not result in monolayer formation. The large negative potential is known to reduce disulfides to thiolate anions,[11] which readies the system for monolayer formation. We compared these results with conventional incubation of the microelectrodes in a 1 mM ethanolic Fc-peptide solution for 5 days at room temperature. The resulting films were assessed electrochemically by cyclic voltammetry (CV), chronoamperometry (CA) and differential pulse voltammetry (DPV) (see ESI). The film thickness for the films was measured by ellipsometry and gave values of 9(3) Å for both electrodeposited and incubated monolayers (excluding **1-a** and **2-a**), which compares well with the calculated value for film thickness of 9(2) Å (n_S = 0.25 and K_S = 3.46 for the substrate, η = 1.40, see ESI).

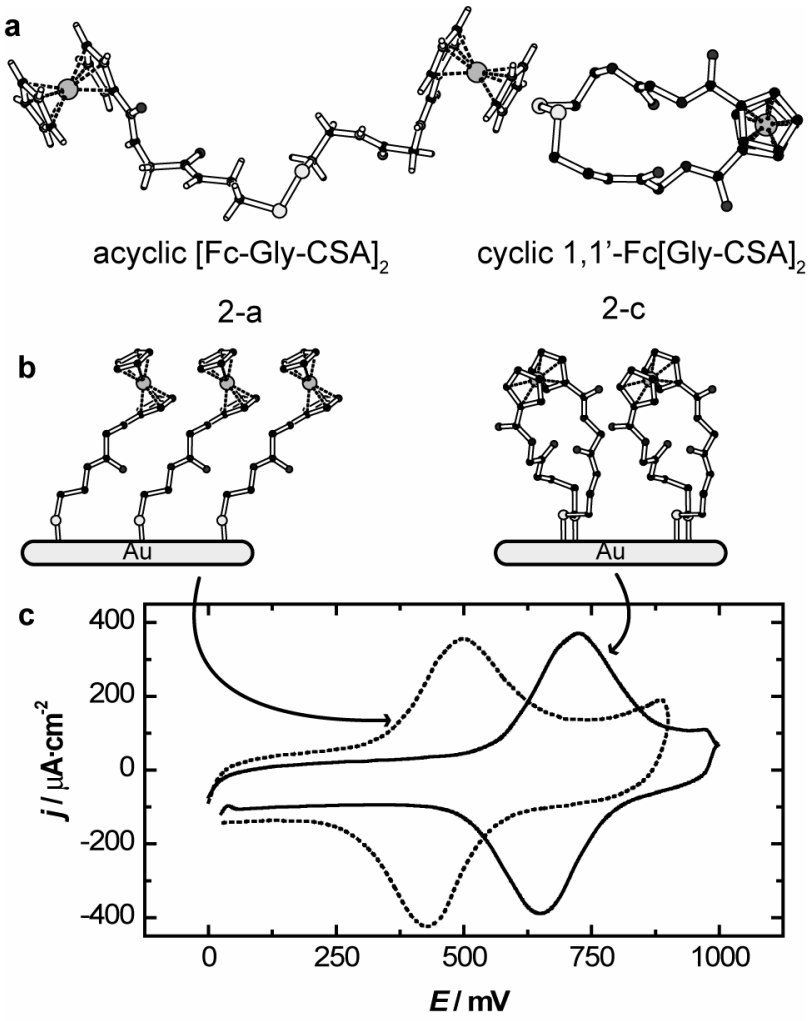

Figure 2.1 a) Crystal structure of acyclic [Fc-Gly-CSA]$_2$ (2-a) and cyclic 1,1'-Fc[Gly-CSA]$_2$ (2-c) b) Schematic representation of the resulting Fc-peptide surfaces. c) Cyclic voltammograms of 2-c (solid line) and 2-a (broken line) films on Au microelectrodes (d = 25 μm). 2.0 M $NaClO_4$ supporting electrolyte, scan rate 1000 Vs^{-1}, Pt mesh auxiliary and Ag/AgCl (3.5 M KCl) reference electrode.

The surfaces were also characterized by X-ray photonspectroscopy (XPS) showing identical signals for both the electrodeposited and incubated film (see supplementary data 2.4). CV was carried out on a custom-built potentiostat and CA was carried out using CHInstruments potentiostat model 660B. All electrochemical measurements were carried out in water using at least 5 different Fc-peptide modified gold microelectrodes

to ensure reproducibility (2 M $NaClO_4$ supporting electrolyte, reference electrode: Ag/AgCl/3.5 M KCl, Pt mesh auxiliary electrode).

The electron withdrawing capability of the amides makes the disubstituted Fc more difficult to oxidize. All electrochemical parameters are included in Table 2.1. Integration of the Faradaic current provides the Fc surface concentration,[12] from which a specific area per molecule can be calculated. The theoretical area (calculated from crystal structure data)[9, 10] of the acylic Fc-peptides and 1,1'-cyclo-Fc-peptides are ~30 and ~40 $Å^2 \cdot molecule^{-1}$, respectively.

Electro-deposited films of Fc-peptides, gave consistently higher surface concentration compared to films obtained by conventional incubation, suggesting that electro-deposition gives a tighter packed film. It is noteworthy that the difference in the molecular footprint obtained for 1,1'-Fc-peptide films prepared by electro-deposition and standard incubation are large. For acyclic Fc-peptides this difference is still significant. The electro-deposition of the 1,1'-cyclo-Fc-peptides results in a 2 to 3 times greater surface coverage than the incubation method. It appears that packing is significantly less tight if the films are prepared by incubation.

Table 2.1 Summary of electrochemical parameters analyzed by CV and CA. Value in parentheses is the standard deviations from 5 electrode measurements.

	Electrodeposition from EtOH			
Compound	$E^{0'}$ / mV	$k_{ET} \times 10^3$ / s^{-1}	Specific Area / $Å^2 \cdot molecule^{-1}$	Surf. Conc. $\times 10^{-10}$ / $mol \cdot cm^{-2}$
1-c	670(7)	9.5	45(7)	3.7
1-a	465(9)	8.0	40(7)	4.2
2-c	688(6)	14.0	47(8)	3.5
2-a	464(6)	13.5	50(8)	3.3
3-c	635(6)	12.0	68(9)	2.4
3-a	490(7)	6.0	36(5)	4.6
4-c	670(7)	12.0	60(9)	2.8
4-a	488(7)	9.5	65(8)	2.6
5-c	686(8)	17.0	60(8)	2.8
5-a	484(7)	11.0	72(8)	2.3

* Error for k_{ET} calculations was 1.5 x 10^3 s^{-1}

The full-width-at-half-maximum, E_{fwhm} (see ESI), is a useful parameter that assesses the homogeneity of the Fc environment. The redox signal for all Fc-peptide films prepared in this study exhibit widths that exceeds the ideal, E_{fwhm} of 90 mV,[13] indicating the presence of some lateral interactions between the molecules in these films. H-bonding presumably plays an important role as was shown before in films of the acyclic Fc-peptides.[13-18] Interestingly, there is little difference between the films formed from cyclic and acylic Fc-peptides. However, Fc-peptide films formed by electro-deposition have a lower E_{fwhm} values (160(10) mV versus 210(20) mV). This difference points to a more uniform film if electro-deposition is used.

The ET kinetics of all films were assessed by CV and CA and are summarized in Table 2.1 and 2.S3 (see ESI). The methods were described before.[18] There are two key results of our kinetic study: a) the k_{ET} for films prepared by electro-deposition or by incubation are the same; b) the k_{ET}s for Fc-peptide films of cyclic Fc-peptides are higher compared to the corresponding acyclic systems. A probable explanation for the faster ET kinetics for the cyclic systems is their inherent ability to establish two Au-S linkages, allowing ET to proceed along both peptide spacers. It is also interesting to note that the most amino acid systems exhibit faster k_{ET} compared to compounds **1-a** and **1-c** having only a cystamine spacer. The amino acid chain may allow for better packing on the surface due to intermolecular H-bonding interactions thereby increasing the rigidity of the linker. Confirmation that both sulfur atoms of the cyclo systems are bound to the gold comes form reductive desorption experiments. As stated above Fc is a one-electron redox probe and sulfur is known to undergo a one electron reductive desorption at sufficiently negative potentials. Thus, DPV experiments were carried out in H_2SO_4 for the Fc and KOH for the Au-S reduction due to the instability of Fc at high pH values.

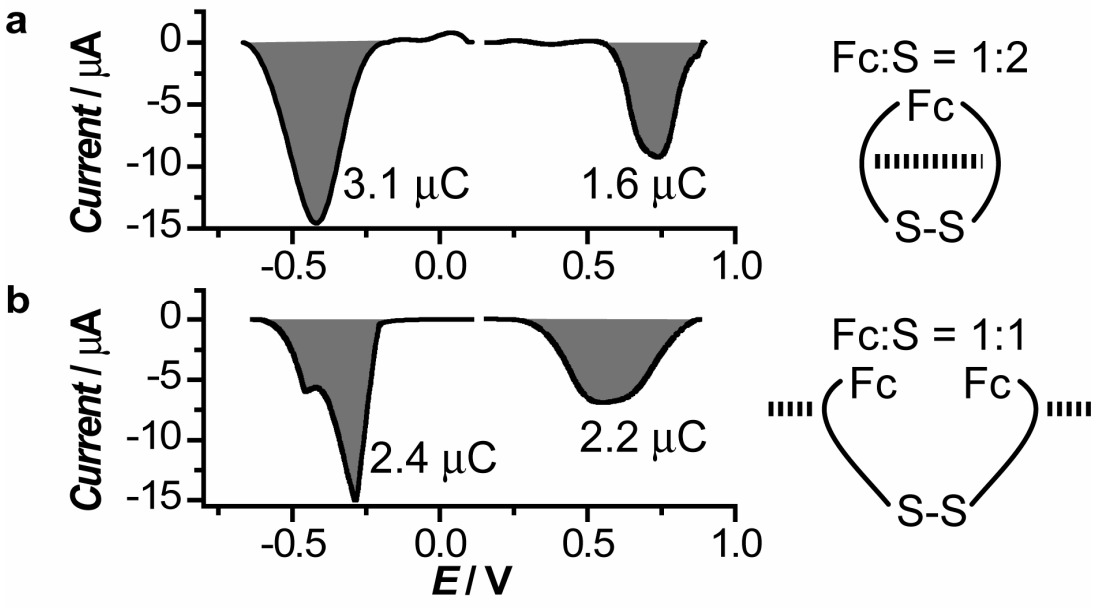

Figure 2.2 DPVs of a) cyclo and b) acyclic, FcGly derivatives. Integrated peak currents for cyclo- and acyclic-derivatives are in a 1:2 and 1:1 ratio, respectively, indicating both sulfur atoms of the cyclo derivatives are bound to the Au surface. The hatched lines in the models represent H-bonding patterns found in the crystal structure.

The integration of the Fc and sulfur reduction for both the acyclic and cyclo FcGly derivatives **2-a** and **2-c** are shown in Figure 2.2. The ratio of the integrated area between the Fc and sulfur reduction peaks shows that the cyclo system has a 1:2 (Fc:S) ratio and the acyclic derivative has a 1:1 (Fc:S) ratio which, is evidence that both sulfur atoms of the cyclo derivatives were bound to the Au surface. The shoulder in Fig. 2b, at *ca.* -0.45 V, is attributed to the decomposition of Fc at high pH. Additionally, crystal structure data supports this claim because the cyclo derivatives participate in intramolecular H-bonding and the acyclic derivatives exhibit intermolecular H-bonding.

In summary, we have presented an electrochemical method to form Fc-peptide monolayers from Fc-peptide disulfides, giving raise to well-packed monolayers on gold. This method should find wide-spread applications for the formation of monolayers from

disulfides. Our studies allowed a direct comparison of the ET kinetics of cyclic and acyclic Fc-peptide disulfide systems. Our results show faster ET kinetics for the cyclic systems compared to the acyclic systems, which may be result of the enhanced rigidity of the molecules on the surface. We are now investigating this phenomenon in more detail and hope to compare our results to the growing number of ET studies on other Fc-peptide systems[18-21] in order to get additional mechanistic insight.

Funding from NSERCC is acknowledged. HBK is the Canada Research Chair in Biomaterials.

2.3 Notes and References

1. M. W. J. Beulen, M. I. Kastenberg, F. van Veggel, and D. N. Reinhoudt, *Langmuir*, **1998**, 14, 7463-7467.
2. M. T. Lee, C. C. Hsueh, M. S. Freund, and G. S. Ferguson, *Langmuir*, **2003**, 19, 5246-5253.
3. M. D. Porter, T. B. Bright, D. L. Allara, and C. E. D. Chidsey, *J. Am. Chem. Soc.*, **1987**, 109, 3559-3568.
4. B. Rai, P. Sathish, C. P. Malhotra, Pradip, and K. G. Ayappa, *Langmuir*, **2004**, 20, 3138-3144.
5. L. H. Dubois, B. R. Zegarski, and R. G. Nuzzo, *Langmuir*, 1986, **2**, 412-417.
6. L. Cheng, J. P. Yang, Y. X. Yao, D. W. Price, S. M. Dirk, and J. M. Tour, *Langmuir*, **2004**, 20, 1335-1341.
7. D. J. Campbell, B. R. Herr, J. C. Hulteen, R. P. VanDuyne, and C. A. Mirkin, *J. Am. Chem. Soc.*, **1996**, 118, 10211-10219.
8. C. Naud, P. Calas, and A. Commeyras, *Langmuir*, **2001**, 17, 4851-4857.
9. I. Bediako-Amoa, R. Silerova, and H. B. Kraatz, *Chem. Commun.*, **2002**, 2430-2431.
10. S. Chowdhury, G. Schatte, and H. B. Kraatz, *J. Chem. Soc., Dalton Trans.*, **2004**, 1726-1730.
11. H. Ron and I. Rubinstein, *J. Am. Chem. Soc.*, **1998**, 120, 13444-13452.
12. S. W. Han, H. Seo, Y. K. Chung, and K. Kim, *Langmuir*, **2000**, 16, 9493-9500.
13. K. Seo, I. C. Jeon, and D. J. Yoo, *Langmuir*, **2004**, 20, 4147-4154.
14. T. Moriuchi, K. Yoshida, and T. Hirao, *Organometallics*, **2001**, 20, 3101-3105.
15. P. Saweczko, G. D. Enright, and H. B. Kraatz, *Inorg. Chem.*, **2001**, 40, 4409-4419.
16. T. Moriuchi, A. Nomoto, K. Yoshida, A. Ogawa, and T. Hirao, *J. Am. Chem. Soc.*, **2001**, 123, 68-75.
17. T. Moriuchi, A. Nomoto, K. Yoshida, and T. Hirao, *Organometallics*, **2001**, 20, 1008-1013.

18. I. Bediako-Amoa, T. C. Sutherland, C. Z. Li, R. Silerova, and H. B. Kraatz, *J. Phys. Chem. B*, **2004**, 108, 704-714.

19. T. Morita, S. Kimura, *J. Am. Chem. Soc*., **2003**, 125, 8732-8733.

20. a) S. Sek, R. Moszynski, A. Sepiol, A. Misicka, R. Bilewicz, *J. Electroanal. Chem.* **2003**, *550-551*, 359-364; b) S. Sek, A. Sepiol, A. Tolak, A. Misicka, R. Bilewicz, *J. Phys. Chem. B* **2004**, *108,* 8102-8105.

21. M.M. Galka, H.-B. Kraatz, *ChemPhysChem* **2002**, 3, 356-359

2.4 Supplementary Data

Table 2S.1 Electrochemical parameters calculated from CV experiments using the electrochemical deposition and incubation methods.

	Incubation			**Electrodeposition**		
	ΔE_p / **mV**	E_{fwhm} / **mV**	I_a/I_c	ΔE_p / **mV**	E_{fwhm} / **mV**	I_a/I_c
1-c	90(8)	200(15)	1.00(9)	90(9)	190(10)	0.92(5)
1-a	120(6)	240(15)	1.00(9)	120 (10)	220(10)	1.00(5)
2-c	60(8)	180(10)	0.90(9)	60(7)	170(8)	1.00(5)
2-a	65(5)	195(10)	1.00(9)	140(10)	175(8)	0.92(5)
3-c	85(7)	190(15)	0.90(9)	55(7)	160(8)	0.94(5)
3-a	90(5)	200(15)	1.00(9)	111(10)	190(10)	0.90(5)
4-c	80(7)	210(8)	0.90(5)	55(7)	170(8)	0.98(5)
4-a	85(5)	230(15)	0.90(5)	120(10)	190(10)	1.00(5)
5-c	70(5)	200(10)	0.90(5)	62(7)	157(10)	0.90(3)
5-a	95(7)	210(10)	0.90(5)	110(10)	190(10)	0.90(3)

Table 2S.2 Electrochemical parameters calculated from CV for the incubation method. This is complementary data to Table 2.1 of the paper.

	$E^{0'}$ / mV	$k_{ET} \times 10^3$ / s^{-1}	***Specific Area /*** $Å^2 \cdot molecule^{-1}$
1-c	660(9)	8.0	120(9)
1-a	473(6)	7.0	50(3)
2-c	682(8)	13.0	150(20)
2-a	445(9)	12.0	78(8)
3-c	624(8)	11.0	141(20)
3-a	468(8)	6.9	53(9)
4-c	665(9)	11.0	130(25)
4-a	484(7)	10.0	70(10)
5-c	680(7)	14.0	220(10)
5-a	476(9)	11.0	101(9)

* Error for k_{ET} calculation was 2 x 10^3 s^{-1}

Background (non-Faradaic current) correction for all CVs was made in custom written software by fitting a polynomial curve. Pinholes in the film were analyzed by taking the difference between the gold oxide reduction peak in sulfuric acid CVs of a bare Au electrode and a Fc-peptide film protected electrode. Only 5-7% of the surface was oxidized to gold oxide if the film was prepared by electro-deposition compared to 15-20% of Au was oxidized to gold oxide in films prepared by the incubation method. The electron transfer kinetics was evaluated according to methods described in reference 18.

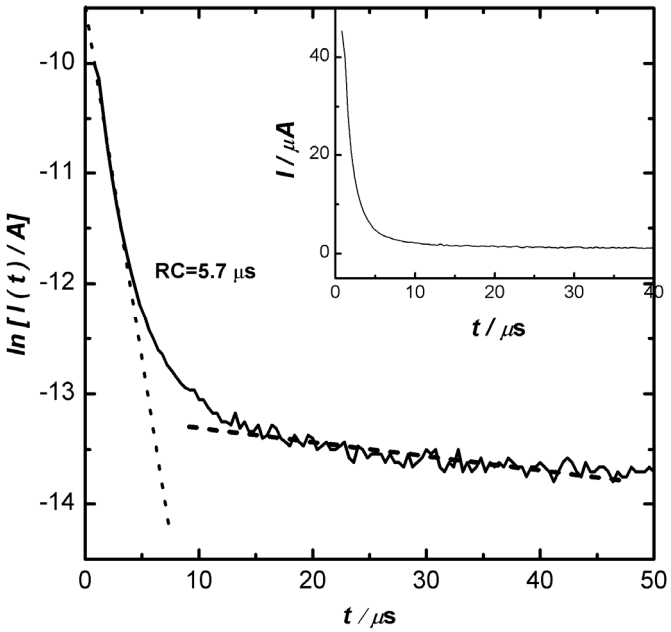

Figure 2S.1 A representative semilog chronoamperometric response from a 400 mV potential jump on an electrodeposited cyclic 1,1'-Fc[GlyCSA]$_2$. 12.5 μm radius Au electrode, 2M $NaClO_4$ supporting electrolyte and a Ag/AgCl/(3.5 M KCl) reference electrode. The RC of 5.7 μs (dotted line) is the time constant of the double layer charging and the linear region (dashed line) is the electron transfer rate at 400 mV overpotential. The inset shows the untransformed data.

k_{et} values that comes from CA are similar to those obtained from CV.

Table 2S.3 Chronoamperometric results from monolayers that were electrodeposited.

Compound	*CA electrodeposition* $k_{ET} \times 10^3$ / s^{-1}
1-c	**7.5**
1-a	**7.0**
2-c	**11.0**
2-a	**12.0**
3-c	**11.0**
3-a	**8.0**
4-c	**10.0**
4-a	**8.0**
5-c	**16.0)**
5-a	**10.5**

Error for k_{ET} calculation was 1.5 x 10^3

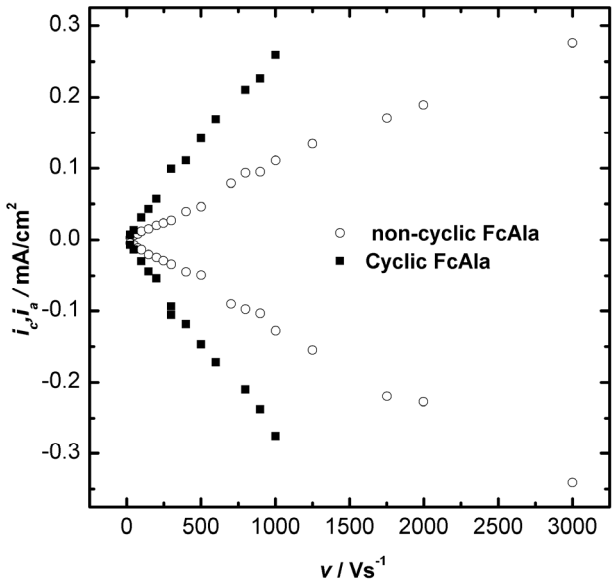

Figure 2S.2 Linear response of anodic and cathodic peak currents for 3-c and 3-a derivatives, indicating successful surface immobilization.

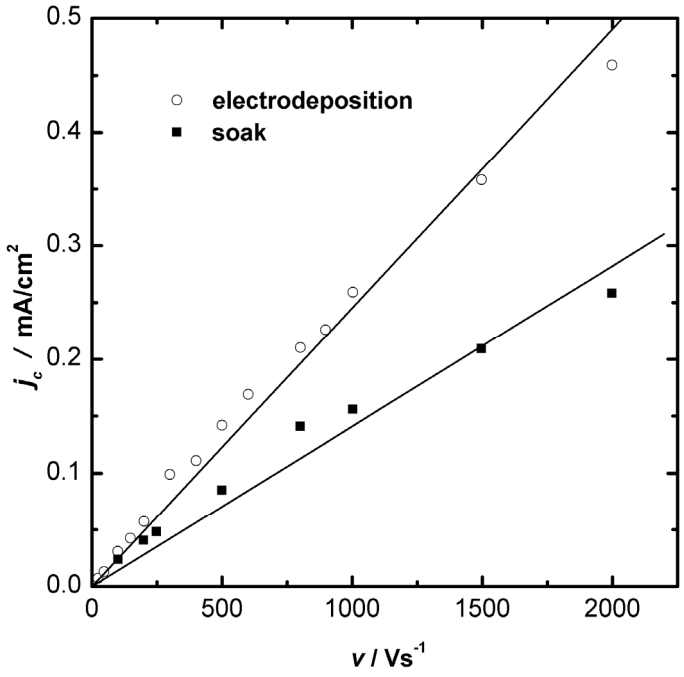

Figure 2S.3 Linear response of anodic peak currents for 3-c using both the incubation and electrodeposition methods, indicating successful surface immobilization.

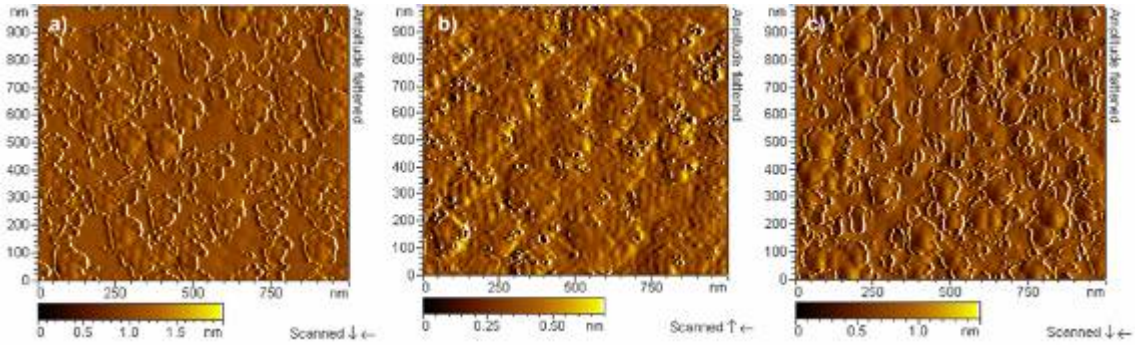

Figure 2S.4 a) AFM image of Au on Si(100); b) AFM image of Au on Si(100) after 400 cycles (0 V to 1.4 V vs. Ag/AgCl (3.5 M KCl)) in 0.5 M H_2SO_4; c) AFM image of Au on Si(100) after electrodeposition of cyclo-1,1'-Fc[AlaCSA]$_2$

Thickness of the monolayers were measured by ellipsometry and gave values 9(3) Å which is in good agreement with data obtained from x-ray crystallography[10] and molecular simulation in Spartan software.

Table 2S.4 Root-Mean-Square (RMS) roughness of 3 AFM images of Figure 2S.4

	RMS (nm)	
	Left Scan Direction	**Right Scan Direction**
Au on Si(100)	2.139	2.058
Au on Si(100) after 400 cleaning cycles	1.196	1.240
cyclo-1,1'-Fc[AlaCSA]$_2$.	1.692	1.678

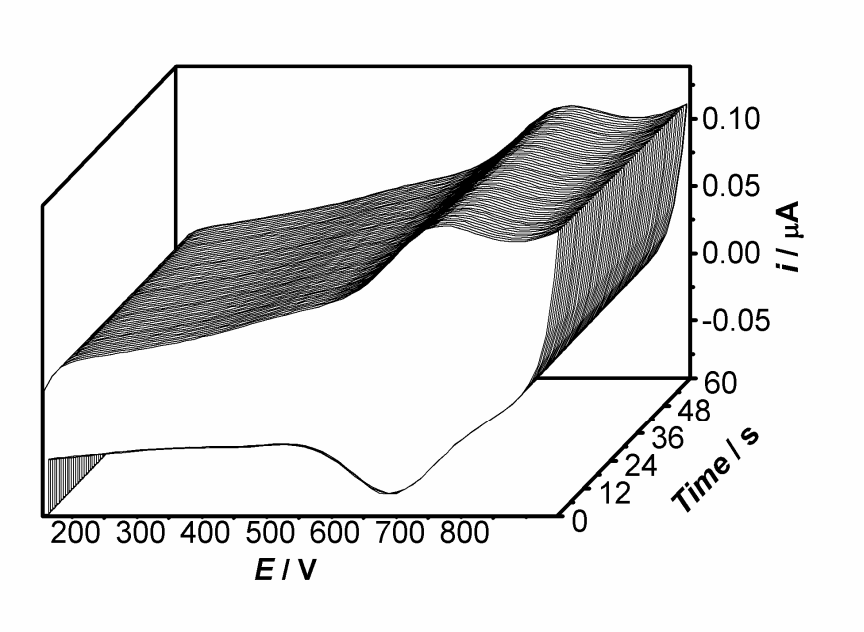

Figure 2S.5 Multiple CVs of cyclo-1,1'-Fc[AlaCSA]$_2$ (3-c) taken every 0.05 seconds for 60 seconds with a 12.5 μm radius Au-modified electrode, 2 M $NaClO_4$ supporting electrolyte and a Ag/AgCl/(3.5 M KCl) reference electrode.

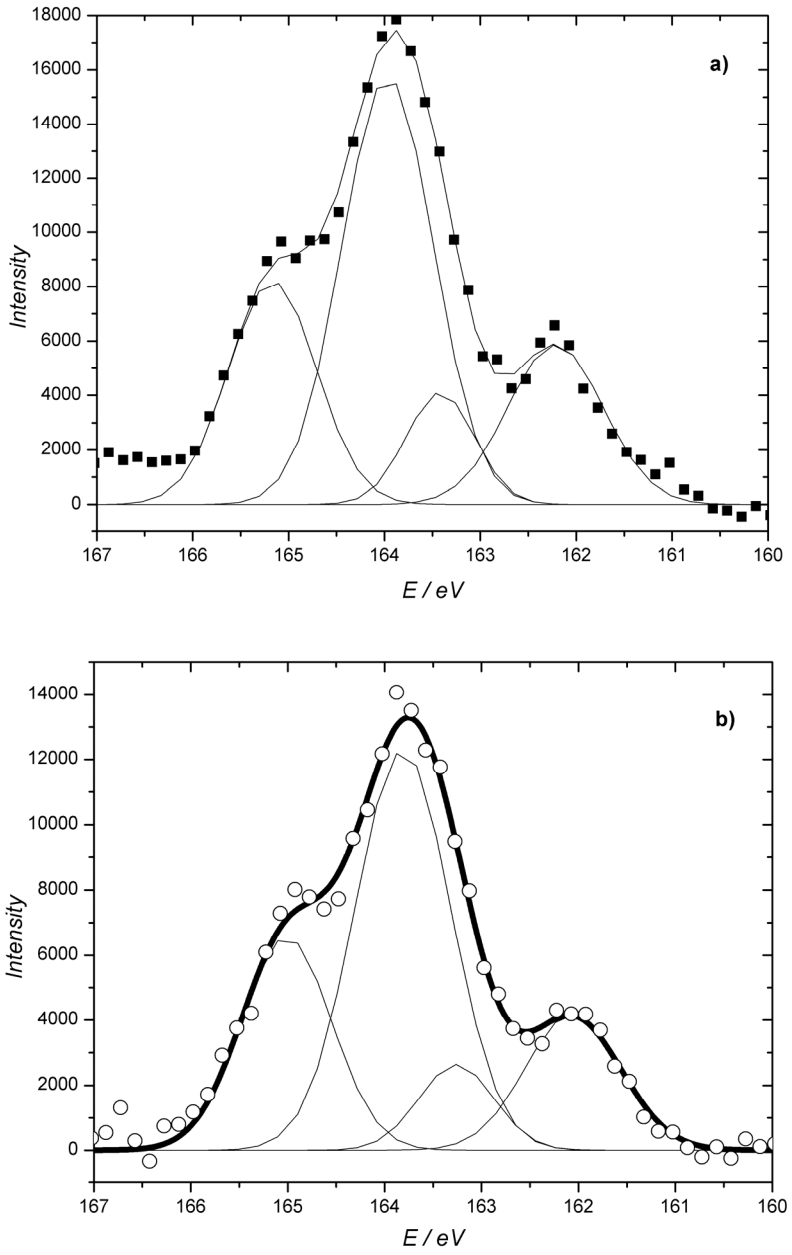

Figure 2S.6 XPS results for sulfur sp2 for a) electrodeposited, b) incubated compound 1-c. Sulfur population in both cases is virtually identical. The similar results were obtained for other cyclic compounds.

Ellipsometry. Au on Si(100) (Platypus Technologies, Inc) wafers were incubated in a 1 mM Fc-peptide ethanolic solution for 5 days and finally rinsed with EtOH and H_2O. A Stokes ellipsometer LSE (Gaertner Scientific Corporation, Skokie, IL, fixed angle (70°), fixed wavelength (632.8 nm)) was used, and the data were collected and analyzed using LGEMP (Gaertner Ellipsometer Measurement Software) on a PC. Ellipsometry constants were as follows: n_S = 0.25 and K_S = 3.46 for the substrate and 1.40 was used as the refractive index of the monolayer.

CHAPTER 3
CAGES ON SURFACES: THIOL FUNCTIONALISATION OF Co(III) SARCOPHAGINE COMPLEXES

This chapter is based on the manuscript by J. M. Harrowfield, G. A. Koutsantonis, H-B. Kraatz, G. L. Nealon, G. A. Orlowski, B. W. Skelton, and A. H. White, *Eur. J. Inorg. Chem.* **2007**, 263–278.

This is the direct result of a collaborative study between the groups of G.A. Koutsantonis (U Western Australia), J.M. Harrowfield (U Strassbourg) and H.-B. Kraatz (U Saskatchewan). I and G. L. Nealon were the main contributors to this manuscript. G.L. Nealon spent two months at the U Saskatchewan (10/05-11/05). During this time, I performed all electrochemical experiments and calculations. The electrochemical part of this manuscript was also written by me. The compounds used in this study were synthesized by G.L. Nealon at U Western Australia. Although, their syntheses and characterizations are an integral part of the manuscript, they do not form part of my work and thus are not included in this chapter. Thus, I am providing a verbatim copy of the portion of the manuscript to which I made major contributions. B.W. Skelton and A.H. White were responsible for the crystal structure analysis. The final version of the manuscript was obtained in an iterative writing process with all three supervisors: J. M. Harrowfield, G. A Koutsantonis, and H-B. Kraatz.

3.1 Connecting Text

Next in my investigations, it was important to elucidate the generality of the electrodeposition method for disulfides described in Chapter 2. Thus, it was decided to embark on a collaborative project, working with cationic sarcophagine-peptide disulfide conjugates. In this chapter, I describe the successful attempts of a potential-assisted surface immobilization of a series of cobalt sacrophagines, which exhibit a redox activity at very high potential. In addition, an example of the dynamic properties of these bioconjugates is described, which will be of relevance in later chapters. Thus, the electrodeposition method, developed initially for Fc-peptide disulfide comjugates, was successfully implemented for cationic peptide conjugates. employed.

3.2 Introduction

Reagent immobilization on surfaces is a sophisticated pathway to materials with a wide range of applications,[1, 2] heterogeneous catalysis being one obvious application, such applications depending on the functionality introduced with the bound reagent, as well as upon the ease and convenience of the immobilization procedure and the stability of the final product. Given the remarkable stability and varied electronic, magnetic and redox properties of metal complexes of the macrobicyclic polyamines known as "sarcophagines" (Figure 3.1),[3] these are species of particular appeal as entities for attachment to surfaces and for various related applications.[4] Reduction potentials for readily accessible species span a range of 2 V,[5] subject to modification in an interfacial environment,[6] and outer-sphere redox processes involving Co complexes, are, for example, known to be rapid steps in reactions leading to photoinduced hydrogen production[7-10] and the reduction of oxygen to hydrogen peroxide.[11] Of practical importance in relation to immobilization of such complexes is the facile synthesis of the ligand in forms with reactive "external" functional groups R (Figure 3.1).[12]

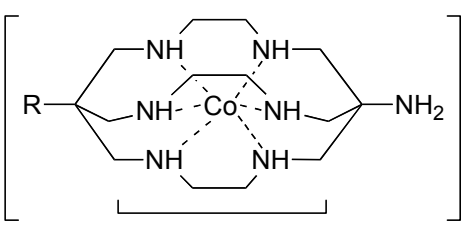

$= [Co(R)(NH_2)sar]^{3+}$ $(R = CH_3, NH_2)$

Cage = sarcophagine = "sar"= 3,6,10,13,16,19-hexa-azabicyclo[6.6.6]icosane

Figure 3.1 Trivial nomenclature used throughout this work

Limited earlier work on surface-bound cage complexes has involved modification of electrodes by impregnation of thin Nafion films on graphite with simple cage complexes,[5] electropolymerisation of a thiophenylmethylamino-cage complex on Pt,[12] and carbodiimide coupling of carboxyl groups on partially oxidized graphite to a diamino-cage complex.[13] Amphiphilic cages[14, 15] have also proved to have interesting biological properties, probably associated with their ability to be bound within membranes.[15] As a simple approach to the immobilization of cage complexes on surfaces, we are currently exploring the use of the well-established surface chemistry of disulfides[1] to form monolayers of cobalt sarcophagine complexes on gold. This is based on the introduction of peptide substituents associated with cystamine units onto the cage, a facile synthesis when starting from readily synthesized glycylated derivatives.[16] The use of peptide based tethering groups is advantageous as the length of the spacer between the surface and the cage moiety can be increased incrementally with relative ease, using common peptide synthetic techniques,[17] and tightly packed monolayers can be formed, presumably aided by extensive hydrogen bonding networks between the amide groups.[18] A similar approach has been applied to the synthesis of ferrocene-decorated peptides as probes for elucidation of the mechanism(s) of electron transfer in proteins.[19]

Our immediate aim in the present work was to synthesize a series of disulfides bearing peptido-cage complex substituents, evaluate their solution electrochemical characteristics. and determine a suitable method for their immobilization onto gold electrodes. Since only a single disulfide substituent is required for surface tethering, our

focus has been on obtaining derivatives of the monosubstituted cage complex $[Co(CH_3)(NH_2)sar]^{3+}$, though the more complicated syntheses of monofunctionalised derivatives of $[Co(NH_2)_2sar]^{3+}$ have also been investigated. These Co(III) complexes exist in stable enantiomeric forms and thus the formation of diastereomeric forms of their oligopeptide derivatives was anticipated, though prior work suggested that differences between such diastereomers should be small.[12]

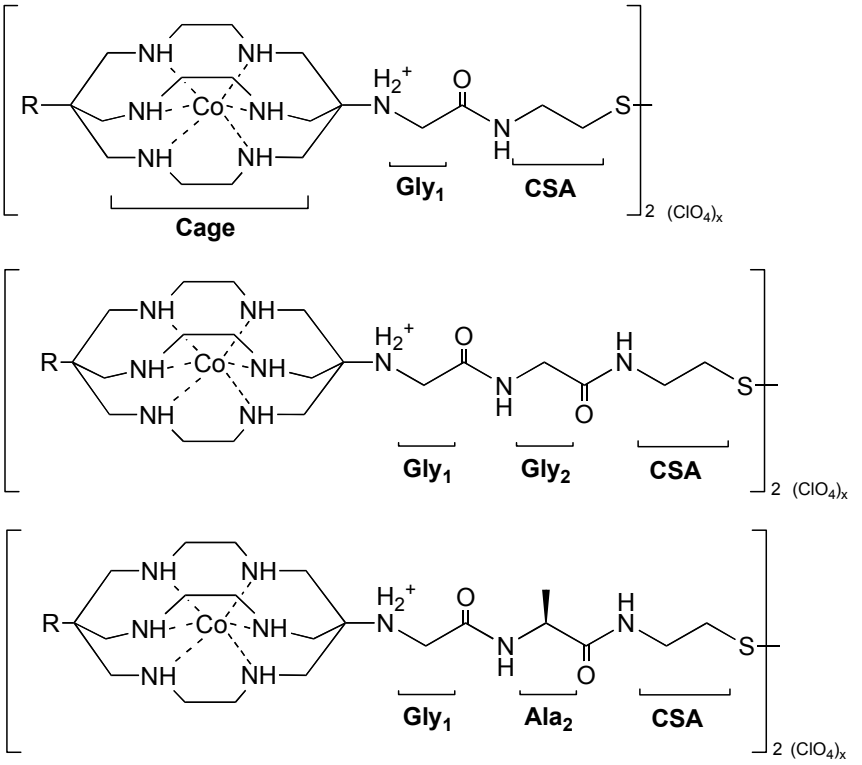

Chart 3.1 General structures of the compounds prepared showing trivial nomenclature used.

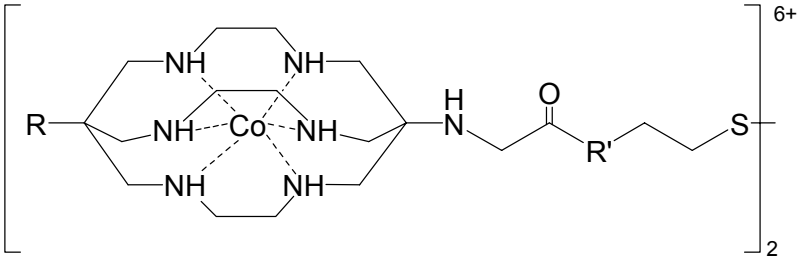

Table 3.1 List of synthesized compounds.

Compound #	R	Cage	R’
2	$-CH_3$	racemic	-Gly-OH
3	$-CH_3$	racemic	$-N(CH_2CO_2H)_2$
4	$-CH_3$	racemic	-Gly-CSA-
5	$-CH_3$	racemic	-Gly-Gly-CSA-
6	$-CH_3$	racemic	-Gly-Ala-CSA-
7	$-NH_2$	racemic	-Gly-CSA-
8	$-NH_2$	Λ-enantiomer	-Gly-CSA-
9	$-NH_2$	Λ -enantiomer	-Gly-Gly-CSA-
10	$-NH_2$	Λ -enantiomer	-Gly-Ala-CSA-

3.3 Electrodeposition

All electrodeposition experiments were performed using a three electrode cell system consisting of Au (25 μm diameter) as working electrode, Pt wire as counter electrode and Ag wire as the reference electrode. Electrodeposition was accomplished by placing

a freshly oxidised microelectrode (electrochemical cycling from –0.4 to +1.2 V *vs*. Pt wire in 0.5 M H_2SO_4) into a 1 mM solution of the analyte in 0.1 M $NaClO_{4(aq)}$ and applying –1.5 V for 30 min. After this period, the electrode was washed with water, then suspended in a vigorously stirred beaker of water for 10 mins, and then 2 M $NaClO_{4(aq)}$ for 30 seconds. All electrochemical measurements were performed using a custom-built potentiostat in 2 M $NaClO_{4(aq)}$ using a three electrode cell system consisting of Au (25 μm diameter) as working electrode, Pt wire as counter electrode and Ag/AgCl as the reference electrode, which was placed in a separate cell and connected to the analyte cell via a salt bridge (KNO_3). The electrochemical cell was enclosed in a grounded Faraday cage, and all electrolytes were degassed with a flow of $N_{2(g)}$ prior to the experiments, and an $N_{2(g)}$ blanket maintained throughout the course of the measurements. All electrochemical measurements were performed on at least 5 different microelectrodes to ensure reproducibility.

3.4 Self-assembly

Monolayers were formed by soaking a freshly cleaned electrode (electrochemical cycling from –0.4 to +1.2 V *vs*. Pt wire in 0.5 M H_2SO_4) in a 1 mM aqueous solution of the complex for 5 days. After this period, the electrodes were treated exactly as above for the electrodeposited materials.

3.5 Solution Electrochemistry

The solution electrochemistry of compounds 2-10 was investigated via Cyclic Voltammetry (CV) and Differential Pulse Voltammetry (DPV) performed in aqueous solution using $NaClO_4$ as supporting electrolyte, and selected data are presented in Table 3..2 depicts typical CV and DPV data for two of the complexes, **4** and **7**. The electrochemical behavior of the compounds was found to be pH sensitive and was often complicated by adsorption effects, particularly at Au or Pt working electrodes, which is consistent with previous work performed on the parent cages.[20] Adsorption behavior at an Au electrode was confirmed via quartz crystal microbalance (QCM) measurements, whereby an increase in mass at the working electrode was observed at the potential corresponding to the pre-wave attributed to an adsorption phenomenon. In order to obtain reproducible results, the electrochemistry was performed in aqueous $NaClO_4$ adjusted to pH 7.3 utilizing a tris(hydroxymethyl)aminomethane (TRIS)/$HClO_4$ buffer. As the data in Table 3.4 show, the compounds display quasi-reversible redox behaviour, as determined from the ΔE values (>0.059 V) and the peak current ratio I_a/I_c being lower than unity for most of the compounds. It is known that the $E_{1/2}$ values for the cages are sensitive to the nature of the apical substituents[20] and this is evident for the compounds synthesised here. The $E_{1/2}$ for compound 2 with one glycyl substituent is shifted by 55 mV to more positive potential than that for compound 3, which is terminated with an iminodiacetate moiety. The nature of the terminal group in compounds 4-10 also affects the $E_{1/2}$ in that there is a significant shift (*ca.* 60-70 mV) to more positive potentials when the methyl group at the apex of the cage is replaced by an

amino group. It is worth noting, however, that the $E_{1/2}$ value does not change when moving from the Gly-CSA to Gly-Gly-CSA and Gly-Ala-CSA derivatives if the group ($-CH_3$ or $-NH_2$) at the apex is held constant. This implies that changing the nature of the substituent beyond the initial –Gly- group does not affect the electronic environment about the Co centre and therefore explains the absence of any significant differences between diastereomers. The lack of an effect on the resulting $E_{1/2}$ value is important when considering the possible use of the complexes as electrocatalysts.

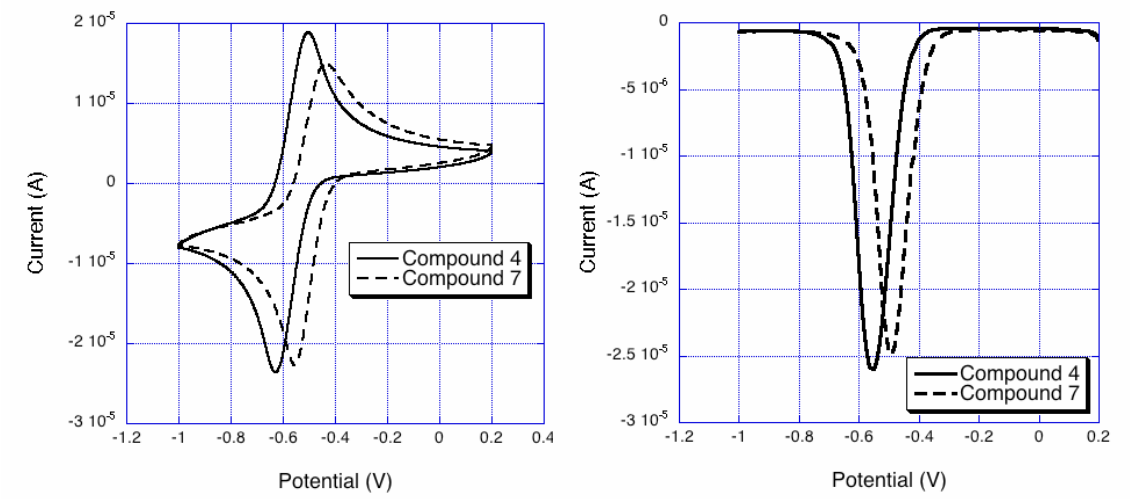

Figure 3.2 (a) Solution CVs of compounds 4 and 7 with GC working electrode at pH 7.3, versus Ag/AgCl (100 mVs^{-1}, 0.1M $NaClO_4$) (b) DPVs of the reduction processes (scan rate 20 mVs^{-1}, pulse amplitude 50 mV).

Table 3.2 Solution electrochemical data for compounds **4-10**. All $E_{1/2}$ values are referenced to the Ag/AgCl reference electrode. Scan Rate 100 mVs^{-1}. Errors are the standard deviations from five measurements.

Compound	$E_{1/2}$ (V)	ΔE (V)	I_a/I_c
2	-0.552(2)	0.074(3)	1
3	-0.607(2)	0.073(2)	1
4	-0.565(3)	0.12(1)	1
5	-0.562(5)	0.09(1)	1
6	-0.563(2)	0.09(1)	0.9
7	-0.494(6)	0.118(5)	0.8
8	-0.497(2)	0.122(2)	0.8
9	-0.497(4)	0.116(5)	0.8
10	-0.496(5)	0.15(1)	0.8

3.6 Surface Electrochemistry

Preparation of gold microelectrodes modified by a film of one of the cage disulfides was achieved using both conventional "self-assembly" (SAM) by soaking the electrodes in aqueous solutions of the disulfides for 5 days, and via electrodeposition (EDM).[18] All surface cyclic voltammograms (CVs) were carried out in H_2O and in the presence of 2 M $NaClO_4$ as supporting electrolyte in order to minimize the *iR* drop. Determination of the surface concentration of the cage was achieved via integration of the Faradaic peak

currents of the cyclic voltammograms. Some of the characteristics of the film are shown in Table3.2.

During repeated experiments it became clear that the films that formed immediately after the electrodeposition and washing steps displayed some unusual characteristics. CVs performed on the fresh films often displayed very small or unobservable current peaks corresponding to the cage species, and if they were present, the $E_{1/2}$ values were shifted to more negative potentials than the normal "equilibrium" potentials. It was found that repeated cycling of the potential, at scan rates from 0.1-10 V s^{-1}, for periods of up to and above 30 min produced CVs that displayed sharper and more intense peak currents, with a reduction in charging current (Figure 3.3). This effect could be explained by a random distribution of molecules on the surface at the start of the electrochemical experiment, which gradually re-arranges to give a more ordered film. It is worth pointing out that the electrostatic repulsion between the cationic Co-conjugates is likely to induce an initial disorder in the film as the Co headgroups maximize their physical separation. Electrochemical cycling might allow greater penetration of the anions into the film, and the enhanced charge neutrality would promote better packing within the film. As the film becomes more ordered, the Co centers become more thermodynamically homogeneous, which helps explain the reduction in peak half-widths during the experiment. A more ordered film would also help to explain the lower charging current observed with time, as a more effective "blocking layer" is formed. A similar effect has been observed in films produced from immobilised Ni(II)/(III) redox species[21] whereby a reduction in capacitive current and sharper Faradaic current peaks were observed with longer exposure times of the modified electrode to the disulfide

solution. To interpret the results, the authors proposed a process whereby an initially random (disordered) film was replaced by a more ordered and compact film via replacement of surface molecules present in defective sites with fresh molecules in solution, whilst the total surface coverage (Γ) remained constant. Whilst replacement of surface bound molecules with those in solution is clearly not possible here, if a surface reorganisation effect is taking place, for example via surface migration of the gold thiolate molecules[22] or the potentially slow cleavage of the disulfide bond, the results between the two experiments would be almost identical. It is worth noting that this effect was more pronounced for the films produced by ED, when compared to those prepared by SA, and this phenomenon may be explained by the relative rates at which the two films are formed. Rapid film formation during ED might not allow the molecules enough time to orient themselves on the surface, which could be exacerbated by the negative potential "pulling" the cationic cage units to the surface, whereas the long time and lack of applied potential in SA would overcome and obviate these effects (Figure 3.4). Thus, in order to obtain stable and reproducible CVs, all freshly prepared films were subjected to the above electrochemical treatment before the determination of the electrochemical parameters shown Table 3.2.

Plotting the peak current against scan rate for monolayers of compound **4** prepared using both SA and ED shows a linear relationship (Figure 3.5), which is expected for a surface adsorbed species.[23] These results indicate the successful immobilization of compound **4** onto the gold surface using both ED and SA techniques.

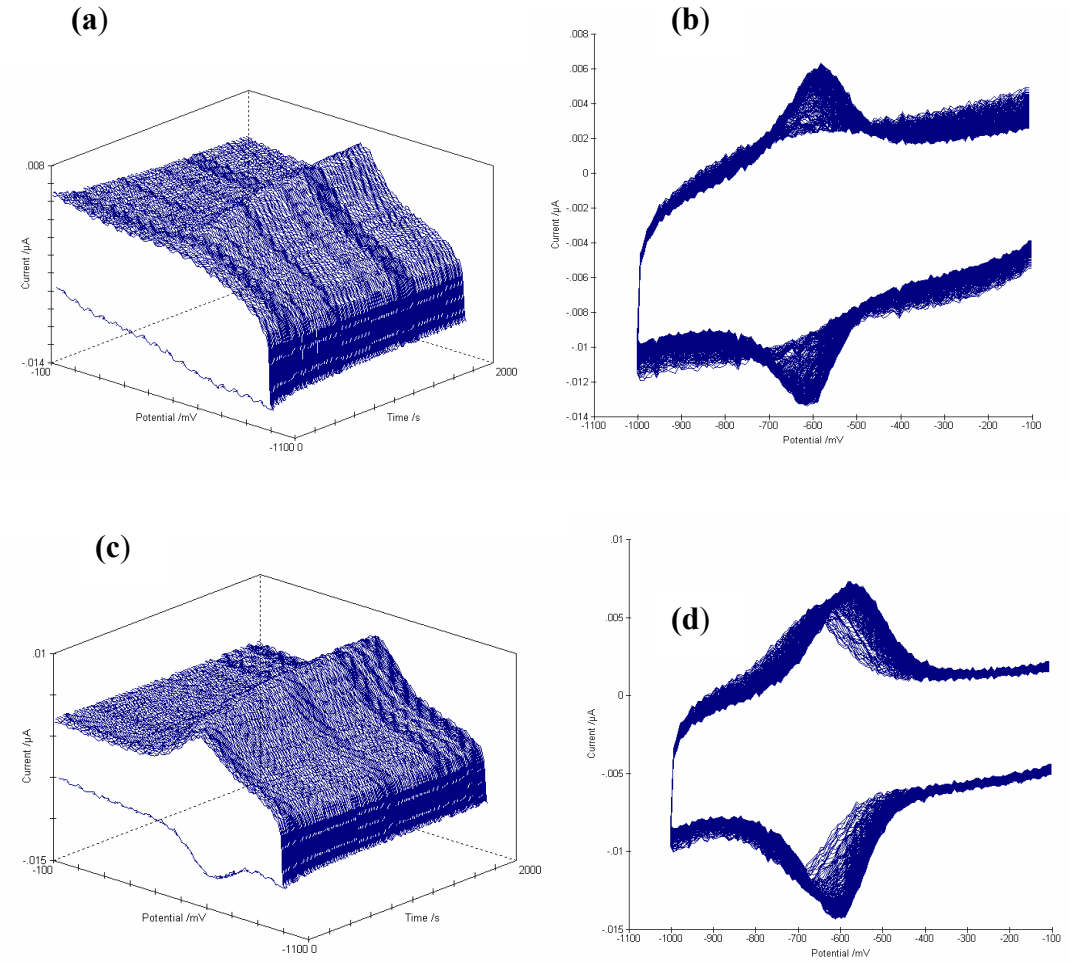

Figure 3.3 (a): Plot of repeated CVs versus time for compound 4 immediately after ED and washing (10 Vs^{-1}) (Note: Potential axis reversed for clarity in (a) and (c)); **(b):** (a) viewed along the current/potential plane; **(c):** same as (a) but for SA; **(d):** (c) viewed along the current/potential plane.

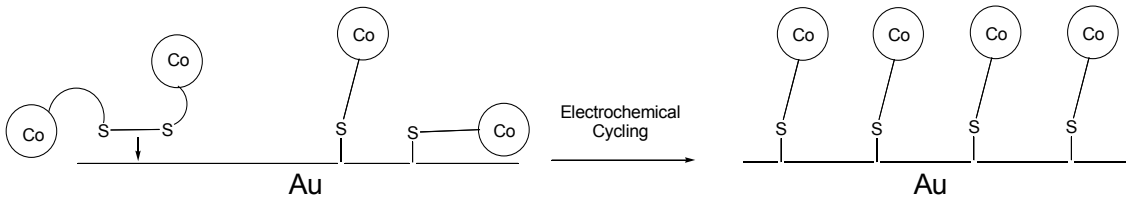

Figure 3.4 Diagram illustrating the possible reorganization process leading to the observed increase in peak current and concomitant sharpening of peaks

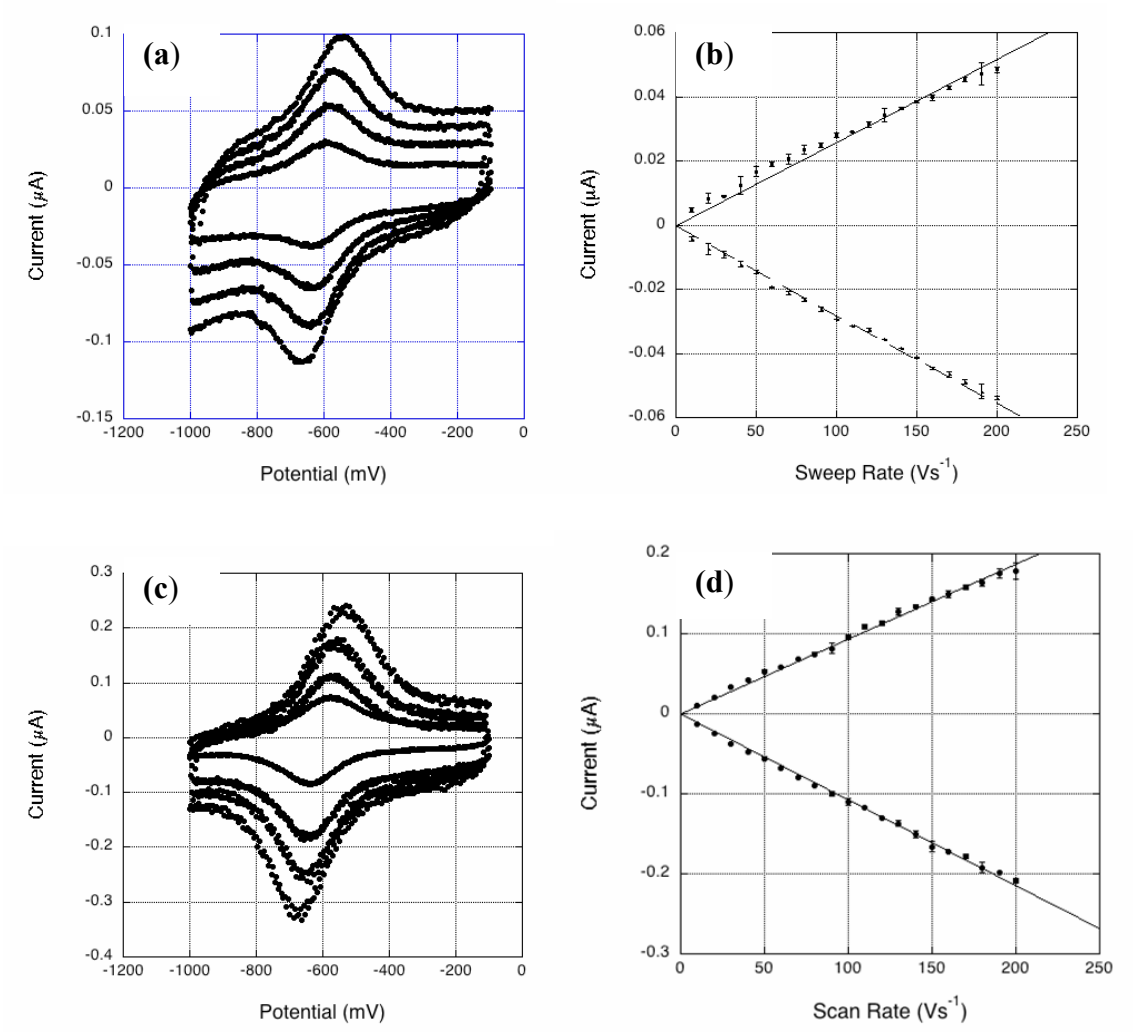

Figure 3.5 (a): CV's obtained at 50, 100, 150 and 200 Vs^{-1} for an EDM of compound 4; (b): Plot of peak current versus scan rate for monolayer in (a); (c): As in (a) but for SAM; (d): As in (b) but for the SAM.

The stability of the monolayers was examined by repeated electrochemical cycling, from the open circuit potential (*ca.* –100 mV) to –1000 mV with a scan rate of 100 Vs^{-1} (Figure 3.6). The signal due to the reduction of the surface-bound Co(III) conjugate shows virtually no loss in signal intensity upon repeated cycling for 100 s, indicating a stable monolayer has been formed.

As the data in table 3.3 indicates, the monolayers formed using both the ED and SA techniques display very similar properties. The experimentally determined values for both films are virtually identical. Both films exhibit a reversible reduction of the Co(III) cage at E^o = -619(4) mV vs Ag/AgCl, which is anodically shifted compared to the solution electrochemistry. The peak separation is non-zero but significantly reduced compared to the solution electrochemistry, indicating potentially an increase in the reversibility of the process on the surface.

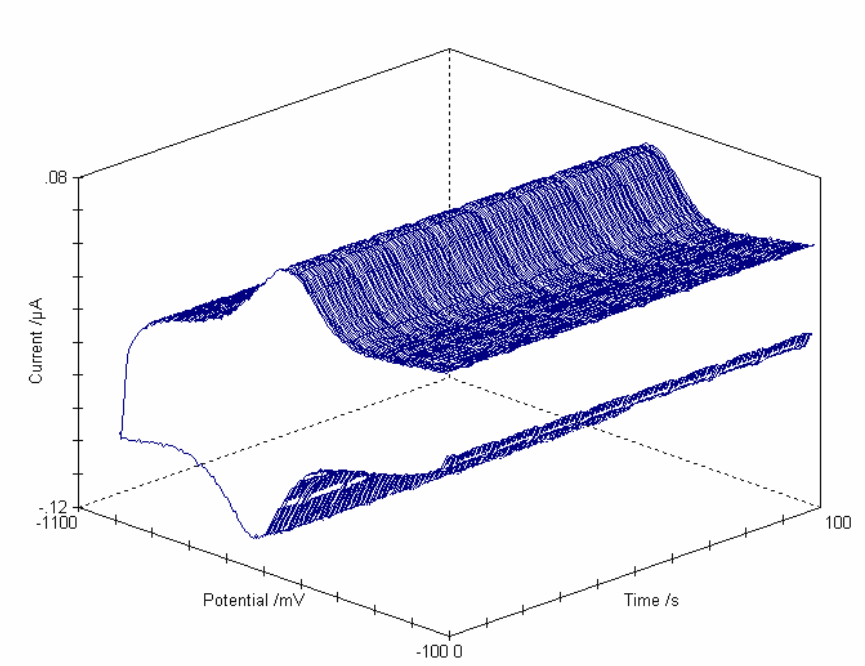

Figure 3.6 Repeated electrochemical cycling for film of compound **4** (100 Vs^{-1}).

This also signifies that there is some barrier for electron transfer through the spacer. As would be expected, the molecular footprint is larger compared to the more compact and

neutral ferrocene conjugates.[18, 24] This can rationalized considering the electrostatic repulsion between the positively charged Co(III)-sarcophagine conjugates on the surface, and the large E_{fwhm} of ~ 200 mV is consistent with this, as theoretical treatments[25, 26] predict a broadening of Faradaic peaks when the film consists of repulsive entities. However it is important to point out that the footprint and thus the surface concentration for films deposited electrochemically and prepared by self-assembly are identical. All of the experimentally determined values for $E_{1/2}$, and importantly, the surface concentration and the related specific area of the molecule are in agreement between the two techniques. This shows that both methods can be used to generate monolayers of the compounds on a gold electrode.

SAMs on Au-coated silicon wafers were also prepared, and the presence of a highly polar moiety on the surface was demonstrated qualitatively by the higher wettability of the modified surface with respect to water, compared to a bare unmodified substrate. Evidence for a monolayer was obtained through the use of ellipsometry, which indicated a film thickness of (7 ± 1 Å) which is lower than the value expected for a fully extended molecule of compound 4 (*ca.* 15 Å). A low value for the film thickness could be due to the molecules lying at an angle to the surface and/or poor surface coverage, but it does suggest that the surface is modified by a monolayer and not a multilayer.

An XPS analysis of a SAM prepared on an Au coated silicon substrate of compound **4** was undertaken in order to define the nature of the adsorption of the compound onto the gold surface. Disulfide chemisorption onto gold is generally believed to occur through a process in which the disulfide bond is broken to give two chemically independent molecules on the surface, bound as thiolates.[22] Peaks corresponding to S, Co, N, O and

C are observed in the XPS spectrum which demonstrates the presence of compound **4** on the substrate. Figure shows the major peak in the S(2p) region at 162 eV, which is consistent with the formation of an Au-S bond,[27] allowing us to conclude that the compound is bound as a thiolate on the surface. The Co binding energy of 781.5 eV is higher than the reported binding energy of 780.5 eV for the related $[Co(NO_2)_2sar]Cl_3$[28], but does fall within the range of binding energy values for the Co(III) N_6 complexes $[Co(en)_3]Cl_3$ and $[Co(NH_3)_6]Cl_3$ of 780.2 –781.8 eV[28, 29], which indicates the cobalt is present as Co(III).

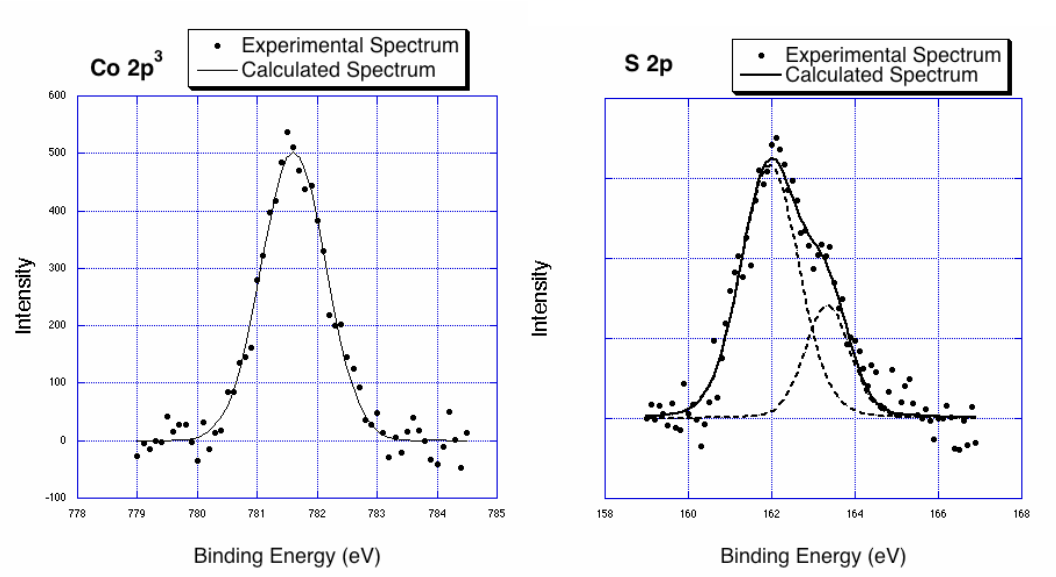

Figure 3.7 (a): XPS of Co $2p^3$ region; (b): S 2p region

3.7 Conclusions

In this paper we have described the synthesis and solution electrochemical behavior of a series of cobalt cage complexes bridged with short disulfide containing peptides. In this way we have demonstrated the efficacy of this synthetic strategy which will allow us to tune "tail" length in a number of applications. We have also shown that it is possible, at least in one case, to immobilize a complex on a gold substrate utilizing the disulfide linkage present. We believe that this undergoes facile cleavage to give initially species, which lack ordering, and subsequent electrochemical cycling allows them to attain thermodynamically stable surface ordering, although this phenomenon requires further study.

The surface attachment of these peptide tethered sarcophagine complexes has allowed us to form modified surfaces containing redox active centres and promise entry to an exciting range of applications.

Acknowledgments

We thank the University of Western Australia for partial funding of this research. GLN was the holder of an Australian Postgraduate Award.

3.8 References

1. Love, J. C.; Estroff, L. A.; Kriebel, J. K.; Nuzzo, R. G.; Whitesides, G. M. *Chem. Rev.* **2005,** *105*, 1103-1169.
2. Daniel, M.-C.; Astruc, D. *Chem. Rev.* **2004,** *104*, 293-346.
3. Sargeson, A. M. *Pure and Applied Chemistry* **1986,** *58*, 1511-1522.
4. Sargeson, A. M. *Coord. Chem. Rev.* **1996,** *151*, 89-114.
5. Jensen, M. H.; Osvath, P.; Sargeson, A. M.; Ulstrup, J. *J. of Electroanal. Chem.* **1994,** *377*, 131-141.
6. Hupp, J. T.; Liu, H. Y.; Lay, P. A.; Petri, W. H. F.; Sargeson, A. M.; Weaver, M. J. *J. of Electroanal. Chem. and Interf. Electrochem.* **1984,** *163*, 371-379.
7. Creaser, I. I.; Hammershoei, A.; Launikonis, A.; Mau, A. W. H.; Sargeson, A. M.; Sasse, W. H. F. *Photochem. and Photobiol.* **1989,** *49*, 19-23.
8. Konigstein, C.; Mau, A. W. H.; Osvath, P.; Sargeson, A. M. *Chem. Commun.* **1997**, 423-424.
9. Launikonis, A.; Lay, P. A.; Mau, A. W. H.; Sargeson, A. M.; Sasse, W. H. F. *Sci. Papers I.P.C.R.* **1984,** *78*, 198-205.
10. Mau, A. W.-H.; Sasse, W. H. F.; Creaser, I. I.; Sargeson, A. M. *Nouv. J. Chimie* **1986,** *10*, 589-592.
11. Gahan, L. R.; Hambley, T. W.; Sargeson, A. M.; Snow, M. R. *Inorganic Chemistry* **1982,** *21*, 2699-2706.
12. Burnet, S.; Choi, M.-H.; Donnelly, P. S.; Harrowfield, J. M.; Ivanova, I.; Jeong, S.-H.; Kim, Y.; Mocerino, M.; Skelton, B. W.; White, A. H.; Williams, C. C.; Zeng, Z.-L. *Eur. J. Inorg. Chem.* **2001**, 1869-1881.
13. Paxinos, A. S.; Gunther, H.; Schmedding, D. J. M.; Simon, H. *Bioelectrochem. Bioenerg.* **1991,** *25*, 425-436.
14. Harrowfield, J. M.; Koutsantonis, G. A.; Nealon, G. L.; Skelton, B. W.; White, A. H. *Eur. J. Inorg. Chem.* **2005**, 2384-2392.

15. Walker, G. W.; Geue, R. J.; Sargeson, A. M.; Behm, C. A. *J. Chem Soc., Dalton Trans.* **2003**, 2992-3001.

16. Donnelly, P. S.; Harrowfield, J. M.; Skelton, B. W.; White, A. H. *Inorg. Chem.* **2000,** *39*, 5817-5830.

17. Bodanszky, M.; Bodanszky, A., *The Practice of Peptide Synthesis*. Second ed.; Springer-Verlag: Berlin, 1994.

18. Orlowski, G. A.; Chowdhury, S.; Long, Y.-T.; Sutherland, T. C.; Kraatz, H.-B. *Chem Commun* **2005**, 1330-1332.

19. Kraatz, H.-B. *J. Inorg. Organomet. Polym. Mat.* **2005,** *15*, 83-106.

20. Bond, A. M.; Lawrance, G. A.; Lay, P. A.; Sargeson, A. M. *Inorg. Chem.* **1983,** *22*, 2010-2021.

21. Gobi, K. V.; Okajima, T.; Tokuda, K.; Ohsaka, T. *Langmuir* **1998,** *14*, 1108-1115.

22. Ulman, A. *Chem. Rev.* **1996,** *96*, 1533-1554.

23. Bard, A. J.; Faulkner, L. R., *Electrochemical Methods*. Second ed.; John Wiley & Sons: 2001.

24. Bediako-Amoa, I.; Sutherland, T. C.; Li, C.-Z.; Silerova, R.; Kraatz, H.-B. *J. Phys. Chem. B* **2004,** *108*, 704-714.

25. Laviron, E. *J. Electroanal. Chem.* **1979,** *100*, 263-270.

26. Matsuda, H.; Aoki, K.; Tokuda, K. *J. Electroanal. Chem.* **1987,** *217*, 15-32.

27. Ishida, T.; Choi, N.; Mizutani, W.; Tokumoto, H.; Kojima, I.; Azehara, H.; Hokari, H.; Akiba, U.; Fujihira, M. *Langmuir* **1999,** *15*, 6799-6806.

28. Achilleos, A. A.; Gahan, L. R.; Hambley, T. W.; Healy, P. C.; Weedon, D. M. *Inorganica Chimica Acta* **1989,** *157*, 209-214.

29. Okamoto, Y.; Nakano, H.; Imanaka, T.; Teranishi, S. *Bull. Chem. Soc. Jpn.* **1975,** *48*, 1163.

CHAPTER 4
EVALUATION OF ELECTRON TRANSFER RATES IN PEPTIDE FILMS: SIMPLIFIED CALCULATION AND THEORY

This chapter is based on the manuscript by G. A. Orlowski, H.-B. Kraatz. "Evaluation of electron transfer rates in peptide films: Simplified calculation and theory". Electrochim. Acta, **2006**, 51, 2934-2937.

I am the main contributor to the manuscript. I have performed all electrochemical experiments and calculations. The first draft of the manuscript was also prepared by me. The final version of the manuscript was obtained in an iterative writing process with my supervisor.

4.1 Connecting Text

Next in our investigations, it became necessary to extract electron transfer rate information from the redox active peptide films prepared by electrochemical deposition as described in the previous chapters. This chapter describes an electrochemical approach to obtain electron transfer rates and reorganization energies for surface-bound redox active ferrocene peptide conjugates. Cyclic voltammetry experiments performed

at 1000 Vs^{-1} were used to extract the electron transfer rates at various temperatures and as a result reorganization energies for two ferrocene-modified peptide films [Fc-Gly-CSA]$_2$ and [Fc-Val-CSA]$_2$ (CSA = cystamine) were estimated. The asymmetry in the Tafel-like plot, which is not related to the dipole moment, was observed for the Val-containing conjugate and suggests some additional effects which are investigated in subsequent chapters.

4.2 Introduction

The study of electron transfer processes in biological systems, such as proteins, DNA and peptides, has received significant attention over the past two decades[1-7]. Marcus-Hush theory provides the theoretical foundation for ET processes, which can be described mathematically by an exponential dependence of the ET rate on the distance between a donor and an acceptor[8,9]. Experimental studies of ET in small peptide models has been studied in solution using photophysical or radiolysis methods to cause electron transfer between a D-A pair.[10-12] More recently solution electrochemical methods were used to evaluate the dissociative ET in small peptides.[13]

With the advent of self-assembly of molecules on surfaces, ET from a redox center, such as ferrocene (Fc), through the molecular spacer material can be probed by a variety of electrochemical methods: CV[14-21,29], CA[22,23], ACV[24,25], EIS[20,21] and finally with SECM[26]. For example, the electrochemistry of Fc-peptide films was reported in which the peptides adopt a hydrogen bonded collagen-like structure. But instead of an exponential relationship between the separation of the redox center from the electrode surface, a linear distance dependence was observed, indicating that tunneling is not the major mechanism in these systems.[16,17] We recently reported on the facile formation of peptide films by electrodeposition of disulfides onto a gold substrates and were able to evaluate the ET process.[14] In this contribution, we would like to outline the electrochemical approach and draw attention to the asymmetry in the Tafel plots of thin

films prepared from the bioorganometallic conjugates $[Fc\text{-}Gly\text{-}CSA]_2$ and $[Fc\text{-}Val\text{-}CSA]_2$ (CSA = cystamine).

4.3 Results and Discussion

In our approach we choose to evaluate film prepared from the Gly conjugate $[Fc\text{-}Gly\text{-}CSA]_2$, and the Val conjugate $[Fc\text{-}Val\text{-}CSA]_2$ according to the electrodeposition method described earlier.[14] The Gly residue is expected to allow more flexibility of the peptide spacer and potentially for a better film, while steric interactions between neighboring the isopropyl groups of the Val residue should make for a more disordered film (Scheme 4.1).

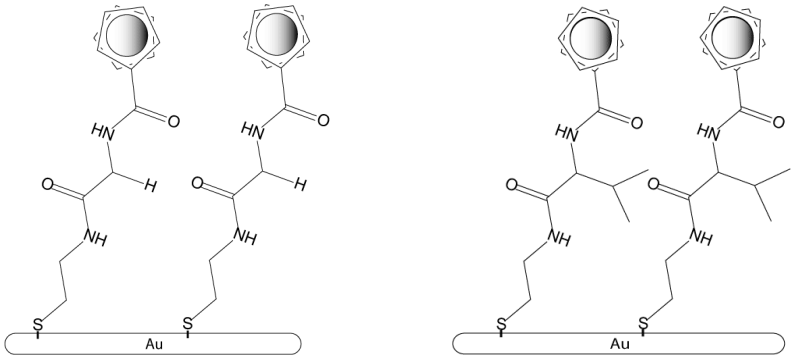

Scheme 4.1 Schematic view of films prepared of $[Fc\text{-}Gly\text{-}CSA]_2$ and $[Fc\text{-}Val\text{-}CSA]_2$ on the gold surface.

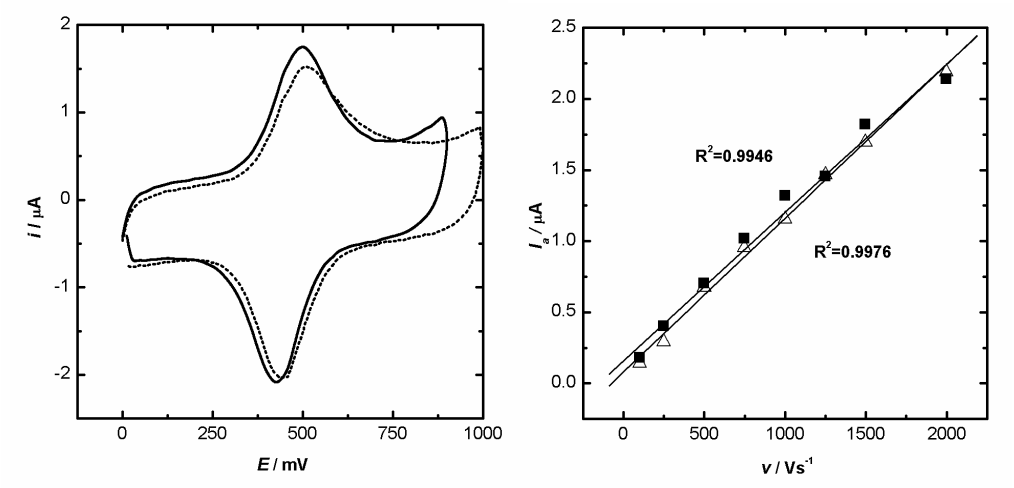

Figure 4.2 Left: CV for films of $[Fc\text{-}Gly\text{-}CSA]_2$ (——) and $[Fc\text{-}Val\text{-}CSA]_2$ (·····) using a gold microelectrode 25 μm radius, scan rate $1000 Vs^{-1}$, Ag/AgCl, Pt-mesh counter. Right: i_P vs scan rate for $[Fc\text{-}Gly\text{-}CSA]_2$ (■) and $[Fc\text{-}Val\text{-}CSA]_2$ (Δ).

The CVs of films prepared by electrodeposition from 1 mM ethanolic solutions of $[Fc\text{-}Gly\text{-}CSA]_2$ and $[Fc\text{-}Val\text{-}CSA]_2$ are shown in Figure 1. Both films exhibit a fully reversible one-electron oxidation wave at E_F = 460 mV for $[Fc\text{-}Gly\text{-}CSA]_2$ and 490 mV for $[Fc\text{-}Val\text{-}CSA]_2$. The peak current ratios for both films are close to unity. The peak separation for both systems at 1000 Vs^{-1} in room temperature is around 65-80 mV. The peaks are broader than what would be for Nerstian behavior. However, peak broadening in our case may be attributed to lateral intermolecular interaction, including H-bonding between the peptide strands, the interaction of the Fc with the solvent or supporting electrolyte (i.e. ion pairing, ClO_4^- as a counter ion or even surface roughness effects (roughness factor in our case 1.1-1.2). In our simplified approach, we assume a near ideal Nernstian behavior.

The linearity of a plot of scan rate versus the peak current i_P for both films confirms the absence of diffusive contributions and indicates the presence of surface bound molecules only.

4.4 Evaluation of the Electron Transfer Kinetics

The Butler-Volmer formalism for surface bound electroactive species is described by:[27]

$$i = nFA(k_f \Gamma_{ox} - k_b \Gamma_{red}) \qquad (4.1)$$

We assume that for an electroactive couple Fc/Fc^+ the process is Nernstian. Thus,

$$\frac{k_f}{k_b} = e^{\frac{nF(E-E_0)}{RT}} \qquad (4.2)$$

$$Ox + e^- \underset{k_b}{\overset{k_f}{\rightleftharpoons}} Red$$

Where $E-E_0 = \eta$ is overpotential, k_f, and k_b are the electron transfer rates for the forward and backward processes.

By combining equation (4.2) with (4.1) equation (4.3) is obtained:

$$i(E) = nFA\left(k_f \Gamma_{ox}(\eta) - \frac{k_f \Gamma_{red}(\eta)}{e^{\frac{nF\eta}{RT}}} \right) \qquad (4.3)$$

Finally equation (4.4), which is the final expression for the calculation of the electron transfer rate, useful for fast ET processes at a high scan rates.

$$\frac{i(E)}{nFA\left(\Gamma_{ox}(\eta) - \frac{\Gamma_{red}(\eta)}{e^{\frac{nF\eta}{RT}}} \right)} = k_f(E) \qquad (4.4)$$

The average value from the oxidation and reduction of the surface bound peptide provides the electron transfer rate k_{ET}.

$$k_{ET} = \frac{k_f + k_b}{2} \qquad (4.5)$$

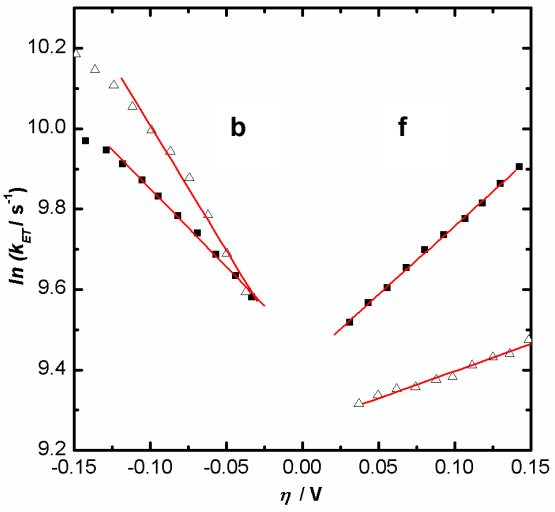

Figure 4.3 ln k_{ET} ploted vs overpotential η according to Equation 4 at 293K. The slope for positive and negative η's is described by the symmetry factor α. $[Fc\text{-}Gly\text{-}CSA]_2$ (■) and $[Fc\text{-}Val\text{-}CSA]_2$ (Δ). k_{ET} calculated from CV at 1000 V/s

Extrapolation of the rate constant to zero overpotential provides k_{ET} from the Tafel plot.

Electron transfer rates obtained with this approach are given in Table 3.1.

Table 4.1: Summary of kET values obtained by cyclic voltammetry (CV) at 1000 Vs-1 and chronoamperometry (CA) and of the Fc-peptide surface concentrations.

	k_{ET} (s^{-1}) [CVat1000Vs^{-1}]	k_{ET} (s^{-1}) [CA] [14]	Surface conc.[mol/cm^2] [14]
$[Fc\text{-}Gly\text{-}CSA]_2$	$12.5x10^3$	$12.0x10^3$	$2.6x10^{-10}$
$[Fc\text{-}Val\text{-}CSA]_2$	$10.0x10^3$	$8.0x10^3$	$3.3x10^{-10}$

* Standard deviation $1.5x10^3$, room temperature, unoccupied space on electrode monitored by Au-oxidation was found to be 5-7%[14].

We found the Laviron[27] method not suitable for our purpose, since the ET process is very fast ($E_p < 200$ mV even at 2000 V/s).

In case of $[Fc\text{-}Gly\text{-}CSA]_2$, the Tafel plot is symmetrical with respect to the oxidation and reduction (Figure 2), and indicates similar barriers for the forward and backward electron transfer steps. For $[Fc\text{-}Val\text{-}CSA]_2$ however, the forward and backward ET steps are very asymmetric. We suggest the following explanation for this interesting observation. Upon forward ET, ClO_4^- anions from the supporting electrolyte are closely associated with the film and may even migrate into the film. For a well-ordered film it may be expected that diffusion in and out of the film is not as strongly affected by a change in the redox potential. For the Val-film, the bulkier, hydrophobic isopropyl substitutents may not allow diffusion of polar solvent and ions from the solution into the film, which may play an important role in the ET of the system.

In order to investigate this in more detail and obtain information about a potential reorganization of the films, variable temperature studies were carried out and evaluated using the Arrhenius equation (4.6), which related the activation energy for a process to the rate constant for a particular reaction:

$$k_{ET} = A_{n,NA} e^{-\frac{E_{a,NA}}{k_b T}} \qquad (4.6)$$

where, $E_{a,NA}$ is activation energy, $A_{n,NA}$ is the frequency factor or Arrhenius prefactor for non-adiabatic reactions[6], k_{ET} is standard rate constant for electron transfer reaction, k_b is the Boltzman constant and T is the temperature in Kelvin. With a good approximation we can state that[22]:

$$E_{a,NA} = \frac{\lambda}{4} \qquad (4.7)$$

where λ is the reorganization parameter.

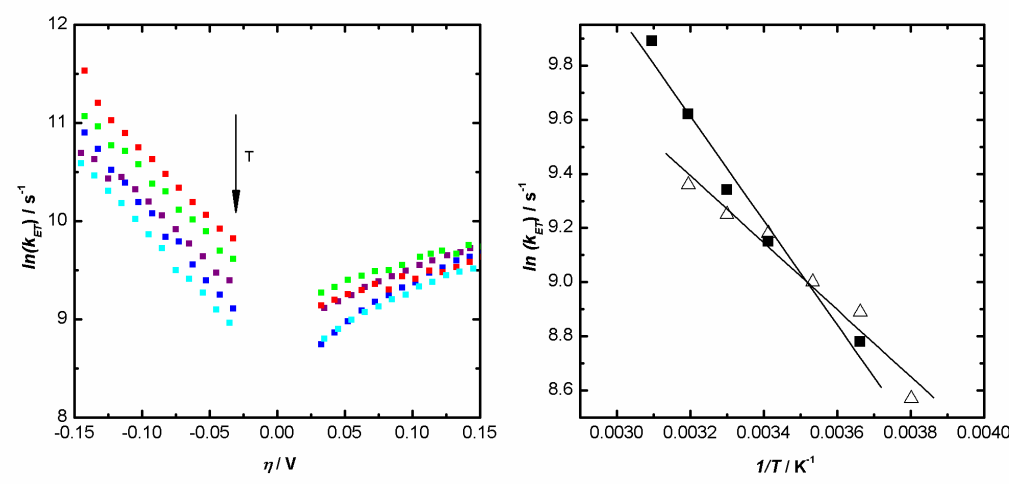

Figure 4.4 Left: variable temperature Tafel plot for $[Fc\text{-}Val\text{-}CSA]_2$ (Temperature from top to bottom: 323K, 313K, 293K, 273K, 263K). Right: Arhenius plot for both monolayers ($[Fc\text{-}Gly\text{-}CSA]_2$ (■) and $[Fc\text{-}Val\text{-}CSA]_2$ (Δ)) where k_{ET} values were obtained from CV at $1000Vs^{-1}$.

The simplified method described above allow for a quick and convenient description of important parameters regarding evaluated films on microelectrodes. This is especially useful for short spacers (i.e. short peptides) and fast ET rates.

A representative series of Tafel plots for the forward and backward electron transfer reaction for film of $[Fc\text{-}Val\text{-}CSA]_2$ obtained over a temperature range of 263 – 323 K are shown in Figure 3. We can observe significant differences in the oxidative and reductive part of the plot. For example, the reduction of the Fc^+ follows the expected trend, whereas the oxidation reaction shows a k_f not at the highest temperature of 323 K, indicating potentially morphological changes in the film or may be the result of

movement within the peptide spacer and potentially interactions with the solvent and/or ions which may have penetrated the film. In particular, the latter may cause serious disturbances in the electron transfer. In these short sequences the electric dipole moment is rather small and it would be expected that this cannot lead to this dramatic effect. Dipole moment effects were reported before by Fox for longer helical Aib-rich peptide sequences[30]. However, for short spacers supported on surfaces, the resulting film is rather poorly structured and allows significant solvent penetration.[28] This could also explain deviation from "ideal" Nerstian behavior and significant broadening of the peaks (from 90mV to 160 mV). The films on the gold surface exhibit a linear relationship of ln k with 1/T (Figure 4.3). As the temperature increases a significant increase in k_{ET} is observed. The activation barrier for the electron transfer process is obtained from the slope of the Arrhenius plot for both system, indicating a difference between the activation parameters for the films of $[Fc\text{-}Gly\text{-}CSA]_2$ and $[Fc\text{-}Val\text{-}CSA]_2$. The reorganization parameters were evaluated according to Equations 4.6, 4.7 and are summarized in Table 4.2.

Table 4.2 Parameters of the films obtained from cyclic voltammetry. Slopes are given for 293K.

Film	E_f [mV]	Reorganization energy [eV]	Slope m [V]	
		λ_o	forward	backward
$[Fc\text{-}Gly\text{-}CSA]_2$	460	0.65 (6)	7.8	-8.0
$[Fc\text{-}Val\text{-}CSA]_2$	490	0.75 (5)	3.4	-13.8

4.5 Summary

In summary, we have investigated the electrochemical properties of two Fc-peptide conjugate films, linked to a gold surface via an Au-S linkage, providing a simplified but detailed procedure for obtaining kinetic information for the electron transfer process. We found significant differences in the forward and backward electron transfer steps. Since the peptides are short, these differences cannot be due to their electric properties such as the dipole moment. Rather we expect that higher penetration of supporting electrolyte and of solvent, in addition to solvation effects account for our observations.

4.6 References

1. P. Kaden, E. Mayer-Enthart, A. Trifonov, T. Fiebig, H.-A. Wagenknecht, *Angew. Chem., Int. Ed.* **2005**, *44*, 1636.

2. M. K. Cichon, C. H. Haas, F. Grolle, A. Mees, T. Carell, *J. Am. Chem. Soc.* **2002**, 124, 13984.

3. T. Morita, S. Kimura, S. Kobayashi, Y. Imanishi, *J. Am. Chem. Soc.* **2000**, 122, 2850.

4. S. O. Kelley, N. M. Jackson, M. G. Hill, J. K. Barton, *Angew. Chem., Int. Ed.* **1999**, 38, 941.

5. J. N. Richardson, S. R. Peck, L. S. Curtin, L. M. Tender, R. H. Terrill, M. T. Carter, R. W. Murray, G. K. Rowe, S. E. Creager, *J. Phys. Chem.* **1995**, 99, 766.

6. C. A. Widrig, C. Chung, M. D. Porter, *J. Electroanal. Chem.* **1991**, 310, 335.

7. J. F. Smalley, S. B. Sachs, C. E. D. Chidsey, S. P. Dudek, H. D. Sikes, S. E. Creager, C. J. Yu, S. W. Feldberg, M. D. Newton, *J. Am. Chem. Soc.*, ACS ASAP.

8. N. S. Hush, *Electrochim. Acta* **1968**, 13, 1005.

9. R. A. Marcus, *J. Chem. Phys.* **1956**, 24, 966.

10. Y.-G. K. Shin, M. D. Newton, S. S. Isied, *J. Am. Chem. Soc.* **2003**, 125, 3722.

11. A. Fedorova, A. Chaudhari, M. Y. Ogawa, *J. Am. Chem. Soc.* **2003**, 125, 357.

12. R. A. Malak, Z. Gao, J. F. Wishart, S. S. Isied, *J. Am. Chem. Soc.* **2004**, 126, 13888.

13. S. Antonello, F. Maran, *Chem. Soc. Rev.* **2005**, 34, 418.

14. G. A. Orlowski, S. Chowdhury, Y.-T. Long, T. C. Sutherland, H.-B. Kraatz, *Chem. Comm.* **2005**, 1330.

15. S. A. Serron, W. S. Aldridge, III, C. N. Fleming, R. M. Danell, M.-H. Baik, M. Sykora, D. M. Dattelbaum, T. J. Meyer, *J. Am. Chem. Soc.* **2004**, 126, 14506.

16. H.-B. Kraatz, I. Bediako-Amoa, S. H. Gyepi-Garbrah, T. C. Sutherland, *J. Phys. Chem. B* **2004**, 108, 20164.

17. I. Bediako-Amoa, T. C. Sutherland, C.-Z. Li, R. Silerova, H.-B. Kraatz, *J. Phys. Chem. B* **2004**, 108, 704.

18. H.-B. Kraatz, *Macromolecular Symposia* **2003**, 196, 39.

19. H. O. Finklea, *J. Phys. Chem. B* **2001**, 105, 8685.

20. S. Sek, A. Sepiol, A. Tolak, A. Misicka, R. Bilewicz, *J. Phys. Chem. B* **2004**, 108, 8102.

21. S. Sek, R. Moszynski, A. Sepiol, A. Misicka, R. Bilewicz, *J. Electroanal. Chem.* **2003**, 550-551, 359.

22. J. F. Smalley, H. O. Finklea, C. E. D. Chidsey, M. R. Linford, S. E. Creager, J. P. Ferraris, K. Chalfant, T. Zawodzinsk, S. W. Feldberg, M. D. Newton, *J. Am. Chem. Soc.* **2003**, 125, 2004.

23. J. F. Smalley, S. W. Feldberg, C. E. D. Chidsey, M. R. Linford, M. D. Newton, Y.-P. Liu, *J. Phys. Chem.* **1995**, 99, 13141.

24. H. O. Finklea, *J. Electroanal. Chem.* **2001**, 495, 79.

25. D. A. Brevnov, H. O. Finklea, *J. Electrochem. Soc.* **2000**, 147, 3461.

26. B. Liu, A. J. Bard, M. V. Mirkin, S. E. Creager, *J. Am. Chem. Soc.* **2004**, 126, 1485.

27. E. Laviron, *J. Electroanal. Chem.,* **1979**, 101, 19–28

28. A. S. Viana, M. Kalaji, L. M. Abrantes, *Langmuir,* **2003**, 19, 9542 -9544

29. T. M. Nahir, R. A. Clark, E. F. Bowden, *Anal. Chem.*; **1994,** 66, 2595-2598

30. E. Galoppini, M. A., Fox *J. Am. Chem. Soc.* **1996,** 118, 2299-2300

4.7 Supplementary Data

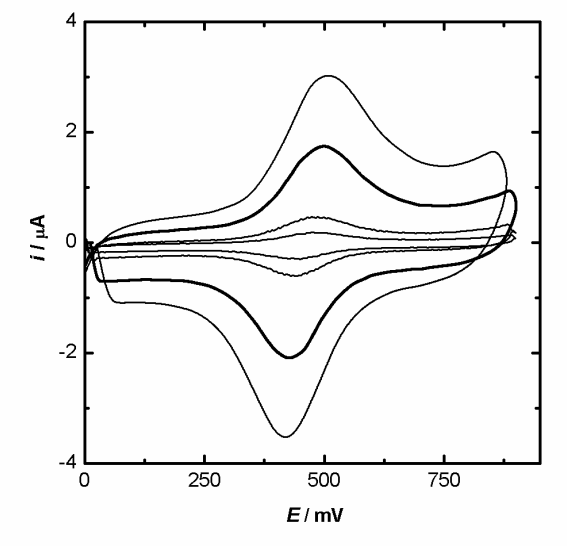

Figure 4S.1 Variable scan rate graph for $[Fc\text{-}Gly\text{-}CSA]_2$ (2000, 1000, 250, 100 Vs^{-1})

CHAPTER 5
REORGANIZATION ENERGIES OF FERROCENE-PEPTIDE MONOLAYERS

This chapter is based on the manuscript by G. A. Orlowski, S. Chowdhury, H.-B.Kraatz "Reorganization energies of ferrocene-peptide monolayers". This manuscript was recently submitted for publication to Langmuir.

I am the main contributor to the manuscript. I have performed all electrochemical experiments and calculations. I am also main author of the hypothesis. S. Chowdhury provided compounds, synthesis of which is described elsewhere.

5.1 Connecting Text

In the previous chapter, the electron transfer rate constants and the reorganizational energies for two Fc-peptide disulfide films were reported, showing an apparent effect on the size of the amino acid side chain. There is very little information available as to the effect of the individual amino acids on the electron transfer and none on their role on the reorganizational energies in organized peptide films. Thus, to deepen our understanding of the electron transfer process through the peptide backbone, we have investigated a series of Fc-peptide conjugates immobilized on gold microelectrodes

using the general method described in Chapter 2. Electrochemical studies on these films were carried out in the presence of a range of counter ions (BF_4^-, ClO_4^-, PF_6^-), allowing me to explore a possible connection between peptide film rigidity and reorganization energy.

5.2 Introduction

Ferrocene terminated self-assembled monolayers are one of the most studied redox-active assemblies on metal surfaces. These films have been extensively used as convenient ensembles with well-defined composition, structure and thickness and can serve as model systems to probe heterogeneous electron transfer (ET).[1-4]

A self-assembled monolayer with an electro-active headgroup can be described essentially as a donor-acceptor system that is linked by a spacer. In this particular arrangement, the electrode and the electro-active headgroup function as the donor acceptor system separated by a spacer molecule.

Investigations have shown that the ET in peptides can occur across long distances separating the donor from the acceptor.[5, 6] The peptide secondary structure, as well as the intramolecular hydrogen bonding network are known to affect the ET process.[5, 7-9] Electrochemical investigations of peptides immobilized on gold surface have become a practical way to study the electron transfer processes and to obtain important parameters like molecular footprint on the surface,[10] interfacial resistance,[11, 12] capacitance, activation and reorganization energies.[13] It was demonstrated by Chidsay[1] and others[13] that the solvation energy of the ferrocene significantly contributes to the activation

energy and thus is affecting ET rate. The orientation of molecules one the surface and its vast impact on the electron rate was described by Mirkin[14] and Kaifer.[15]

Bilewicz and co-workers studied the effect of increasing glycine and alanine amino acids in Fc-peptide films anchored to the gold electrode. Their STM (scanning-tunneling microscopy) results indicated that poly-glycine films were structurally well ordered and extremely well packed (specific area ~30Å^2).[16] Similar surface concentrations were observed for helical polyalanine films,[17] and effects of the dipole on the symmetry of the Tafel plot was also addressed.

Kimura and coworkers addressed the problem of an electron transfer mechanism by working on very long helical peptides. By incorporating non-natural amino acids containing naphthyl[18] or ferrocene[4, 19] residue in the side chain they were trying to find the theory that will explain the nature of long-range electron transfer. "Hopping" electron transfer mechanism was proposed.[20] However, this mechanism is highly contentious as the peptides lacking specific amino acids (e.g. Tyr, Trp) do not display any redox activity in a biologically sensible regime. In a recent STM study, Kimura and coworkers[21] observed that long helical peptides are able to change the length depend on the applied potential.

The electrochemical properties of helical Fc-oligoprolines were investigated in our research group.[22] Oligoprolines are unable to form intra- or inter-strand H-bonding patterns and create inflexible structure. This aspect was used to provide some insight into the complicated mechanism of the ET process. In this system a linear relationship between distance and electron transfer rate was found. In another publication collagen-like peptides (Pro-Pro-Gly unit), which are structurally related to oligoprolines, were

used to explain the effect of inter-strand and intermolecular H-bonding influence on ET process.[23] Interestingly, the effect of the repulsion between Fc head-groups and resultant changes in film structure were observed. Theoretical investigation of molecular motion on long helical structures showed that such formations could be extremely flexible.[24]

In results presented by Kimura, Bilewicz and from our own work, a significant issue arises. How can one distinguish a purely electrochemical response from an electrochemical signal distorted by a molecular motion of the molecules on the surface? The time scale of the electron movement from the ferrocene to the gold surface through the peptide spacer in most electrochemical experiments is often slower than the time scale of molecular motions, especially when external electric field are applied, forcing the molecule to align itself within the field gradient. Clearly, the dynamic properties of the molecules have to be taken into account in order to describe the electron transfer process correctly and one part of the puzzle is a proper description of the reorganization energy of the system and its link to the dynamic properties of the system.

In this contribution, we report the results of a study into the re-organizational parameters for a series of mono and di-substituted ferrocene-peptide conjugates. The effect of rigidity of Fc-peptides on the electron transfer rate will be addressed by evaluation of two types of compounds shown in Figure 5.1. In these systems, the rigidity of the molecule is largely determined by the number of attachment points on the gold surface. While the mono-substituted systems [Fc-Gly-CSA]$_2$ (**1**), [Fc-Ala-CSA]$_2$ (**2**), [Fc-Val-CSA]$_2$ (**3**) and [Fc-Leu-CSA]$_2$ (**4**)will be attached to the surface through only one podant peptide chain, di-substituted systems Fc[Gly-CSA]$_2$ (**5**), Fc[Ala-CSA]$_2$ (**6**), Fc[Val-CSA]$_2$ (**7**), Fc[Leu-CSA]$_2$ (**8**), Fc[Gly-Val-CSA]$_2$ (**9**), Fc[Gly-Ile-CSA]$_2$

(**10**), and Fc[Ile-Ile-CSA]$_2$ (**11**) will have both peptide chains linked to the Au surface, enhancing its rigidity. In this study we are describing the results of a series of electrochemical experiments testing the effects of counter-ions that associate with the ferrocenium ion to varying degrees in order determine the factors responsible for the sometimes atypical electron transfer rates that have been reported in the literature.

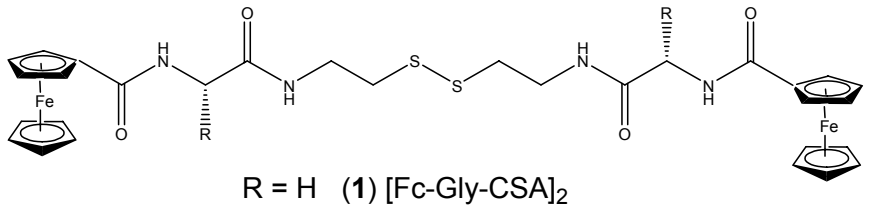

R = H (**1**) [Fc-Gly-CSA]$_2$
R = Me (**2**) [Fc-Ala-CSA]$_2$
R = Pr (**3**) [Fc-Val-CSA]$_2$
R = iBu (**4**) [Fc-Leu-CSA]$_2$

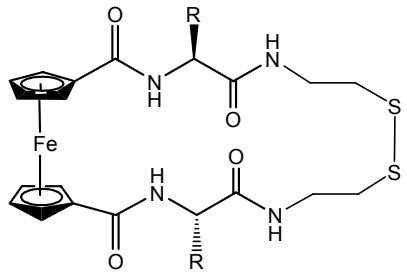

R = H (**5**) Fc[Gly-CSA]$_2$
R = Me (**6**) Fc[Ala-CSA]$_2$
R = iPr (**7**) Fc[Val-CSA]$_2$
R = iBu (**8**) Fc[Leu-CSA]$_2$

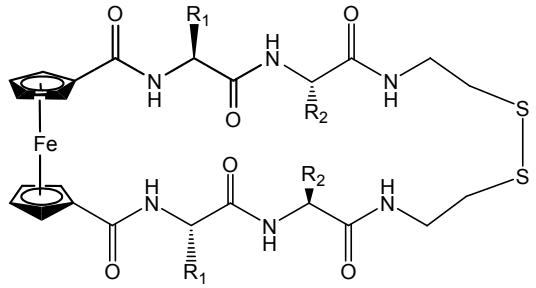

R_1 = H, R_2 = iPr (**9**) Fc[Gly-Val-CSA]$_2$
R_1 = H, R_2 = iBu (**10**) Fc[Gly-Ile-CSA]$_2$
R_1 = iBu, R_2 = iBu **(11)** Fc[Ile-Ile-CSA]$_2$

Figure 5.1 Acyclic and cyclic ferrocene-peptide conjugates used in this study

5.3 Experimental

All Fc-peptide disulfides were immobilized on gold microelectrodes (diameter: 25 μm) by modified potential assisted deposition[25].

Initially, the microelectrode was pre-treated by cycling in 0.5 M H_2SO_4 proceeded by a short oxidation for 0.5 s at 2 V (Figure 5.2). In subsequent stage of the preparation, electrode was cycled in a negative potential range (-0.6 to -2.3 V) to remove all remaining surface oxygen and cover the electrode with a layer of hydrogen atoms. The removal of remaining oxygen is necessary, due to possibility of the reaction between residual oxygen and disulfide compounds. Sulfonates produced in this instance will be only weakly physisorbed on the gold surface, lowering total integrity of the deposited films.

In a deposition step, potential of -1.5 V vs. W (tungsten quasi reference electrode) was applied for 30 min (Figure 2). An Ag/AgCl reference electrode is not suitable for the deposition function mainly due to chloride anion leakage, which can significantly inhibit deposition of disulfide conjugates. 1 to 10 mM ethanolic solution of Fc-peptide conjugates were used without presence of the supporting electrolyte.

Deposited films were ordered and tightly packed and showed surface concentrations of the ferrocene in the regime of 2.3 to 4.6 $*10^{-10}$ mol / cm^2, which can be correlated to the footprint ranging from 45 – 70 $Å^2$ per molecule. An unoccupied surface, estimated by CV in sulfuric acid, was estimated at 5-7 %.

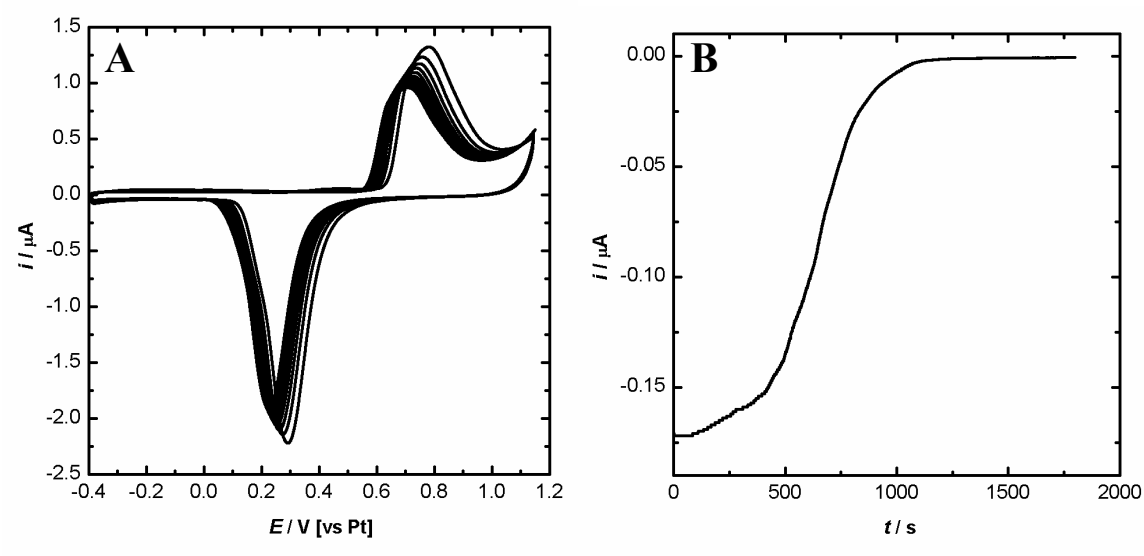

Figure 5.2 A) Typical cyclic voltammogram of gold microelectrode in 0.5 M H_2SO_4 obtained during pretreatment step (10 Vs^{-1} potential versus Pt wire). B) Typical amperometric i-t curve obtained during electrodeposition process. Potential was set to -1.5 V vs. Tungsten wire

All electrochemical experiments were carried out on a custom-built potentiostat EDAS 301 (design and production by Prof A. Baranski, University of Saskatchewan) and CHInstruments CHI660B. Variable temperature studies were conducted with a custom-built Peltier cooler that allows a temperature control of ± 1 ºC. Tungsten wire was used as a quasi-reference electrode to avoid film contamination with "leaking" chlorides ions (potentials given in Table 1 are reported vs. Ag/AgCl) and Pt mesh as an auxiliary electrode. Synthesis of the Fc-peptide conjugates used in this study is described elsewhere.[26, 27]

Comparison of the electron transfer rates, reorganization energies and formal potentials obtained for all the ferrocene peptide conjugates (**1- 11**) in different supporting electrolytes (0.1 M $NaClO_4$, 0.1 M $NaBF_4$ and 0.1M $NaPF_6$) is presented in the main text of this manuscript.

Films were electrochemically characterized by variable temperature cyclic voltammetry. Each experiment was repeated at least 5 times to ensure good reproducibility of the obtained data. Values of electron transfer rates were obtained from CV performed at 1000 Vs^{-1}. Simplified calculations were applied to evaluate reorganization energy. Methodology used to calculate reorganization energy and electron transfer rates is described elsewhere[28] and is based on the theoretical description introduced by Smalley *et al*[3].

$$k_{ET} = A_n e^{-\frac{E_a}{k_b T}} \qquad (5.1)$$

where, E_a is activation energy, A_n is the frequency factor or Arrhenius prefactor for non-adiabatic reactions[6], k_{ET} is standard rate constant for electron transfer reaction, k_b is the Boltzman constant and T is the temperature in Kelvin.

The calculations are based on two major assumptions: ET process is non-adiabatic and electrochemical response is strictly Nerstian.

Equation used to estimate ET rate at 1000 Vs^{-1} is presented below:

$$i(E) = nFA\left(k_f \Gamma_{ox}(\eta) - \frac{k_f \Gamma_{red}(\eta)}{e^{\frac{nF\eta}{RT}}} \right) \qquad (5.2)$$

Where Γ is surface concentration, k_f is a forward ET process, η is overpotential ($E-E^0$). I, n, F and A have their usual meanings.

5.4 Results and Disscussion

Figure 5.3 shows procedure for obtaining reorganization energies from cyclic voltammetry at variable temperatures. Figure 5.3a presents typical cyclic voltammograms (CVs) at five different temperatures. Peak height and broadness is

strongly affected signifying possible structural changes in the film. Figure 5.3b shows the corresponding Tafel plots used to obtain the electron transfer rates. Figures 5.3c and 5.3d represent typical Arrhenius plots used to obtain values for reorganization energy.

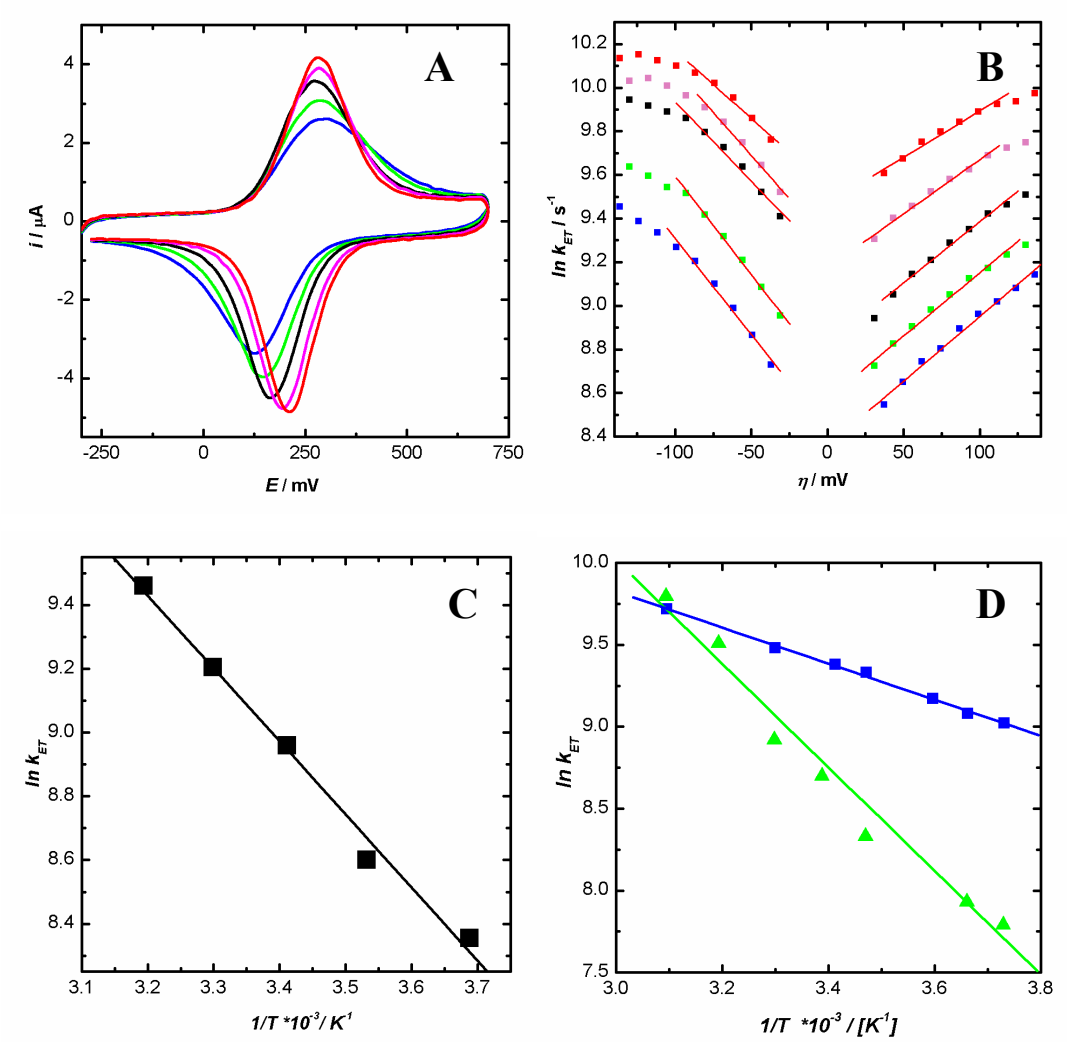

Figure 5.3 (—) 313 K, (—) 303 K, (—) 293 K, (—) 283 K, (—) 273 K, **A)** Variable temperature cyclic voltammetry of surface bound Fc[Ileu-Ileu-CSA]$_2$, 0.1 M $NaClO_4$, 1000 Vs^{-1}**B)** Tafel plot of lnkET vs η for (11) Fc[Ileu-Ileu-CSA]$_2$ Electron transfer rate dependency on the temperature, calculated at 1000 V/s. **C)** Arhenius plot for monolayer of Fc[Ileu-Ileu-CSA]$_2$ (11) (■) where k_{ET} values were obtained from CV at 1000 Vs^{-1}. **D)** Arhenius plot for monolayers [Fc-Ala-CSA]$_2$ (2) (■) and Fc[Ala-CSA]$_2$ (6) (■) where k_{ET} values were obtained from CV at 1000 Vs^{-1}.

The peak separation and peak broadness are strongly affected by the temperature. This effect can be explained by orientation and morphological[29] changes within the film. At higher temperatures, increased molecular motion of the Fc-peptides may allow for more simultaneous discharge and better ordering of the film (sharper peak and less diversity within monolayer). We can hypothesize that at lower temperature, there will be less molecular motion resulting in a number of local environments for the Fc groups, each contributing to the broadening of the peak. The immobilized molecules will respond slowly to any changes and the chance of simultaneous redox reaction will be smallest leading to broad peaks and large peak separations. The films on the gold surface exhibit a linear relationship of ln*k* versus 1/T (Figure 5.3d). As the temperature increases a significant increase in k_{ET} is observed. The activation barrier for the electron transfer process is obtained from the slope of the Arrhenius plot.

In Table 5.1, the formal potentials, the reorganization energies and the average electron transfer rates in different supporting electrolytes for all Fc-peptide conjugates (**1** - **11**) and are presented.

Table 5.1 Comparison of formal potentials, reorganization energies and k_{ET}`s of ferrocene peptide conjugates **1 - 11**.

	PF_6^-				ClO_4^-				BF_4^-			
Compound	**E^0 [mV]**	**lnA_n [s^{-1}]**	**λ[eV]**	**k_{ET} * 10^3 [s^{-1}]**	**E^0 [mV]**	**lnA_n [s^{-1}]**	**λ [eV]**	**k_{ET} * 10^3 [s^{-1}]**	**E^0 [mV]**	**lnA_n [s^{-1}]**	**λ [eV]**	**k_{ET} * 10^3 [s^{-1}]**
1	*462*	16.6	0.76	10.0	*464*	15.4	0.65	8.2	*446*	13.6	0.52	5.0
2	*480*	13.5	0.48	6.6	*490*	15.4	0.71	4.4	*450*	17.2	0.86	5.9
3	*437*	16.1	0.76	6.0	*488*	16.2	0.75	7.1	*450*	16.0	0.79	5.2
4	*504*	11.9	0.30	8.0	*484*	13.7	0.48	7.5	*432*	14.3	0.59	5.1
5	*679*	12.3	0.34	8.5	*688*	14.1	0.52	8.2	*716*	14.4	0.52	11.0
6	*654*	11.6	0.28	7.6	*635*	12.3	0.33	9.0	*662*	13.3	0.45	7.2
7	*654*	11.9	0.26	12.0	*686*	12.3	0.31	10.0	*592*	14.3	0.52	9.5
8	*682*	11.0	0.19	9.9	*686*	12.2	0.29	12.0	*667*	13.8	0.45	11.4
9	*625*	14.3	0.52	9.8	*658*	13.1	0.40	10.0	*671*	15.4	0.62	10.6
10	*661*	13.7	0.48	8.2	*641*	12.4	0.35	8.0	*600*	15.3	0.65	7.2
11	*670*	14.6	0.57	8.4	*600*	14.7	0.59	7.0	*636*	13.2	0.41	9.6

k_{ET} error = $1.0*10^3$ s^{-1} , λ error = 0.06 eV, E^0 error = 8 mV
E^0 is reported vs. Ag/AgCl, k_{ET} is measured at 295 K

It is interesting to note that these systems display an unusual distance relationship. Compared to ferrocene-alkanethiol monolayers in which the electron transfer rate k_{ET} is decreasing exponentially with distance, k_{ET} for Fc-peptides investigated here, does not follow the same distance relationship. For example, comparing the k_{ET} for compounds **9** - **11** to those of the shorter Fc-peptides, it is apparent that the rates are similar even though the distance for these dipeptide conjugates almost doubled from 9 Å for the shorter Fc-conjugates **1** – **8** to 15 Å (film thickness determined by ellipsometry). Potentially the difference is caused by more extensive H-bonding in these longer peptide conjugates.

The reorganization energy mainly depends on anionic solvation of the ferrocene.[30] The strength of the ion-pair created with Fc^+ mainly depends on the hydration level of the counter ion. The interactions with the Fc^+ group are decreasing in the following manner $PF_6^- > ClO_4^- > BF_4^-$. The reorganization energy in the case of the PF_6^- anion is smaller than that observed for BF_4^-, which can suggests that the weakly associated BF_4^- anions can easier penetrate deep into the film causing structural changes and thus increases the reorganization energy of the system. Anions that associate more strongly with the Fc^+ cation, such as PF_6^-, will not penetrate the film and will maintain strong interactions with the Fc^+ cation, the result is a lower reorganization energy λ for most systems investigated. The reverse order of the reorganization energy dependence on counter-ion observed in the case of Gly containing films, it is likely to be caused by difference in organization of the films. We can speculate that glycine containing Fc-films are uniform throughout the surface providing H-bond saturated layer efficiently affecting film response toward approaching counter-ions, where other compounds that

has side groups i.e methyl or propyl provide additional separation and limit H-bonding interactions between neighboring molecules.[7,9]

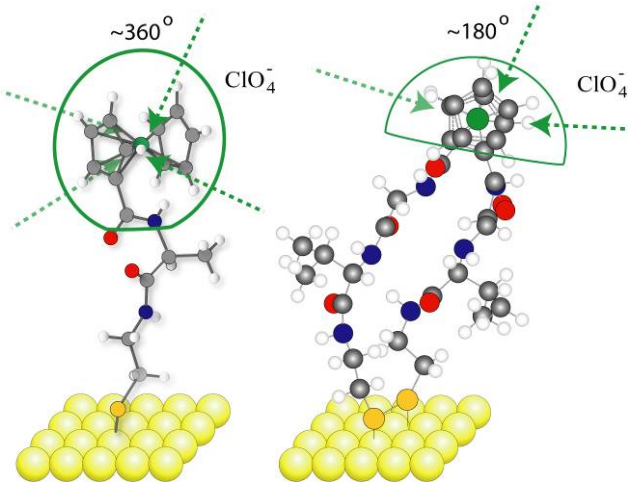

Figure 5.4 Graphical visualization of the differences in the access areas of the counter ion to ferrocenium. Comparison of $[Fc\text{-}Ala\text{-}CSA]_2$ (**2**) with $Fc[Gly\text{-}Val\text{-}CSA]_2$ (**9**) ferrocene- peptide films.

λ in the case of the cyclic Fc-conjugates **5 - 8** is on an average lower by 30-50% when compared to the acyclic Fc-peptide conjugates **1 – 4,** containing the same amino acid linker. Such behavior can be rationalized by evaluating the access of the counter-ion to the ferrocenium moiety. In the case of cyclic compounds, access to the Fc/Fc^+ moiety can be spatially limited thus resulting in lower reorganization energy. Impeded access of the solvent and counter-ion to the Fc^+ moiety provides a possible explanation (Figure 4). In addition, the cyclic compounds **5 - 11** have limited degrees of freedom, which reduce their surface dynamics. Especially important seems to be the freedom of rotation, which is present in the case of conjugates **1 – 4**, allowing a better interaction with the approaching solvent/counter-ion molecules enabling it to change its orientation

on the surface (Figure 5.5). Similar conclusions can be reached by evaluating $\ln A_n$ prexponential factor. Ln A_n has always slightly higher value for acyclic compounds **1** – **4** and ranges from 12 to 17, where for cyclic compounds shows values between 11 and 14. This may suggest that molecular mobility/ferrocenium access can also have some impact on A_n value.

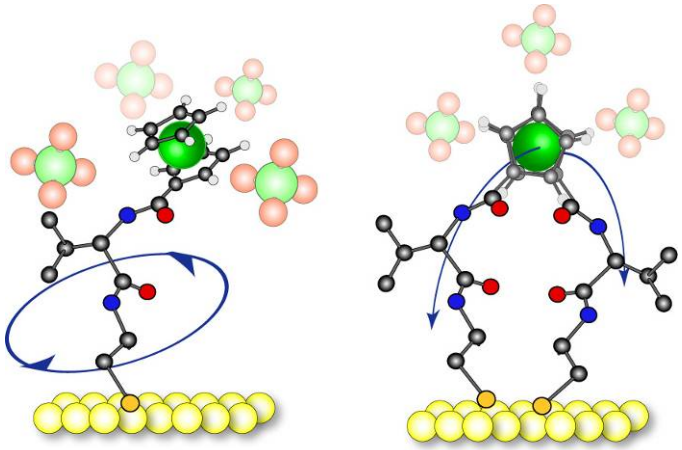

Figure 5.5 Representation of potential dynamics of the Fc-peptide conjugates on a gold surface. Left: very high mobility and freedom to rotate for monosubstituted Fc-peptide conjguates. Right: limited flexibility reducing the ability to change orientation as a solvent/counter ions approach.

An indirect confirmation of molecular mobility can be obtained from measurements of the film capacity. The capacity was measured at two potentials. At 0 mV (vs. Ag/AgCl) the interactions of the counter ions with Fc are negligible, whereas at 900 mV, a potential well above the oxidation potential of Fc, the Fc^+ has very strong interactions with counter ions. Figure 5.6 shows the result of a typical AC experiment for compounds **2** and **6**. The ACVs of both compounds clearly show that the capacitance for a acyclic compound **2** (5.5 $\mu F/cm^2$) is larger compared to the cyclic less flexible system **6** (0.7 $\mu F/cm^2$).

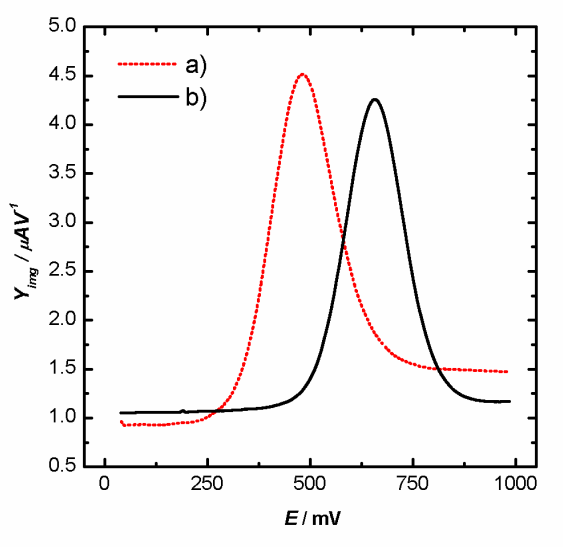

Figure 5.6 AC Voltammetry of a) Fc[Ala-CSA]$_2$ (**6**) b) [Fc-Ala-CSA]$_2$ (**2**) The capacity change measured at 0 mV and 950 mV for a) ΔC = 0.7 μF/cm2 for b) 5.5 μF/cm^2

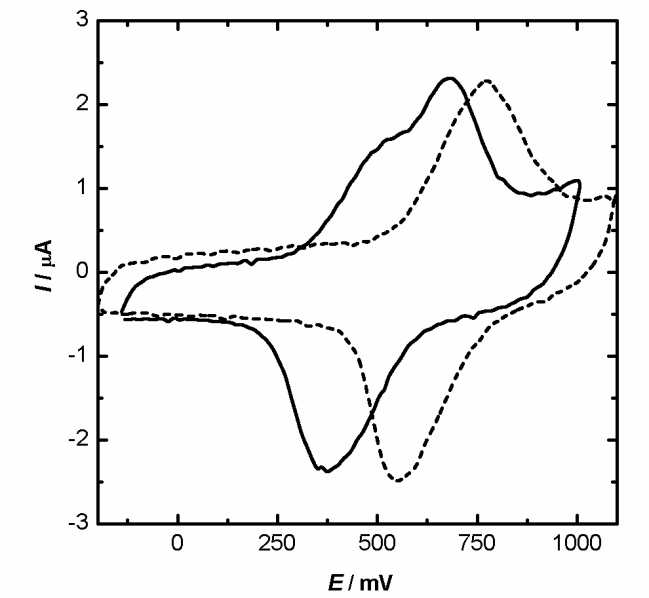

Figure 5.7 Cyclic voltammograms of (----) Fc[Ala-CSA]$_2$ (**6**) and (—) [Fc-Ala-CSA]$_2$ (**2**). Scan rate 1000 Vs^{-1} in 0.1 M $NaBF_4$ as a supporting electrolyte. Compound 2 shows significant phase separation (double oxidation peak) and broadened reduction peak.

The electron transfer rates k_{ET} evaluated for the rigid cyclic Fc-peptide conjugates (**5 - 8**) is, in most cases, faster than the k_{ET} obtained for their corresponding non-cyclic system compounds **1 - 4**. As expected, the k_{ET}s of the cyclic compounds **5 - 11** are virtually unaffected by the presence of different counter-ions and only minor variations of the k_{ET}s were observed (Table 5.1). In contrast, for the non-cyclic conjugates **1 – 4,** the k_{ET}s are significantly lower when weakly associating counter-ion are present.

Ferrocene phase separation, described by B. Lennox[31-33] and others,[30] was observed in the case of the linear Fc-peptide conjugates **3** and **4.** A representative CV is shown in Figure 5.7. We can speculate that the agglomeration might be a result of weak hydrophobic interactions between peptide side-groups (iPr, iBu), which will subsequently leads toward a tighter packing of the ferrocene units. Doubled or broadened oxidation peak was mostly observed when weakly associative BF_4^- was employed (Figure 5.8).

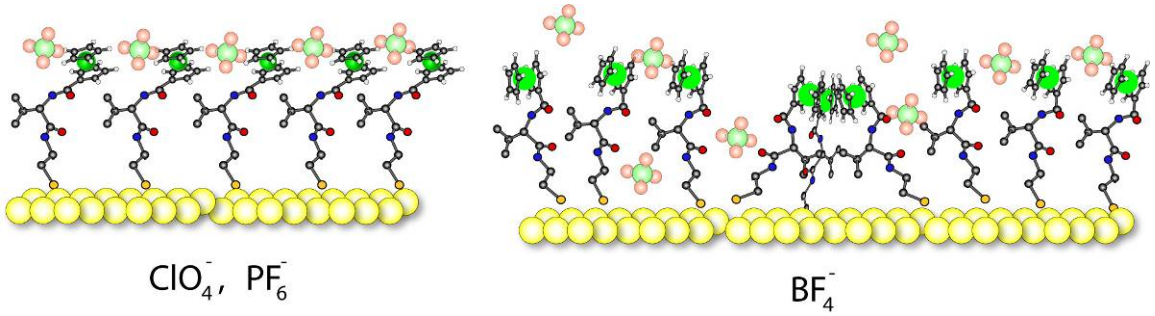

Figure 5.8 Effect of the counter-ion on the agglomeration of the ferrocene.

Weak interactions of the BF_4^- counter-ion with Fc^+ were not able to disrupt the aggregation of the Fc-conjugates on the surface. PF_6^- and ClO_4^- anions were strongly attracted to the Ferrocenium group and as a result more organized films were formed and thus agglomeration was not possible (see Figure 5.8). An aggregation was not observed with any of the cyclic Fc-peptide conjugates **5 – 11**, suggesting again such conjugates have limited flexibility/mobility of on the surface. The investigations on the appearance of the double peak will be pursued further in the future. A possibility to control aggregation by applying different counter-ion will be also investigated.

5.5 Summary

In this contribution, we have investigated the electron transfer properties of cyclic and non-cyclic ferrocene-peptide cystamine conjugates, which differ in the number of podant peptide substitutents and thus in the number of attachment point on the gold surface. Cyclic systems have two peptide chains linking the Fc group to the surface, making it more rigid compared to the non-cyclic analogue. We can hypothesize that this in turn influences the electron transfer process.

In addition, we observed a significant influence in the electron transfer kinetics on the nature of the counterion and its ability to associate with the ferrocene/ferrocenium couple. Counterions were chosen for the ability to associate with the redox couple. BF_4^- exhibits the weakest association while PF_6^- has the strongest interaction. The reorganization energies for the Fc-peptide cystamine films exhibit the highest

reorganization trends for the BF_4^- counterion and the lowest for the PF_6^- counterion. The dynamics of the Fc-peptide cystamine conjugates on the surface as well as more dramatic changes within the double layer that are associated with improved access of counterions to the Fc^+, were described. It is evident that electron transfer can be strongly affected by three major parameters: molecular mobility of the peptide conjugates on the surfaces, the strength of the ion-pair created between Fc^+ and counter-ion, as well as spatial access of the counter-ion to Fc^+.

It was intriguing to note the aggregation of some of the Fc-peptide conjugates. This clearly calls for additional investigations into this behavior since it appears that the aggregation of the conjugates is potential dependent and can be controlled.

Acknowledgments

This work was supported by the National Science and Engineering Research Council of Canada. H.-B.K. is Canada Research Chair in Biomaterials.

5.6 References

1. Chidsey, C. E. D. *Science (Washington, DC, U. S.)* **1991,** 251, 919-922.

2. Finklea, H. O.; Yoon, K.; Chamberlain, E.; Allen, J.; Haddox, R. *J. Phys. Chem. B* **2001,** 105, 3088-3092.

3. Smalley, J. F.; Finklea, H. O.; Chidsey, C. E. D.; Linford, M. R.; Creager, S. E.; Ferraris, J. P.; Chalfant, K.; Zawodzinsk, T.; Feldberg, S. W.; Newton, M. D. *J. Am. Chem. Soc.* **2003,** 125, 2004-2013.

4. Kitagawa, K.; Morita, T.; Kimura, S. *Langmuir* **2005,** 21, 10624-10631.

5. Beratan, D. N.; Betts, J. N.; Onuchic, J. N. *Science* **1991,** 252, 1285-1288.

6. Beratan, D. N.; Onuchic, J. N.; Winkler, J. R.; Gray, H. B. *Science* **1992,** 258, 1740-1741.

7. Sek, S.; Maicka, E.; Bilewicz, R. *Electrochim. Acta* **2005,** 50, 4857-4860.

8. Ogawa, M. Y.; Moreira, I.; Wishart, J. F.; Isied, S. S. *Chem. Phys.* **1993,** 176, 589-600.

9. Kraatz, H.-B.; Bediako-Amoa, I.; Gyepi-Garbrah, S. H.; Sutherland, T. C. *J. Phys. Chem. B* **2004,** 108, 20164-20172.

10. Rowe, G. K.; Creager, S. E. *Langmuir* **1994,** 10, 1186-1192.

11. Creager, S. E.; Rowe, G. K. *J. Electroanal. Chem.* **1997,** 420, 291-299.

12. Weber, K.; Hockett, L.; Creager, S. *J. Phys. Chem. B* **1997,** 101, 8286-8291.

13. Weber, K. S.; Creager, S. E. *J. Electroanal. Chem.* **1998,** 458, 17-22.

14. Herr, B. R.; Mirkin, C. A. *J. Am. Chem. Soc.* **1994,** 116, 1157-1158.

15. Wang, Y.; Cardona, C. M.; Kaifer, A. E. *J. Am. Chem. Soc.* **1999,** 121, 9756-9757.

16. Sek, S.; Moszynski, R.; Sepiol, A.; Misicka, A.; Bilewicz, R. *J. Electroanal. Chem.* **2003,** 550-551, 359-364.

17. Sek, S.; Tolak, A.; Misicka, A.; Palys, B.; Bilewicz, R. *J. Phys. Chem. B* **2005,** 109, 18433-18438.

18. Watanabe, J.; Morita, T.; Kimura, S. *J. Phys. Chem. B* **2005,** 109, 14416-14425.

19. Kitagawa, K.; Morita, T.; Kawasaki, M.; Kimura, S. *J. Polym. Sci., Part A: Polym. Chem.* **2003,** 41, 3493-3500.

20. Morita, T.; Kimura, S. *J. Am. Chem. Soc.* **2003,** 125, 8732-8733.

21. Kitagawa, K.; Morita, T.; Kimura, S. *Angew. Chem., Int. Ed.* **2005,** 44, 6330-6333.

22. Galka, M. M.; Kraatz, H.-B. *Chem. Phys. Chem.* **2002,** 3, 356-359.

23. Bediako-Amoa, I.; Sutherland, T. C.; Li, C.-Z.; Silerova, R.; Kraatz, H.-B. *J. Phys. Chem. B* **2004,** 108, 704-714.

24. Mandal, H. S.; Kraatz, H.-B. *Chem. Phys.* **2006,** 326, 246-251.

25. Orlowski, G. A.; Chowdhury, S.; Long, Y.-T.; Sutherland, T. C.; Kraatz, H.-B. *Chem. Commun.* **2005**, 1330-1332.

26. Chowdhury, S.; Sanders, D. A. R.; Schatte, G.; Kraatz, H.-B. *Angew. Chem., Int. Ed. Engl.* **2006,** 45, 751-754.

27. Chowdhury, S.; Schatte, G.; Kraatz, H.-B. *J. Soc. Chem. Dalton Trans.* **2004**, 1726-1730.

28. Orlowski, G. A.; Kraatz, H.-B. *Electrochim. Acta* **2006,** 51, 2934-2937.

29. Sumner, J. J.; Creager, S. E. *J. Phys. Chem. B* **2001,** 105, 8739-8745.

30. Valincius, G.; Niaura, G.; Kazakeviciene, B.; Talaikyte, Z.; Kazemekaite, M.; Butkus, E.; Razumas, V. *Langmuir* **2004,** *20*, 6631-6638.

31. Lee, L. Y. S.; Lennox, R. B. *Langmuir* **2007,** 23, 292-296.

32. Lee, L. Y. S.; Sutherland, T. C.; Rucareanu, S.; Lennox, R. B. *Langmuir* **2006,** 22, 4438-4444.

33. Lee, L. Y. S.; Lennox, R. B. *PhysChemPhys* **2007,** 9, 1013-1020.

CHAPTER 6
THE EFFECT OF ALKALI METAL IONS ON THE ELECTROCHEMICAL BEHAVIOR OF FERROCENE-PEPTIDE CONJUGATES IMMOBILIZED ON GOLD SURFACES

This chapter is based on the manuscript by G. A. Orlowski, S. Chowdhury, H.-B.Kraatz "The Effect Of Alkali Metal Ions On The Electrochemical Behavior Of Ferrocene-Peptide Conjugates Immobilized On Gold Surfaces". The manuscript was recently submitted for publication to Electrochimica Acta.

I am the main contributor to this manuscript. I have performed all electrochemical experiments and calculations as well as written the first draft of the manuscript. S. Chowdhury provided all Fc-peptides, the synthesis of which is described elsewhere. The final version of the manuscript was obtained in an iterative writing process with my supervisor.

6.1 Connecting Text

In the previous chapter, the interactions of counter-ions with Fc-peptide conjugates were described together with the reorganizational properties of the Fc-peptide films. In this chapter effect of cations on the Fc-peptide films is investigated in detail in order to provide a complete picture of the electrochemical properties of Fc-peptide films on gold surfaces. Research on the electron transfer in DNA films suggested that cations can

significantly change the conductivity of the DNA double-strand. In this chapter, the impact of different alkali metal cations on the electron transfer in peptide films was explored. Notable changes in the ET caused by the presence of cations were observed. Alkaline metals cations are found to affect surface organization of the Fc-peptide films as well. This chapter completes the study of the electrochemical properties of Fc-peptide films.

6.2 Introduction

Metal interactions with peptides and proteins are playing a crucial role in controlling vital cell functions. In particular, interactions of Na^+ and K^+ are important in this context. Protein-metal interactions involving Li^+ are of pharmacological relevance. Peptides offer a number of possible binding sites for metal ions. The metal binding properties of amino acids and peptides are influenced by the steric properties of the particular amino acid and of neighboring amino acids in the peptide chain[1, 2]. In the absence of specific metal binding side chains, such as immidazole or carboxylates, alkali metal ions coordinate to the amide carbonyl oxygens. Ab initial calculations of the interactions of Gly with alkali metal ions showed that the free binding enthalpy decreases on going from Li^+ to Cs^+.[3] Alkali metal coordination to peptides can induce significant conformational changes in the peptide structure, as is the case for K^+-binding to the cyclodepsipeptide valinomycin resulting in the formation of an octahedrally coordinated K^+-peptide complex. Calculations by Ma and Tsang clearly show that K^+

binding to Gly-Gly and Ala-Ala causes significant structural changes in the dipeptide as long as the coordination involved amide C=O groups[4].

In our research, we have been interested in exploiting ferrocene (Fc)-modified peptides for monitoring the interaction with neutral substrates [5]. We recently reported the interaction of a histidine conjugate with metal ions in solution and shown that Li^+ causes significant changes in the secondary structure of the Fc conjugate, presumably due to the interaction with the proximal amide C=O [6]. At present, there are no studies available of surface-bound Fc-peptide conjugates with metal ions. In present study, we have focused on the investigation of the electrochemical behavior of Fc-peptide conjugates bound to gold surfaces in the presence of the alkali metal series. Films prepared from mono- and disubstituted Fc-peptide cystamine (CSA - H_2N-$(CH_2)_2$-S-S-$(CH_2)_2$-NH_2) conjugates were compared: [Fc-Gly-CSA]$_2$ (**1**), [Fc-Ala-CSA]$_2$ (**2**), [Fc-Val-CSA]$_2$ (**3**), [Fc-Leu-CSA]$_2$ (**4**), Fc[Gly-CSA]$_2$ (**5**), Fc[Ala-CSA]$_2$ (**6**), Fc[Val-CSA]$_2$ (**7**), Fc[Leu-CSA]$_2$ (**8**), Fc[Gly-Val-CSA]$_2$ (**9**), Fc[Gly-Ile-CSA]$_2$ (**10**), and Fc[Ile-Ile-CSA]$_2$ (**11**) (see Figures 6.1 and 6.2).

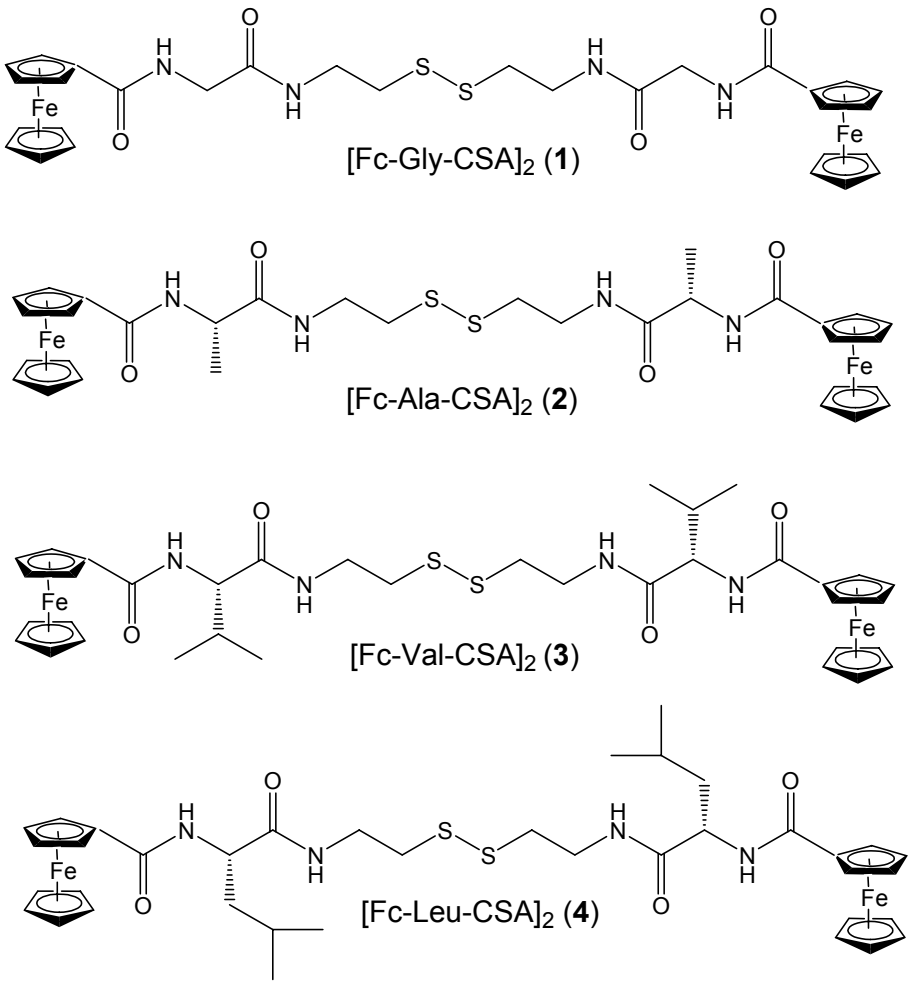

Figure 6.1 Nomenclature and chemical drawings of the acyclic Fc-peptide compounds

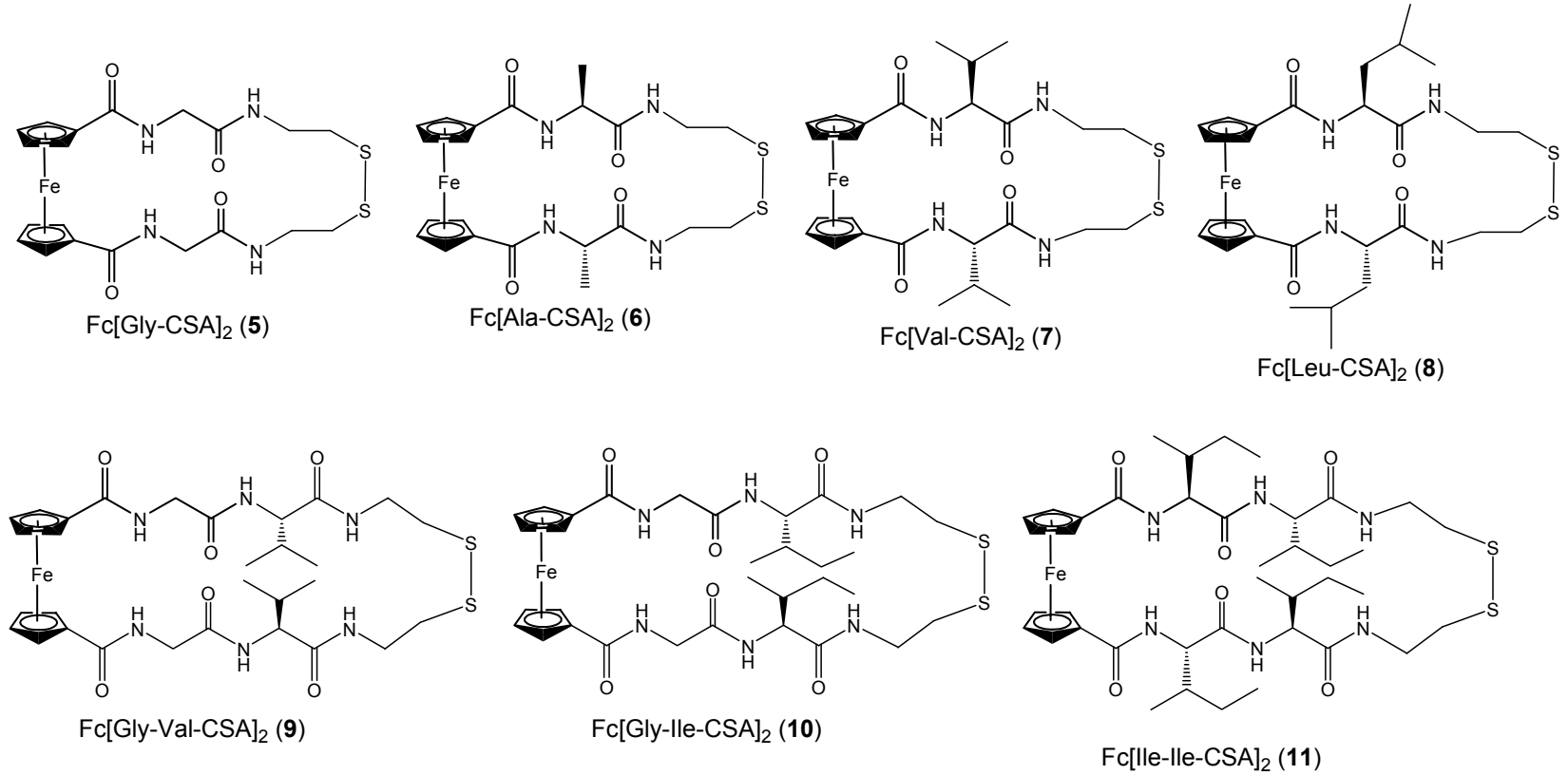

Figure 6.2 Nomenclature and chemical drawings of the cyclic Fc-peptide compounds

6.3 Experimental

All electrochemical experiments were carried out on a home-built potentiostat (production and design Professor A. Baranski, University of Saskatchewan) and a CH Instruments CHI 660B. Ag/AgCl (BAS) was used as a reference electrode and Pt mesh as an auxiliary electrode. Synthesis of the compounds used in this study is described elsewhere [7, 8]

Electrodeposition method used in this study[9] required a pre-treatment step in which gold microelectrode was cycled in 0.5 M H_2SO_4 proceeded by an oxidation for 0.5 s at 2.0 V. In the final preparation step, the electrode was cycled in a negative potential range (-0.6 to -2.3 V) to reduce all remaining surface oxygen and cover the electrode with a layer of hydrogen atoms. Fc-peptide cystamine conjugates **1** - **11** were immobilized on gold microelectrodes (diameter: 25 μm) by electrochemical deposition method,[9] using 10 mM solutions of Fc-peptides **1** – **11** in pure ethanol. A potential of -1.8 V vs. Ag/Ag^+ (quasi reference electrode) in the absence of supporting electrolyte was applied for 30 min to the gold microelectrode. A silver wire was used as a quasi-reference electrode instead typical Ag/AgCl reference electrode during the electrodeposition step to avoid contamination of the gold surface with chlorides. Presence of the chlorides (leaking from Ag/AgCl electrode) lowered Fc-peptide concentration on the surface and quite often resulted in complete inhibition of the film formation. Modified electrodes were washed with copious amounts of ethanol and water then dried under a stream of nitrogen. Each experiment was repeated at least five times to ensure high reproducibility. Electrodeposition, as described in reference 9, allowed

for fast deposition and provided tightly packed Fc-peptide films (Table 6.2). Fc-peptide films obtained that way had improved surface organization and reproducibility when compared to Fc-films obtained by typical "incubation" method.

Electrochemical scans were carried out using the Fc-peptide modified gold microelectrode (25 μm) as a working electrode. Pt wire was used as a counter electrode and a Ag/AgCl reference electrode (BAS, 3 M KCl) at a scan rate of 100 V s^{-1} and 1000 V s^{-1} in 50 mM $HClO_4$ with the addition of 25 mM alkali metal perchlorate salt ($XClO_4$, X = Li^+, Na^+, K^+, Rb^+, Cs^+). The concentration of metal alkali perchlorates was kept below their respected maximum solubility. Addition of perchloric acid to alkali metal solutions maintains a constant pH, as well as similar ionic strength throughout all experiments.

6.4 Results and Discussion

It is well known that Fc immobilized on the surface is highly sensitive to counter ions used as the supporting electrolyte.[10, 11] In order to minimize counter-ion effects, we kept the counter ions and its concentration approximately constant and varying the concentration of cations by addition of the alkali metals perchlorates. Our experimental data shows that the ClO_4^- concentration has only a small effect on the formal potential of the Fc-peptide monolayers.

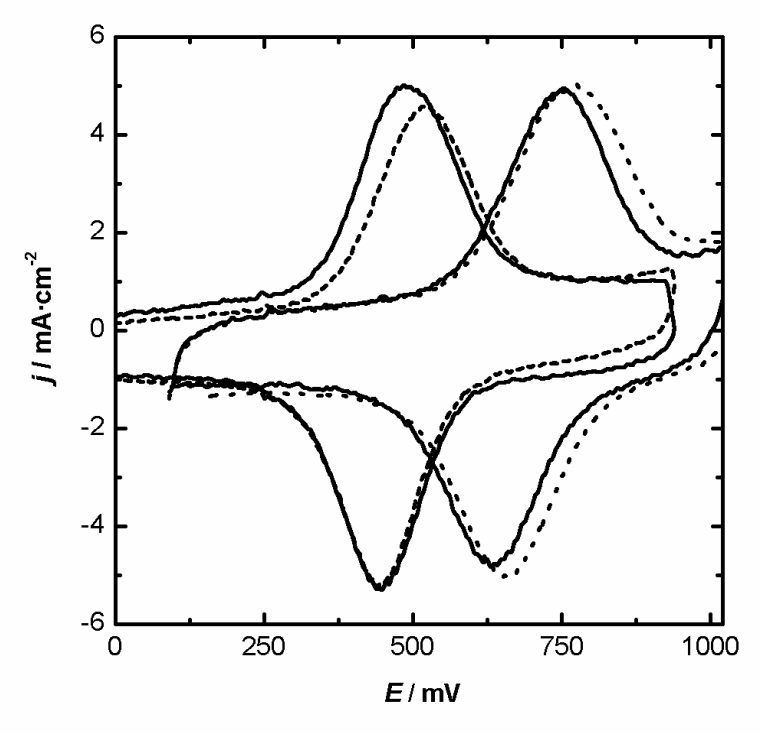

Figure 6.3 Fc-peptide film behavior in the presence of alkaline metals. CV of **1** $[Fc\text{-}Gly\text{-}CSA]_2$ and **5** $Fc[Gly\text{-}CSA]_2$ in 25 mM $XClO_4$ / 50 mM $HClO_4$ (—) X = Li^+ ; (----) X = Rb^+

In 75 mM $HClO_4$ solution, all Fc-peptide cystamine (CSA) films displayed a fully reversible one electron oxidation at a scan rate of 100 Vs^{-1} and 1000 Vs^{-1} respectively. Figure 3 shows a set of typical CVs for the monosubstituted Fc derivative $[Fc\text{-}Gly\text{-}CSA]_2$ (**1**) and for the 1,n'-disubstituted $Fc[Gly\text{-}CSA]_2$ (**5**). This redox response is typical for the two monosubstituted Fc conjugates **1** and **2** and for the disubstituted conjugates **5** – **11**. Table 1 summarizes our experimental findings. The monosubstituted Fc conjugates **1 – 4** exhibit formal potentials E^0 between 385 to 415 mV versus Ag/AgCl with peak separations ΔE_P of 15 to 85 mV indicating facile electron transfer.

Table 6.1 Formal potentials and peak separation values for a series of Fc-peptide films (data presented for CV collected at 100 Vs^{-1})

Cmpd	*H*		*Li*		*Na*		*K*		*Rb*		*Cs*	
	E^0	ΔE	E^0	ΔE	E^0	ΔE	E^0	ΔE	E^0	ΔE	E^0	ΔE
1	415	**50**	375	**45**	400	**35**	410	**60**	400	**80**	395	**50**
2	390	**45**	440	**55**	470	**85**	450	**40**	445	**75**	460	**55**
3	415	**60**	385	**20**	395	**40**	390	**10**	400	**10**	450	**100**
4	385	**15**	410	**45**	370	**20**	410	**35**	385	**25**	460	**80**
5	610	**20**	590	**110**	650	**80**	595	**45**	620	**105**	595	**100**
6	590	**70**	585	**70**	590	**65**	560	**50**	560	**80**	590	**60**
7	585	**80**	545	**80**	570	**30**	570	**35**	560	**45**	580	**35**
8	570	**75**	570	**90**	560	**84**	580	**80**	580	**85**	560	**75**
9	605	**20**	570	**50**	630	**30**	660	**20**	635	**20**	680	**20**
10	635	**70**	600	**40**	635	**15**	620	**40**	650	**40**	620	**60**
11	610	**40**	590	**45**	650	**90**	655	**75**	580	**40**	660	**100**

Errors: **ΔE** ±15 mV, $\mathbf{E^0}$ ±15 mV

The oxidation of the disubstituted Fc conjugates **5** – **11** is observed at more anodic potentials as is expected for disubstituted ferrocenes in a potential range of E^0 of 570 to 635 mV versus Ag/AgCl with larger peak separations ΔE_P of 20 to 110 mV compared to the monosubstituted systems.

Upon addition of metal perchlorate salts, the redox potentials E^0 as well as the peak shape and peak separation of the oxidation and reduction process are affected (see Figures **3** and **4**). The following changes may indicate structural changes within the film in addition to changes in the kinetics of the electron transfer through the peptide linker.

Such electrochemical response might be also explained by differences in the electrolyte/cation penetration into the film. Large ΔE_P were observed for compounds **5** and **11** in the presence of Cs^+.

Table 6.2 Surface concentrations of compounds **1 – 11**

Compound	Surface concentration $\Gamma \times 10^{-10}$ (mol/cm^2) [9]
1	3.3
2	4.6
3	2.6
4	2.3
5	3.5
6	2.4
7	2.8
8	2.8
9	1.7
10	1.4
11	1.3

Error: $\pm 0.4 \times 10^{-10}$ mol/cm^2

It is interesting to note that the redox behavior of the two monosubstituted Fc conjugates $[Fc\text{-}Val\text{-}CSA]_2$ **3** and $[Fc\text{-}Leu\text{-}CSA]_2$ **4** is more complex. Both Fc-conjguates display a "double oxidation" (see Figure 4). Both conjugates possess bulky hydrophobic side-chains (isopropyl for **3** and isobutyl for **4**). The hydrophobic nature of the side-chain may be responsible for a specific packing interaction on the surface minimizing the exposure of these hydrophobic sidechains to water, presumably resulting in association of these Fc-conjugates on the gold surface, effectively resulting in a phase separation. Similar redox responses were reported by B. Lennox[12-14] , C. E. D. Chidsey[15], Creager[16-19] and others[20-29] for Fc-alkanenthiols and were related to a ferrocene agglomeration (similarly to Figure 6.5) occurring on the gold surface where

island-like Fc-agglomerated structures were suggested. Usually symmetrical broadening, or even additional oxidation and reduction peaks were described. An agglomerated Fc group has a different formal potential when compared with a Fc that it is in not-agglomerated form, resulting in the appearance of additional second oxidation and reduction peak. Importantly, the corresponding disubstituted Fc systems do not exhibit such a redox behavior, presumably due to significantly lower mobility of the molecules on the surface due to both peptide chains being linked to the Au surface. In the case of monosubstituted conjugates **3** and **4**, the mobility is less restricted allowing the conjugates to cluster creating island-like features on the surface.

Interestingly cations introduced into the solution have feasible effect on the electrochemical response. In the presence of alkali metal ions, the two redox signals are affected differently (Figure 6.4), suggesting that metal ions interact differently with the two different peptide environments present in the surface agglomerated peptide conjugates. The presence of these cations in the solvent may even promote aggregation (Figure 6.4).

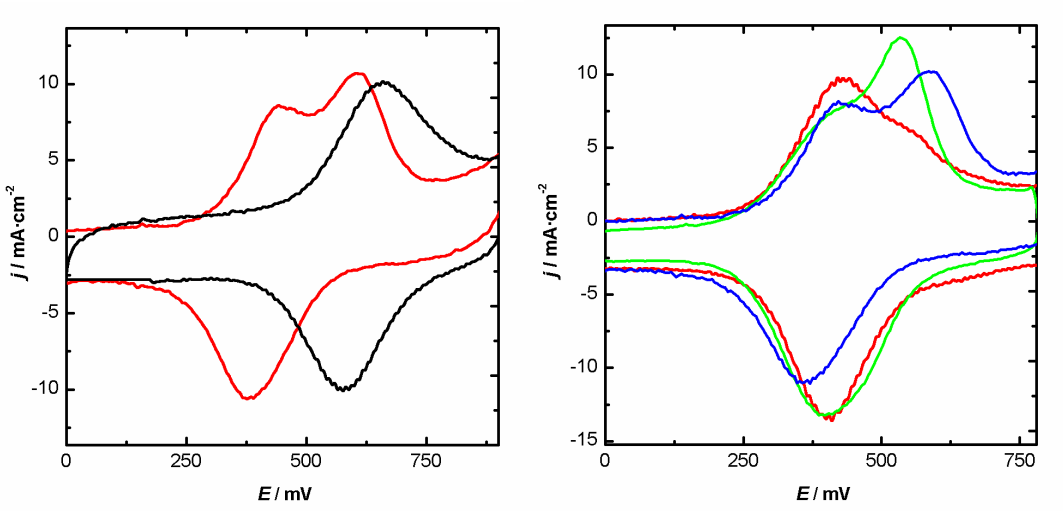

Figure 6.4 Right: Cyclic voltammetry recorded at 100 Vs^{-1} for compound **3** in the presence of Li^+ (–), Na^+ (–), and Cs^+ (–) perchlorate. Left: comparison of cyclic voltammograms recorded for compounds **3** and **7** at 100 Vs^{-1} in Cs^+ containing solutions.

In contrast to Fc-alkanethiol films, our Fc-peptide films of compounds **3** and **4** exhibit a single reduction process. A possible explanation for this phenomenon is presented in Figure 6.5 An agglomerated state is broken when the Fc group is oxidized and significant repulsion occurs between the Fc^+ groups. This repulsion may then result in a redistribution of Fc-peptides on gold surfaces. We have observed significant repulsion before in films of Fc-collagen conjugates[30]. In these systems, three Fc-peptide strands are forming a supramolecular H-bonded helix, bringing the three Fc groups in close proximity. Upon oxidation in Fc-collagens, the H-bonding interactions holding the three individual strands together adjusts in an effort to accommodate the electrostatic repulsion between the cationic Fc^+ groups.[30]

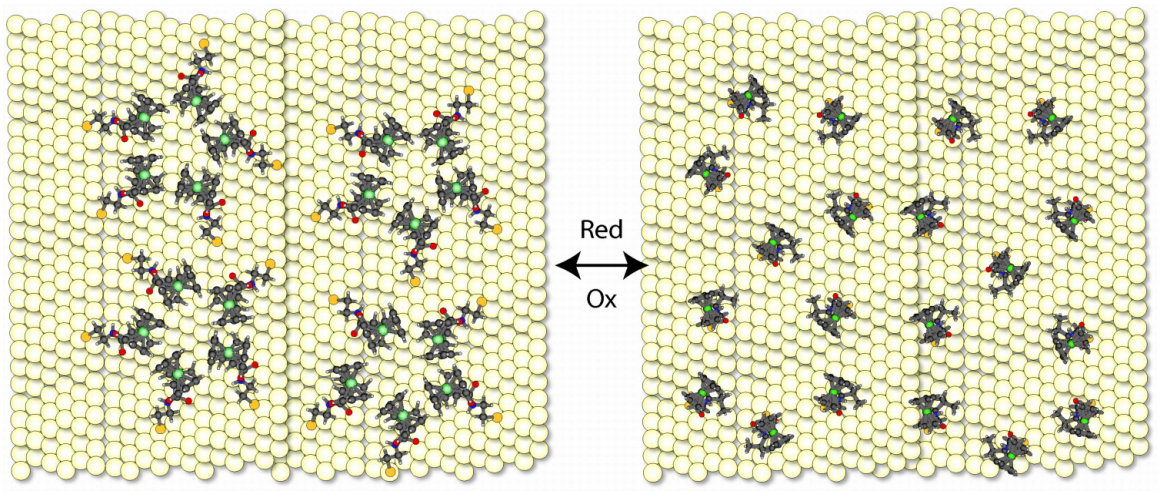

Figure 6.5 Proposed organization of [Fc-Val-CSA]$_2$ (**3**) and of [Fc-Leu-CSA]$_2$ (**4**) on the surface caused by cations and counter ion. Hydrophobic "tail" from Val or Leu is oriented toward other hydrophobic groups creating micelle-like structures bringing ferrocene groups close together, which is likely to coexist with non-agglomerated state. After oxidation, ferrocennium groups repel each other creating purely non-agglomerated film.

We also notice that the integrated charge ratio for these monosubstituted Fc-peptide conjugates **3** and **4**, obtained by dividing the area of oxidation peaks by area of the reduction peak, is higher than unity and ranges from 1.5 to 1.7 for Li and Cs respectively. This observation cannot be rationalized by a loss of oxidized Fc-peptide from the surface. In fact, prolonged cycling clearly showed no loss in signal intensity, which is expected if any redox active material is lost from the electrode surface. We offer an alternative explanation, which takes into account additional pseudo-capacitive response from mobile monosubstituted Fc-peptide conjugates. This in fact to some extent could account for this unusual ratio.

Current of the second oxidation peak in each case showed linear dependency with the scan rate. Peak separation between second oxidation wave and reduction ranges from 100 mV at 100 Vs^{-1} to more than 300 mV at 1000 Vs^{-1}. First oxidation wave showed peak separation 10 to 100 mV depending on the peptide linker and cation (Table 6.1) at 100 Vs^{-1}. Differences in the peak separation were even smaller at 1000 V s^{-1} and ranged between 125 and 200 mV.

Small variations in the differential capacity of the Fc-peptide films can be reported. Lowest capacity of 8 ± 2 μF/cm^2 was observed in solutions containing K^+ and H^+. Highest capacity of 12 ± 2 μF/cm^2 was observed in case of Na^+ and Li^+.

Table 6.3 Influence of alkaline cations on basic electrochemical parameters of the Fc-peptide film. k_{ET} values were determined at a scan rate of 1000 Vs^{-1} according to the procedure described elsewhere[31].

	$k_{ET}[s^{-1}]$ *10^3 ±1.5	
cations	***Fc[Gly-CSA]$_2$***	***Fc[Ile-Ile-CSA]$_2$***
H^+	**9.0**	**11.5**
Li^+	**3.0**	**11.0**
Na^+	**4.5**	**8.0**
K^+	**7.0**	**8.0**
Rb^+	**6.0**	**12.0**
Cs^+	**3.5**	**6.5**

Having observed an effect of cations on the electrochemical response for Fc-peptide conjugates presumably by altering the structure of the Fc-peptides on the gold surface raises the question if the presence of various cations can alter the electron transfer kinetics in Fc-peptide films? We measured the electron transfer kinetics for two disubstituted peptide systems Fc[Gly-CSA]$_2$ (**5**) and Fc[Ile-Ile-CSA]$_2$ (**11**). Table 6.2 summarizes the experimental results. Both films show significantly lower k_{ET}s in the

presence of Cs^+. The difference between Rb and Cs cations is striking, showing an almost twofold decrease in the ET rate for Cs^+ compared to Rb^+. The size of hydrated Rb and Cs cation is identical and has an approximate size of 2.28 Å. We rationalize these results by suggesting that the presence of cations alters the agglomeration and orientation of the Fc-peptide conjugates on the surface, altering the observed electron transfer kinetics. To the best of our knowledge, such effect was never observed before.

6.5 Summary

We have immobilized a series of Fc-peptide conjugates and investigated the electrochemical response of these films in the presence of alkali metal cations Li^+ to Cs^+. In some cases, significant changes in the redox responses were observed in the form of changes in the formal potential E^0 (for up to 100 mV) and in changes in the peak separation ΔE_P (up to 90 mV). Observed changes in electrochemical response can be explained by invoking differences in film penetration by respected cations.

Two of the monosubstituted Fc-peptide systems investigated (**3**) and (**4**) exhibited agglomeration on the surface, presumably due to the hydrophobic amino acids Val and Leu, which causes association of the Fc-peptide conjugates on the surface to form clusters and has been observed before for Fc-alkanethiols films. $[Fc\text{-}Val\text{-}CSA]_2$ (**3**) and $[Fc\text{-}Leu\text{-}CSA]_2$ (**4**) exhibit two oxidation waves but only a single reduction wave. The appearance of the uncommon single reductive peak is explained by proposing increased mobility of the monosubstituted Fc-peptide compounds and a redistribution of the systems on the surface due to electrostatic repulsion between the

Fc^+ groups. The presence of alkali metal ions alters the ability of the Fc-peptides to aggregate on the surface or by changes in the orientation of the Fc group in the film, which in turn affects the observed rate of electron transfer.

Acknowledgement

This work was supported by the National Science and Engineering Research Council of Canada. H.-B.K. is the Canada Research Chair in Biomaterials.

6.6 References

1. M. Remko, B. M. Rode, *J. Phys. Chem. A* **2006**, 110, 1960-1967.
2. A. H. Eder, S. Saetia, B. M. Rode, *Inorg. Chim. Acta* **1993**, 207, 3-10.
3. S. Hoyau, G. Ohanessian, *Chemistry Eur. J.* **1998**, 4, 1561-1569.
4. C. H. S. Wong, N. L. Ma, C. W. Tsang, *Chemistry. Eur. J.* **2002**, 4909 – 4918.
5. P. Saweczko, G. D. Enright, H.-B. Kraatz, *Inorg. Chem.* **2001**, 40, 4409-4419.
6. S. Chowdhury, G. Schatte, H.-B. Kraatz, *Eur. J. Inorg. Chem.* **2006**, 988-993.
7. S. Chowdhury, D. A. R. Sanders, G. Schatte, H.-B. Kraatz, *Angew. Chem., Int. Ed.* **2006**, 45, 751-754.
8. S. Chowdhury, G. Schatte, H.-B. Kraatz, *Dalton. Trans.* **2004**, 1726-1730.
9. G. A. Orlowski, S. Chowdhury, Y.-T. Long, T. C. Sutherland, H.-B. Kraatz, *Chem. Commun.* **2005**, 1330-1332.
10. P. D. Beer, P. V. Bernhardt, *J. Chem. Soc., Dalton Trans.* **2001**, 1428-1431.
11. P. D. Beer, J. J. Davis, D. A. Drillsma-Milgrom, F. Szemes, *Chem. Commun.* **2002**, 1716-1717.
12. L. Y. S. Lee, R. B. Lennox, *Phys. Chem. Chem. Phys.* **2007**, 9, 1013-1020.
13. L. Y. S. Lee, R. B. Lennox, *Langmuir* **2007**, *23*, 292-296.

14. L. Y. S. Lee, T. C. Sutherland, S. Rucareanu, R. B. Lennox, *Langmuir* **2006**, *22*, 4438-4444.

15. C. E. D. Chidsey, C. R. Bertozzi, T. M. Putvinski, A. M. Mujsce, *J. Am. Chem. Soc.* **1990**, 112, 4301-4306.

16. G. K. Rowe, S. E. Creager, *Langmuir* **1991**, 7, 2307-2312.

17. S. E. Creager, K. Weber, *Langmuir* **1993**, 9, 844-850.

18. G. K. Rowe, S. E. Creager, *Langmuir* **1994**, 10, 1186-1192.

19. G. K. Rowe, S. E. Creager, *J. Phys. Chem.* **1994**, 98, 5500-5507.

20. E. Sabatani, I. Rubinstein, *J. Phys. Chem.* **1987**, 91, 6663-6669.

21. D. M. Collard, M. A. Fox, *Langmuir* **1991**, 7, 1192-1197.

22. K. Uosaki, Y. Sato, H. Kita, *Langmuir* **1991**, 7, 1510-1514.

23. K. Weber, S. E. Creager, *Anal. Chem.* **1994**, 66, 3164-3172.

24. T. Kondo, M. Takechi, Y. Sato, K. Uosaki, *J. Electroanal. Chem.* **1995**, 381, 203-209.

25. J. N. Richardson, S. R. Peck, L. S. Curtin, L. M. Tender, R. H. Terrill, M. T. Carter, R. W. Murray, G. K. Rowe, S. E. Creager, *J. Phys. Chem.* **1995**, 99, 766-772.

26. J. N. Richardson, G. K. Rowe, M. T. Carter, L. M. Tender, L. S. Curtin, S. R. Peck, R. W. Murray, *Electrochim. Acta* **1995**, 40, 1331-1338.

27. G. K. Rowe, M. T. Carter, J. N. Richardson, R. W. Murray, *Langmuir* **1995**, 11, 1797-1806.

28. Y. Sato, F. Mizutani, K. Shimazu, S. Ye, K. Uosaki, *J. Electroanal. Chem.* **1997**, 434, 115-119.

29. J. J. Calvente, R. Andreu, M. Molero, G. Lopez-Perez, M. Dominguez, *J. Phys. Chem. B* **2001**, 105, 9557-9568.

30. I. Bediako-Amoa, T. C. Sutherland, C.-Z. Li, R. Silerova, H.-B. Kraatz, *J. Phys. Chem. B* **2004**, 108, 704-714.

31. G. A. Orlowski, H.-B. Kraatz, *Electrochim. Acta* **2006**, 51, 2934-2937.

CHAPTER 7

SUMMARY AND CONCLUSIONS

7.1 Electrodeposition

In the previous chapters, I demonstrated that electrodeposition is very versatile method and can be applied for the immobilization of a range of different molecules containing disulfide bonds (Chapter 2 & 3). Therefore one of the objectives of my thesis outlined in the introduction was successfully completed. A scheme that compares typical "soaking" and electrodeposition method is presented in Figure 7.1.

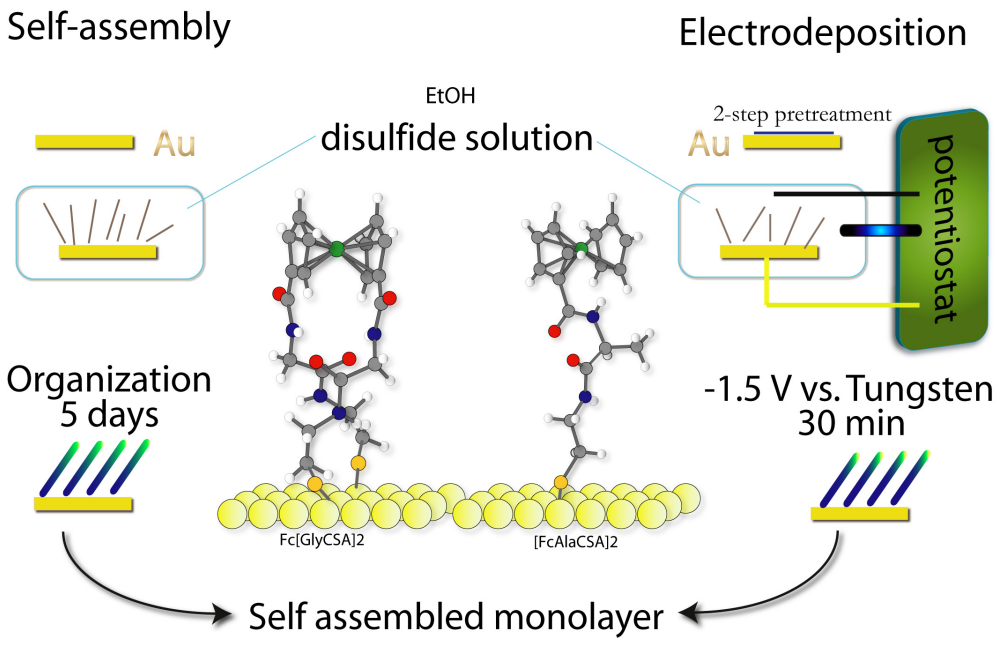

Figure 7.1 Comparison of the incubation and electrodeposition methods showing the different conditions and time requirements

Films prepared by electrochemical deposition were tightly packed and well ordered. However, it was also shown in chapters 3 and 4 that the electrodeposition process in cases of amino acid residues with bulky alkyl chains (valine and leucine) can cause additional structural changes and lack of organization of the film. This method allows significant time to be saved, especially when compared to the typical self-assembly by the lengthy immersion of an electrode surface in a disulfide solution. The electrodeposition method developed for disulfides in this thesis should find widespread application for the deposition various films derived from disulfides on gold surfaces. In Figure 7.2, the electrochemical responses of the electrodeposited mixed films are presented.

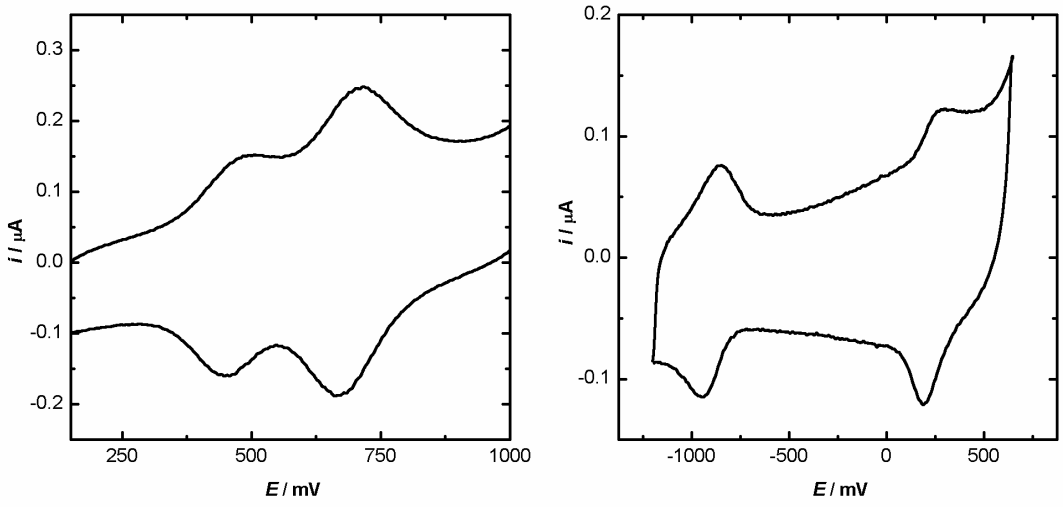

Figure 7.2 Two examples of electrochemically deposited mixed monolayers. Left: CV of mixed cyclic Fc[Ala-CSA]$_2$ and acyclic [Fc-Ala-CSA]$_2$. Right: CV of the monolayer composed of Co-sar and [Fc-Ala-CSA]$_2$.

Rapid and efficient deposition of the various single and mixed disulfide modified compounds should enable a completely new section of surface chemistry to become readily accessible. For example, this method may enable the rapid and efficient assembly of a range of disulfide-containing molecules onto surfaces that can be screened for their performance in solar energy conversion. Surface preparation and screening by traditional incubation methods would not be time efficient. Thus, the electrodeposition method described in this thesis will help to shorten significantly the time required and in addition, the films will have improved packing. This may facilitate research in molecular electronics, biosensing and molecular devices.

7.2 Electron Transfer and Peptide Films

In this thesis, it was successfully established that the current description of ET in peptides may not be sufficient and further development in this field should take into the account additional parameters. It was shown that electron transfer is mainly affected by hydrogen bonds. The effect of hydrogen bonding is mostly detectable in the case of glycine containing Fc-peptide conjugates. Such compounds are known to engage in inter- and intramolecular hydrogen bonding.[1-3] Both cyclic and acyclic compounds showed identical ET rate $8.2*10^3$ s^{-1} when ClO_4^- was used as the supporting electrolyte (Chapter 5). These results suggest that H-bonding is one of major parameters affecting ET, similarly to the observations made by Bielewicz[2, 3] and Kraatz.[4] H-bonding present in Fc-Gly systems: $Fc[Gly\text{-}CSA]_2$ (two attachments with surface) versus $[Fc\text{-}Gly\text{-}CSA]_2$ (only single connection with surface) was able to overcome differences in ET

originating from the variations in flexibility of the molecules on the surface. A comparison of the reorganization energies (Chapter 5) for both of these compounds (0.65 eV in ClO_4^- and 0.52 eV in BF_4^- for acyclic $[Fc\text{-}Gly\text{-}CSA]_2$ and 0.52 eV in ClO_4^- and BF_4^- for $Fc[Gly\text{-}CSA]_2$) further supports the hypothesis that H-bonding can affect ET by actually limiting dynamics of the molecules on the surface. For an immobilized molecule to change the orientation and engage in interactions with the counter-ion, it has to overcome H-bonding from the neighboring glycine containing conjugates.

Interestingly, longer Fc-peptide conjugates with a glycine subunit that engage in intra-molecular H-bonding[5] exhibit unusually fast ET rates ($1*10^4$ s^{-1} for $Fc[Gly\text{-}Val\text{-}CSA]_2$ and $8*10^3$ s^{-1} for $Fc[Gly\text{-}Ile\text{-}CSA]_2$). For these longer peptide conjugates, it is expected that the ET rate will significantly decrease with the distance. However, our experimental results indicate otherwise. The evidence presented in chapter 5 provides important auxiliary information that H-bonding may indeed be a major parameter governing ET in peptides.

It was also shown that the number of the attachments of the Fc-peptide conjugate on a gold surface has a tremendous effect on the ET rate. The best example to illustrate this influence is to compare two Fc-peptide conjugates that are containing alanine as a bridging element. $[Fc\text{-}Ala\text{-}CSA]_2$ is linked to the gold surface with a single Au-S-peptide linkage, while the integrity of $Fc[Ala\text{-}CSA]_2$ is maintained linking it to the gold surface with two Au-S-peptide linkages The electron transfer rate for $Fc[Ala\text{-}CSA]_2$, which is attached with two peptide wires to the gold surface, is more then two times higher with a k_{ET} of $9.0*10^3$ s^{-1}, compared to the k_{ET} of $[Fc\text{-}Ala\text{-}CSA]_2$, which is $4.4*10^3$ s^{-1} and has only single connection with the gold surface. The effect of

rigidity/counter-ion access on the reorganization energy can be also observed in this example. The reorganizational energy due to the increased freedom to rotate[6, 7] and re-arrange towards the approaching molecules of the counter-ion is always higher in the case of acyclic compound ($[Fc\text{-}Ala\text{-}CSA]_2$ 0.71 eV versus 0.33 eV for the more constrained $Fc\text{-}[Ala\text{-}CSA]_2$). This observation important suggests that the dynamic properties of the molecules on the surface is affecting to the observed ET rates. The unusual ET rates can be explained by introducing considering the dynamic properties of the molecules on the surface as was suggested by other researchers.[8, 9]

The proximity of the bulky hydrophobic groups is strongly affecting not only the ET rate but also the reorganization energy. The shielding of the ferrocene is the best observable for $[Fc\text{-}Leu\text{-}CSA]_2$ and $Fc[Leu\text{-}CSA]_2$. Both compounds have the lowest reorganization energy of all Fc-conjugates, determined at 0.48 eV and 0.29 eV in ClO_4^-. An even smaller reorganization energy was observed in strongly associating counter-ion PF_6^- 0.30 eV for acyclic and record low 0.19 eV for cyclic conjugate. Interestingly electron transfer rates were one of the fastest observable $8.0*10^3$ and $1.2*10^4$ s^{-1} for cyclic conjugate. This result seems to indicate that counter-ions are one of factor influencing the ET rate. The effect on the ET of the buried, in alkene chains, ferrocene groups was reported before.[10] The results presented in chapter 5 strongly suggest that not only exposure of the ferrocene to the incoming counter-ions is important but also neighboring hydrophobic groups that are able significantly impede Fc-peptide film penetration by counter-ions and therefore the ET process are of relevance. The observations described above are significantly enhancing our knowledge about solvent and counter-ions effect imposed on Fc-conjugated films. This knowledge could be

further developed and tested by in-depth studies of much more complicated structures like proteins containing electroactive groups.

Another interesting observation is made that acylclic compounds containing hydrophobic groups, such as Val and Leu in the case of the peptide conjugates [Fc-Val-CSA]$_2$ and [Fc-Leu-CSA]$_2$, have the tendency to agglomerate on the surface. Importantly, the agglomeration appears to be triggered by anions present in solution. Agglomeration was especially pronounced in the presence of the weakly associating counter-ion BF_4^-. A second oxidation peak from agglomerated ferrocene groups are observed. Agglomeration was never observed in the case of more rigid cyclic compounds, lending support to the hypothesis that flexibility of the linkage and the dynamic properties of the peptide conjugates are ultimately responsible for the observed behaviour. The results described in chapters 3 and 5 significantly expand our present knowledge about hydrophobic sidegroups and their interactions in close proximity of the ferrocene/ferrocenium and their direct effect on the ET.

The asymmetry in the forward and back electron transfer rates as shown by the asymmetry in the Tafel plots, reported in chapter 4, obtained for Fc-valine conjugate immobilized on the surface, contradict observations made by other groups which attributed asymmetry in electron transfer to a strong dipole moment.[11-13] Very short peptides used in our study do not have strong dipole moment. Such observations as described in chapter 4 may be rationalized in terms of surface organization of the molecules and limited solvent/counter-ion penetration into the film. This initial result gave rise to an in depth investigation into the role of the counter anion in chapter 5. Our investigations clearly show that the ability of the counter-ion to associate with the

ferrocenium cation has a tremendous effect on the reorganization energy of the system. Previous reports by Razumas[14] and Leech[15] described only shifts of the formal potential without any in dept analysis of the parameters governing the electrochemical response of the Fc-films. In essence, the stronger the interaction of the counter-ion with the ferrocenium cation, the lower the organization energy. Values for λ between 0.2 and 0.3 eV for the PF_6^- and 0.4 - 0.5 eV for weakly associating BF_4^- in a case of cyclic Fc-conjugates were observed. Accordingly, the acyclic compounds had λ value between 0.3 - 0.7 eV for the strongly associating anion PF_6^- and between 0.5 – 0.9 eV for the weakly associating anion BF_4^-. Interestingly, the changes in the reorganization energy were always higher for the more flexible acyclic molecules. For example, for. [Fc-Ala-CSA]$_2$ λ increases from 0.48 eV in PF_6^- to 0.86 eV in BF_4^-, while the increases in λ for the cyclic and more ridig Fc[Ala-CSA]$_2$ are significantly lower (λ = 0.28 eV for PF_6^- and 0.45 eV for BF_4^-). Interestingly, the fastest ET rates were always observed for the strongly associating PF_6^- counter-ion. Experimental data presented in this thesis clearly indicate that the association between the counter-ion and the ferrocenium cations affects the film dynamics. Based on this result, it can be concluded that the ordering of the molecules within the film and/or the dynamic properties of the individual molecules have a direct effect not only on the observed ET rates but also on the reorganization energy of the system. These results carry enormous importance that should enhance our understanding of the parameters governing ET in proteins.

In my research described in Chapter 6, I was able to demonstrate that the presence of different cations can significantly affect the observed ET rate of the system. Li^+ and Cs^+, through completely different mechanism, were able to cause major changes

in the organization of the Fc-peptide films. Valine and leucine-containing films were prone to agglomeration in the presence of Li^+ or Cs^+. The CVs for these Fc-peptide films exhibit a second oxidation wave characteristic of systems that agglomerate on the surface. The organization of the molecules agglomeration was affecting the measured ET rates mainly by affecting dynamic properties of the molecules on the gold surface. Cyclic compounds showed major changes in the redox potential as well as oxidation/reduction peak separation. Gaining control over the agglomeration of the molecules on the surface may provide a method for the construction of "smart" switchable materials. Clearly, this has to be investigated in more detail but it can be envisioned that cation-triggered structural changes maybe be a valuable contribution leading to new stimuli-responsive films.. A more immediate application may be to exploit this property for the construction of peptide-based cation detectors.

As described in chapters 2, 4, and 5, the interactions that are occurring between neighboring molecules, like H-bonding between glycine subunits or the agglomeration of the ferrocenes caused by lateral hydrophobic associations between bulky valine and leucine side-chains, were responsible in a significant way for the reorganization energies and ET rates in the Fc-peptide films. This information should guide future researchers toward better understanding of the dynamic properties of peptide based films.

The major objectives of this work were achieved, and in summary we can conclude that in the literature[8, 9, 16, 17] some important parameters (peptide mobility/flexibility, strength of the ion pairing, interactions with neighboring molecules, cation interactions) that are affecting the ET process in peptides were overlooked. Work

described in this thesis provides a deeper understanding of the electron transfer process through peptide chains and a better understanding of the behavior and properties of Fc-peptide films. Even a small change in the side-chain of the peptide (-methyl group exchanged for iso-butyl) can cause dramatic changes not only in the ET rate but also in the film surface organization. A small change in the concentration or addition of different cation can be directly responsible for unusual electrochemical response that was observed.

7.3 References

1. Sek, S.; Moszynski, R.; Sepiol, A.; Misicka, A.; Bilewicz, R., *J. Electroanal. Chem.* **2003,** 550-551, 359-364.

2. Sek, S.; Sepiol, A.; Tolak, A.; Misicka, A.; Bilewicz, R., *J. Phys. Chem. B* **2004,** 108, 8102-8105.

3. Sek, S.; Maicka, E.; Bilewicz, R., *Electrochim. Acta* **2005,** 50, 4857-4860.

4. Bediako-Amoa, I.; Sutherland, T. C.; Li, C.-Z.; Silerova, R.; Kraatz, H.-B., *J. Phys. Chem. B* **2004,** 108, 704-714.

5. Chowdhury, S.; Sanders, D. A. R.; Schatte, G.; Kraatz, H.-B., *Angew. Chem., Int. Ed.* **2006,** 45, 751-754.

6. Viana, A. S.; Jones, A. H.; Abrantes, L. M.; Kalaji, M., *J. Electroanal. Chem.* **2001,** 500, 290-298.

7. Viana, A. S.; Abrantes, L. M.; Jin, G.; Floate, S.; Nichols, R. J.; Kalaji, M., *Phys. Chem. Chem. Phys.* **2001,** 3, 3411-3419.

8. Morita, T.; Kimura, S., *J. Am. Chem. Soc.* **2003,** 125, 8732-8733.

9. Malak, R. A.; Gao, Z.; Wishart, J. F.; Isied, S. S., *J. Am. Chem. Soc.* **2004,** 126, 13888-13889.

10. Sumner, J. J.; Creager, S. E., *J. Phys. Chem. B* **2001,** 105, 8739-8745.

11. Fox, M. A.; Galoppini, E., *J. Am. Chem. Soc.* **1997,** 119, 5277-5285.

12. Fujita, K.; Bunjes, N.; Nakajima, K.; Hara, M.; Sasabe, H.; Knoll, W., *Langmuir* **1998,** 14, 6167-6172.

13. Sek, S.; Tolak, A.; Misicka, A.; Palys, B.; Bilewicz, R., *J. Phys. Chem. B* **2005,** 109, 18433-18438.

14. Valincius, G.; Niaura, G.; Kazakeviciene, B.; Talaikyte, Z.; Kazemekaite, M.; Butkus, E.; Razumas, V., *Langmuir* **2004,** 20, 6631-6638.

15. Ju, H.; Leech, D., *Phys. Chem. Chem. Phys.* **1999,** 1, 1549-1554.

16. Isied, S. S.; Ogawa, M. Y.; Wishart, J. F., *Chem. Rev. (Washington, DC, U. S.)* **1992,** 92, 381-394.

17. Miura, Y.; Kimura, S.; Imanishi, Y.; Umemura, J., *Langmuir* **1998,** 14, 6935-6940.

APPENDIX A

UNIVERSITY OF CALGARY

CHEMISTRY

Science
Science B/325
Telephone: (403) 220-7559
Fax: (403) 289-9488
Email: sutherlt@ucalgary.ca

May 14, 2007

To: Whom it may concern

Re: Permission to Grzegorz Orlowski

Grzegorz Orlowski has my permission to use the following article for the purpose of his Doctoral thesis.

Orlowski, G. A.; Chowdhury, S.; Long, Y.-T.; Sutherland, T. C.; Kraatz, H.-B. *Chemical Communications* **2005**, 1330-1332.

Sincerely,

Todd Sutherland
Assistant Professor

2500 University Drive N.W., Calgary, Alberta, Canada T2N 1N4 • www.ucalgary.ca

4.05.2007

Re: Permission

I hereby grant Grzegorz Orlowski my permission to use the following article for the purpose of his Ph.D. thesis.

Orlowski, G. A.; Chowdhury, S.; Long, Y.-T.; Sutherland, T. C.; Kraatz, H.-B. Chemical Communications 2005, 1330-1332.

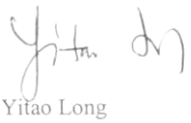

Dr Yitao Long
Department of Chemistry
University of Saskatchewan
110 Science Place
S7N5C9 Saskatoon

Subject: Antwort: Permission
From: VCH-RIGHTS-and-LICENCES <RIGHTS-and-LICENCES@wiley-vch.de>
Date: Thu, 24 May 2007 08:41:57 +0200
To: Grzegorz Orlowski <gro012@mail.usask.ca>

Dear Mr Orlowski,

Thank you for your email.

We hereby grant permission for the requested use expected that due credit is given to the original source.

Please note that we only grant rights for a printed version, but not the rights for an electronic/ online/ web/ microfiche publication.

With kind regards

Bettina Loycke
****
Bettina Loycke
Copyright & Licensing Manager
Wiley-VCH Verlag GmbH & Co. KGaA
Boschstr. 12
69469 Weinheim
Germany

Phone: +49 (0) 62 01- 606 - 280
Fax: +49 (0) 62 01 - 606 - 332
Email: rights@wiley-vch.de

Wiley Bicentennial: Knowledge for Generations
1807-2007

Grzegorz Orlowski
<gro012@mail.usask.ca>

23.05.2007 20:42

An: rights@wiley-vch.de
Kopie:
Thema: Permission

Permission to use co-authored materials in to Ph. D. thesis

I hereby grant permission to Grzegorz Orlowski, Dept of Chemistry, University of Saskatchewan, to use any published and unpublished material that I am co-authoring as a part of his Ph.D. thesis.

Somenath Chowdhury
Department of Chemistry
McMaster University
Hamilton, ON L8S 4M1
Telephone: 905 525 9140 ext 26317
Email: chowsom@mcmaster.ca

Subject: EJIC paper permission for use
From: George Koutsantonis <gak@chem.uwa.edu.au>
Date: Tue, 15 May 2007 16:44:04 +0800
To: gro012@mail.usask.ca
CC: ahw@chem.uwa.edu.au, Jack Harrowfield <harrowfield@chimie.u-strasbg.fr>, gnealon@chem.uwa.edu.au, bws@crystal.uwa.edu.au, Bernie Kraatz <bernie.kraatz@usask.ca>

Dear Grzegorz,

I, as correspondence author and on behalf of the other authors, agree that you, Grzegorz Orlowski, can use published materials that we co-authored with you as a part of your Ph.D. thesis.

Regards,

George

--
Dr George Koutsantonis
Chemistry, M313
School of Chemical and Biomedical Sciences
University of Western Australia
35 Stirling Highway,
Crawley, Perth, 6009
Australia
Ph: +61 8 6488 3177
Fax: +61 8 6488 7247
Group Website: http://chem181.chem.uwa.edu.au/Koutsantonis_Group

Subject: Co-authorship permissions
From: Gareth Nealon <gnealon@chem.uwa.edu.au>
Date: Tue, 15 May 2007 16:36:37 +0800
To: Grzegorz Orlowski <gro012@mail.usask.ca>

Re: Co-authorship rights for the manuscript: Eur. J. Inorg. Chem., 2007, pp. 263-278. DOI: 10.1002/ejic.200600626

To Whom it May Concern,

I agree that Grzegorz Orlowski can use published materials that I am co-authoring with him as a part of his Ph.D. thesis.

Yours Sincerely

Gareth Nealon